Author version: *Mar. Pet. Geol*, vol.58; 2014; 29-98

Geologic implications of gas hydrates in the offshore of India: Krishna-Godavari Basin, Mahanadi Basin, Andaman Sea, Kerala-Konkan Basin

Pushpendra Kumar[a], Timothy S. Collett[b,], Ray Boswell[c], James R. Cochran[d], Malcolm Lall[e],Aninda Mazumdar[f], Mangipudi Venkata Ramana[g], Tammisetti Ramprasad[f], Michael Riedel[h], Kalachand Sain[i], Arun Vasant Sathe[a], Krishna Vishwanath[e], U.S. Yadav[a], NGHP Expedition 01 Scientific Party

[a] Oil and Natural Gas Corporation Ltd, KDM Institute of Petroleum Exploration, 9 Kaulagarh Road, Dehradun 248195, Uttarakhand, India

[b] U.S. Geological Survey, Denver Federal Center, MS-939, Box 25046, Denver, CO 80225, USA

[c] U.S. Department of Energy, National Energy Technology Laboratory, 626 Cochran's Mill Rd., Pittsburgh, PA 15236, USA

[d] Lamont Doherty Earth Observatory, Columbia University, Palisades, NY 10964, USA

[e] Directorate General of Hydrocarbons, Plot No 2, Sector 73, Noida, India

[f] National Institute of Oceanography, Donapaula, Goa 403004, India

[g] Mauritius Oceanography Institute, Victoria Avenue, Mauritius

[h] Natural Resources Canada, 9860 West Saanich Road, Sidney, British Columbia V8L 4B2, Canada

[i] National Geophysical Research Institute, Uppal Road, Hyderabad 500007, India

Editor's Note

This report is part of a two-report series that summarizes the results of the Indian National Gas Hydrate Program Expedition 01 (NGHP-01). This report (Kumar et al., this issue) in this series reviews the occurrence and geologic controls on gas hydrates in the Krishna-Godavari Basin, the Mahanadi Basin, the Andaman Sea, and the Kerala-Konkan Basin, while the first report in this series summarizes the overall operational and scientific accomplishments of NGHP-01 (Collett et al., this issue).

Abstract

Gas hydrate resource assessments that indicate enormous global volumes of gas present within hydrate accumulations have been one of the primary driving forces behind the growing interest in gas hydrates. Gas hydrate volumetric estimates in recent years have focused on documenting the geologic parameters in the "gas hydrate petroleum system" that control the occurrence of gas hydrates in nature. The primary goals of this report are to review our present understanding of the geologic controls on the occurrence of gas hydrate in the offshore of India and to document the application of the gas hydrate petroleum system approach to the study of gas hydrates.

National Gas Hydrate Program of India executed the National Gas Hydrate Program Expedition 01 (NGHP-01) in 2006 in four areas located on the eastern and western margins of the Indian Peninsula and in the Andaman Sea. These areas have experienced very different tectonic and depositional histories. The peninsular margins are passive continental margins resulting from a series of rifting episodes during the breakup and dispersion of Gondwanaland to form the present Indian Ocean. The Andaman Sea is

bounded on its western side by a convergent margin where the Indian plate lithosphere is being subducted beneath southeast Asia.

NGHP-01 drilled, logged, and/or cored 15 sites (33 holes) in the Krishna-Godavari Basin, 4 sites (5 holes) in the Mahanadi Basin, 1 site (2 holes) in the Andaman Sea, and 1 site (1 hole) in the Kerala-Konkan Basin. Holes were drilled through standard drilling for the purpose of f logging-while-drilling and dedicated wireline logging; as well as through the use of a variety of standard coring systems and specialized pressure coring systems.

NGHP-01 yielded evidence of gas hydrate from downhole log and core data obtained from all the sites in the Krishna-Godavari Basin, the Mahanadi Basin, and in the Andaman Sea. The site drilled in the Kerala-Konkan Basin during NGHP-01 did not yield any evidence of gas hydrate. Most of the downhole log inferred gas hydrate and core recovered gas hydrate were characterized as either fracture-filling material in clay dominated sediments or as pore-filling or grain-displacement particles disseminated in both fine- and coarser-grain sediments. Geochemical analyses of gases obtained from sediment cores recovered during NGHP-01 indicated that the gas in most all of the oceanic hydrates in the offshore of India is derived from microbial sources; only one site in the Andaman Sea exhibited limited evidence of a minor thermogenic gas source. The gas hydrate petroleum system concept has been used to effectively characterize the geologic controls on the occurrence of gas hydrates in the offshore of India.

1. Introduction

As reviewed in Collett et al., (this issue), the National Gas Hydrate Program Expedition 01 (NGHP-01) began on 28 April 2006 with the arrival of the research drill ship *JOIDES Resolution* in Mumbai, India, and ended 113.5 days later in Chennai, India. Ultimately 21 drill sites were established during NGHP-01 with 15 of the sites in the Krishna-Godavari Basin, 4 sites in the Mahanadi Basin, 1 site in the Andaman Sea, and 1 site in the Kerala-Konkan Basin (Figure 1).

This report provides a technical review of the geologic controls on the occurrence of gas hydrate in the Krishna-Godavari Basin, the Mahanadi Basin, the Andaman Sea, and in the Kerala-Konkan Basin (Figure 1), including a hole-by-hole synopsis of the evidence for gas hydrates at each of the NGHP-01 drill sites established during the expedition (Table 1). This report also summarizes the scientific results of the NGHP-01 expedition efforts as presented in the XX technical reports that make up this special issue of the Journal of Marine and Petroleum Geology (Table 2A). Additional studies of data and samples obtained through the NGHP-01 expedition has led to the publication of XX additional journal articles and reports not included in this special issue; the scientific results associated with these additional contributions have been summarized in this report (Tables 2B). This report concludes with a systematic review of the gas hydrate petroleum systems that control the occurrence of gas hydrate in the offshore of India.

2. NGHP-01 Expedition geologic setting

2.1. Krishna-Godavari Basin

The Krishna-Godavari Basin is a proven petroliferous basin along the east coast of India. The onshore portion of the basin covers an area of approximately 15,000 square kilometers, while the offshore portion covers an area of at least 25,000 square miles extending seaward to the 1,000 m isobath. The basin

contains about 5 km of sediments with several depositional sequences, ranging in age from Late Carboniferous to Pleistocene (Curray et al., 1982).

The eastern continental margin of India formed as the result of rifting between India and the rest of East Gondwanaland (Australia/Antarctica) in the Late Jurassic and Early Cretaceous. Plate reconstructions place the eastern Indian margin adjacent to Enderby Land in East Antarctica with the northern margin of "Greater India" along the western margin of Australia (Scotese et al., 1988; Powell et al., 1988). Rifting began in the Late Jurassic at about 160 Ma with breakup at about 130 Ma (Powell et al., 1988).

The basin came into existence following rifting along eastern continental margin of Indian Craton in early Mesozoic. The down-to-the-basement faults which define the series of horst and grabens cascading down towards the ocean are aligned NE-SW along Precambrian Eastern Ghat trend.

Sediment input to the Bay of Bengal is dominated by the Ganges-Brahmaputra River system, which drains much of the Himalayas. The resulting sediment influx has built the Bengal Fan, the world's largest sediment accumulation (Alam, et al., 2003). The sediment thickness reaches a maximum of over 22 km on the Bangladesh shelf (Curray, 1991) and over 2 km of fan sediments are found at 2°S lat (Curray et al., 1982), some 2,500 km to the south. Additional sediment is supplied from the Indian sub-continent via the Krishna and Godavari rivers. Studies of seismic data from the Krishna-Godavari Basin, as reviewed by Ramana et al., (2009), reveals a complex seafloor topography that is dominated by a series of deep water fault controlled incised fan-like systems that could have delivered reservoir quality turbidite sands deep into the basin.

2.2. Mahanadi Basin

The geologic history of the Mahanadi Basin is similar to that of the Krishna-Godavari Basin. The Late Jurassic rift structures along the eastern margin of India cut across older NW-SE-trending Permian-Triassic Gondwana grabens including the Mahanadi and Pranhita-Godavari grabens (Sastri et al., 1981). The Mahanadi graben appears to have a continuation in Antarctica as the Lambert graben (Federov et al., 1982). These structures served to delineate the fluvial drainage system throughout the evolution of the margin to the present; and they now contain the Mahanadi and Godavari Rivers, respectively. Both rivers have a high sediment transport (Sastri et al., 1981; Biksham and Subrahmanyam, 1988) and both rivers have built substantial deltas so that sedimentation at the drill sites established during NGHP-01 show features typical of deepwater deposits, including large regional fans, cut and filled channels and abundant growth faulting. Thus, it was predicted that the sediments to be drilled at the proposed drill sites would likely include well-defined channelized fan deposits. The Mahanadi Basin was considered favorable for the presence of gas hydrate because of the input of the large, potentially coarse-grained, sediment volumes along with organic-rich sediments from the nearby Mahanadi and Brahmani river systems (Ramana et al., 2006).

2.3. Andaman Sea

The Andaman Sea, located on the eastern edge of the Bay of Bengal, is an active back-arc basin. The convergent-oblique movement of the Indian plate as it subducts underneath the Burma plate causes compressive north-south wrench tectonics (Alam et al., 2003). A backarc system developed when the overriding plate was stretched and rifted, causing the creation of two distinct plates, the Sunda plate and the Burma plate with an intervening spreading center. Backarc spreading began in the early Miocene, approximately 25 Ma. Current plate boundaries were formed about 3 Ma (Curray, 1991). The plates are currently separating at a rate of 3.76 cm/yr (Raju et al., 2004).

The Andaman Islands are a volcanic island arc system located on the western edge of the Andaman Sea. The only currently active volcano in the system, Barren Island, appears on the northern edge of the Andaman Islands, approximately 135 km north of Port Blair. The area is seismically active and is known for the magnitude nine, Sumatra-Andaman earthquake that occurred south of the Andaman Islands on December 26, 2004. Most of the earthquake activity clusters around the Andaman Islands and the Burma-Sunda spreading center (Raju et al., 2004).

The Site NGHP-01-17 , in the Andaman Sea, is located between the Andaman Islands and the backarc-spreading center. An accretionary wedge lies to the west of the Andaman Islands. The NGHP-01-17 drill site is approximately 60 km west of the Burma-Sunda spreading center, a north-south trending feature located near 93°40' E long.

Terrigenous sediments in the Andaman Sea are supplied by the Irrawaddy River, which runs through central Myanmar and flows into the northern Andaman Sea. One core, collected in the central Andaman Sea on the *R/V Marion Dufresne* in 1977, contained a lithology dominated by terrigenous muddy clay and nannofossil carbonate ooze (Colin et al., 1998). A similar lithology was expected at the site drilled during NGHP-01.

2.4. Kerala-Konkan Basin

The western continental margin of India formed during two rifting events. The first was the rifting of India and the Seychelles from Madagascar in the Late Cretaceous. Magnetic anomalies in the Mascarene Basin date this rifting to about 84 Ma (Dyment, 1991). The Seychelles Platform was still attached to the southern portion of the western Indian margin at this time. Rifting between the Seychelles and India occurred near the Cretaceous-Tertiary boundary (65 Ma) accompanied by the extensive volcanism of the Deccan flood basalts (Duncan and Pyle, 1988).

In the Arabian Sea, the main sources of sediment are the Indus River that drains into the northernmost portion of the Arabian Sea and the Narmuda and Tapti rivers that empty into the Gulf of Cambay, north of 20°N lat. Sediment thickness reaches about 10 km on the Indus shelf and decreases to about 5 km at 22°N lat in the center of the basin (Clift et al., 2001). Sediment thickness in the Cambay and Bombay offshore basins (on the continental shelf at the mouth of the Gulf of Cambay) may also reach 8–10 km, but thickness decreases rapidly moving off the shelf into deeper water (Rao, 2001). South of the Gulf of Cambay, the Western Ghats range form a 600–2,200-m-high escarpment at a distance of only 10–70 km from the coast. The escarpment serves as the main drainage divide for the continent. As a result, rivers arising within 50 km of the Arabian Sea drain eastward into the Bay of Bengal and only short rivers flow across the Kongan-Kanara lowlands to the Arabian Sea.

The surficial sediment in the area of the NGHP-01-1 drill site on the west coast is primarily globigerina clay (Rao, 2001). Ramaswamy et al., (1991) estimated from a set of sediment traps deployed across the Arabian Sea near 15°N lat that almost all of the river's discharge is retained on the shelf, with less than 5% percent deposited in the deeper parts of the basin. Thus, large sediment deposits and turbidite sequences were not expected at Site NGHP-01-1.

A basement ridge, the Pratap Ridge, runs parallel to the coast in the upper continental slope region (Subrahmanyam et al., 1991) resulting in the formation of a series of offshore basins under the shelf and upper slope. These basins contain 2–4 km of sediment (Rao, 2001). Farther offshore, the Chagos-Laccadive Ridge parallels the southwestern margin of India south of ~15°N lat and continues across the Indian Ocean as the trace of the Réunion hotspot, which was responsible for the Deccan basalts

(Duncan, 1990). The west coast drill site (NGHP-01-01) is located nearly on line with the Chagos-Laccadive Ridge just north of where it disappears as a bathymetric feature. Seismic lines show an apparent basement high beneath the site that comes to within about 450 m of the seafloor. Rao's (2001) isopach map shows slightly less than 1,000 m of sediment in this region.

3. NGHP-01 site summaries

3.1. *Krishna-Godavari Basin*

Site NGHP-01-02

Site NGHP-01-02 (Prospectus Site KGGH03-A) is located at the far southwestern end of the Krishna-Godavari Basin study area (Figure 1). The water depth at this site is ~1,058 m. This site was not cored; only LWD data was obtained from two holes. The seismic-imaged stratigraphy at this site is characterized by a ridge with steeply dipping stratigraphy (Figure 2). The depth of the seismic identified bottom-simulating reflector (BSR) at this site was estimated at ~171 mbsf.

The LWD-acquired resistivity log (Figure 3) in Hole NGHP-01-02B shows a general negative correlation with porosity, suggesting that little or no gas hydrate is present. The only exception may be a series of thin, elevated resistivity zones within the interval 70–170 mbsf.

Site NGHP-01-03

Site NGHP-01-03 (Prospectus Site GDGH05-A) is located at the southwestern end of the Krishna-Godavari Basin study area (Figure 1). The water depth at this site is ~1076 m. The seismically-imaged stratigraphy at this site (Figure 4) is characterized by seafloor-parallel to slightly inclined beds to a depth of ~125 mbsf. Below this depth the sediment dips to the northwest. A BSR can be identified at a depth of ~209 mbsf. A total of three holes were drilled at Site NGHP-01-03. Hole NGHP-01-03A was drilled for LWD data collection (Figure 5). Hole NGHP-01-03B was cored to 300 mbsf (Figure 6). Hole NGHP-01-03C was spot cored to 198 mbsf, then drilled and wireline logged to a total depth of 300 mbsf.

The lithostratigraphy recovered at Site NGHP-01-03 is similar to the lithostratigraphy drilled at Sites NGHP-01-05, NGHP-01-10, and NGHP-01-12 on the Krishna-Godavari slope. One notable difference is that Sites NGHP-01-10 and NGHP-01-12 contain significantly less silt/sand laminae beds than Site NGHP-01-03 and NGHP-01-05. In addition, because Site NGHP-01-03 was cored to a greater depth (300 mbsf), a new section of stratigraphy that was apparently not reached at Sites NGHP-01-05, NGHP-01-10, or NGHP-01-12 was recovered.

The presence of gas hydrate at Site NGHP-01-03 was inferred from small increases in resistivity on the LWD data in Hole NGHP-01-03A (Figure 5); however, no gas hydrate was recovered on the catwalk and no significant infrared (IR) anomalies were detected. Much of the interstitial Cl^- concentration profile between 60 mbsf and the BSR is dominated by concentrations near the modern seawater value or slightly depleted relative to modern seawater (Figure 6). The depleted Cl^- concentrations may reflect low concentrations of gas hydrate disseminated in the sediments within the gas hydrate stability zone at this site. Two pressure cores obtained from near the depth of the BSR, exhibited gas volumes in excess of solubility with estimated gas hydrate saturations of less than 1% (Figure 6). The log and core data from Site NGHP-01-03 suggests that gas hydrate may have been disseminated at low concentrations within the sediment as pore-filling particles or grain-displacement material possibly in fractures.

Site NGHP-01-04

Site NGHP-01-04 (Prospectus Site KGGH01) is located in the central part of the Krishna-Godavari Basin study area (Figure 1). The water depth at this site is ~1,081 m. This site was not selected as a primary coring site and only LWD data were recorded. Site NGHP-01-04 is located within a well-developed slope-basin, with a clear BSR at a depth of ~182 mbsf (Figure 7).

The resistivity and formation density well log curves in Hole NGHP-01-04A generally mirror each other (Figure 8), so that the Archie computed water saturation is close to 100 % throughout most of the logged interval. The only exceptions are in the intervals 53–61 mbsf and 80–100 mbsf. The shallower interval corresponds to a low measured density and thus may be due to an underestimation of density in the shallow enlarged part of the hole. On the other hand, the interval 80–100 mbsf is more likely to contain gas hydrate because it corresponds to a resistivity high and because the LWD borehole resistivity images show possible evidence of high-resistivity hydrate-filled fractures.

Site NGHP-01-05

NGHP-01-05 (Prospectus Site KGGH02-A) is located in the central part of the Krishna-Godavari Basin study area (Figure 1). The water depth at this site is ~945 m. The seismic data from this site images a distinct BSR, which cuts inclined, parallel stratigraphic horizons (Figure 9). The BSR is estimated at a depth of 125 mbsf.

At Site NGHP-01-05, a total of five holes (NGHP-01-05A through NGHP-01-05E) were drilled and two of these were cored (NGHP-01-05C and NGHP-01-05D); Hole NGHP-01-05C was cored to 200.0 mbsf and Hole NGHP-01-05D was cored to 201.0 mbsf. Holes NGHP-01-05A and NGHP-01-05B were drilled for LWD data acquisition (Figure 10) and Hole NGHP-01-05E was drilled for wireline and vertical seismic profile (VSP) logging.

The sedimentary sequence cored at Site NGHP-01-05 was assigned to a single lithostratigraphic unit, composed of nannofossil-bearing-to-rich clay with limited silt/sand laminae.

Gas hydrate was inferred from the LWD data at Site NGHP-01-05 and recovered in some cores on the catwalk (where the signs of gas hydrate dissociation were identified through “cold spots” observed on IR imaging). In general, gas hydrate occurrences at this site were interpreted to be disseminated accumulations at low concentrations within the sediment as pore-filling particles or grain-displacement material possibly in fractures (Figure 11). Two interstitial water samples associated with IR cold spots showed that the gas hydrate existed within silt beds. However, X-rays and logs from pressure cores also documented that gas hydrate was present as vein fills and in some horizontal bands. Two pressure cores obtained from near the depth of the BSR, were determined to have gas hydrate saturations of less than 1% (Figure 11). Four additional pressure cores from the interval 77-87 mbsf yield gas hydrate saturations ranging from 0.6 to 8.0 percent. The strongest evidence for gas hydrate from the acquired LWD data is in the intervals 55–94 mbsf (Hole NGHP-01-05A) and 53–90 mbsf (Hole NGHP-01-05B), where the computed Archie-resistivity derived gas hydrate saturations reach a maximum of about 60% (Figure 10). The significant difference in the core and resistivity log derived gas hydrate saturations cannot be easily explained, but it is likely due to the fact that resistivity well log calculations often overestimate gas hydrate saturations in fracture dominated reservoirs as reviewed by Collett et al., (this volume).

Site NGHP-01-06

Site NGHP-01-06 (Prospectus Site KGGH04) is located in the central part of the Krishna-Godavari Basin (Figure 1). The water depth is ~1,160 m. This site was not selected as a primary coring site and only LWD data were obtained from Hole NGHP-01-06A.

Seismic data show that Site NGHP-01-06 is located in a typical sequence of Krishna-Godavari Basin ridges and basins (Figure 12). A BSR is visible throughout most of the area and is best imaged where it cross-cuts steeply-dipping reflectors at a depth of 210 mbsf. Below the BSR, high-amplitude reflectors may be the result of free gas, whereas higher amplitude reflectors above the BSR are suggestive of the possible presence of gas hydrate in the sediments.

Resistivities logged in Hole NGHP-01-06A show a general negative correlation with porosity (Figure 13), suggesting that little or no gas hydrate is present. However, further detailed Archie analysis of the resistivity and porosity log data suggests that some amount of gas hydrate could be present in several intervals between ~100 and ~200 mbsf. The most prominent occurrence is at 137–148 mbsf, where the computed gas hydrate saturation reaches a maximum of about 25%.

Site NGHP-01-07

Site NGHP-01-07 (Prospectus Site KGGH06-A) is located in the northern part of the Krishna-Godavari Basin study area (Figure 1). The water depth at this site is ~1,285 m. Site NGHP-01-07 is located within the Reliance Industry Ltd. D6 exploration block.

At Site NGHP-01-07, a distinct BSR is imaged cross-cutting inclined beds at a depth of 188 mbsf (Figure 14). In general, the seafloor deepens to the southeast, but is interrupted by a ridge to the north, which is elevated 45–50 m above the surrounding topography. Two distinct seismic reflections can be identified within the sediment package overlying the BSR at Site NGHP-01-07: a strong reflector at ~70 mbsf and a high-reflectivity band between 130 mbsf and 150 mbsf are seen. Both reflectors are most likely associated with the occurrence of gas hydrate as identified on LWD data (Figure 15).

Four holes were drilled at Site NGHP-01-07: Hole NGHP-01-07A for LWD; Hole NGHP-01-07B for coring to 211.6 mbsf; Hole NGHP-01-07C, a dedicated wireline logging hole that reached a total depth of 184.2 mbsf; and Hole NGHP-01-07D for coring between 231.2 mbsf and 260 mbsf followed by wireline logging (including a VSP survey). The lithostratigraphy at Site NGHP-01-07 is similar to the lithostratigraphy of sites previously drilled in the southern part of the Krishna-Godavari Basin, with the sedimentary section composed of mostly nannofossil-bearing clay to foraminifera-bearing clay. Terrestrial organic matter is also typically high at Site NGHP-01-07 as in the southern Krishna-Godavari Basin sites. However, compared to other Krishna-Godavari Basin sites, sand/silt laminae and beds occur more frequently at Site NGHP-01-07 and sands are more common (gravel is also encountered in one instance).

Gas hydrate was inferred from the LWD data at Site NGHP-01-07 at 75-93 mbsf and 138-152 mbsf in what appears to be two gas hydrate-bearing fracture dominated reservoirs with downhole log computed gas hydrate saturations generally less than 25%. The interstitial water chemistry and IR thermal images at this site were highly variable, which might indicate the presence of small amount of gas hydrate throughout the entire cored section above the BSR (Figure 16). One pressure core from 148.2 mbsf (which is within the depth interval of the deeper of the two resistivity log anomalies) yielded a gas hydrate saturation estimate of 1.1%.

Site NGHP-01-10

Site NGHP-01-10 (Prospectus Site KGGH03-A; GD-3-1) is located at the far southwestern end of the Krishna-Godavari Basin study area (Figure 1). The water depth at this site is ~1,038 m. Site NGHP-01-10 is located 50 m away from industry well GD-3-1, which had previously shown strong evidence for the occurrence of gas hydrate. During NGHP-01, four sites were established to delineate the gas hydrate accumulation in the area of the industry GD-3-1 well, including Sites NGHP-01-10, NGHP-01-12, NGHP-01-13, and NGHP-01-21. For organization purposes, the review discussion associated with each of these sites are handled below in this report in their own separate sections. However, the seismic, well log, and core data from each of these four sites have been merged into one set of images (seismic display - Figure 17; well log display – Figure 18; core display – Figure 19).

Two high-resolution 2D seismic lines were made available to this project to characterize the local geologic setting around Site NGHP-01-10. An additional low-resolution 2D seismic was also made available from this site. The overall area is dominated by strong seismic reflectivity, which is likely the result of free gas below the BSR at an estimated depth of 160 mbsf (Figure 17). The high-resolution 2D seismic lines also show a highly faulted sedimentary sequence between the seafloor and the deeper inferred gas occurrences. Individual horizontal reflectors can be traced for only a few hundred meters at most within this section. Along the southwest margin of NGHP-01-10 drill site, a possible shallow debris flow was identified. This unit pinches out near the location of Hole NGHP-01-10A.

Four holes were drilled at Site NGHP-01-10: Hole NGHP-01-10A for LWD; Hole NGHP-01-10B for APC/XCB and pressure coring, Hole NGHP-01-10C for one APC core, and Hole NGHP-01-10D for APC/XCB and pressure coring to a total depth of 203.8 mbsf. Hole NGHP-01-10D was wireline logged, including a VSP survey. The sedimentary sequence cored and logged at Sites NGHP-01-10, NGHP-01-12, NGHP-01-13, and NGHP-01-21 was assigned to a single lithostratigraphic unit composed mostly of nannofossil-bearing clay. Possible fossil chemosynthetic communities composed of a variety of mollusk shells with some encrusted by carbonatic worm tubes were recovered at both Sites NGHP-01-10 and NGHP-01-12 below about 10–20 mbsf.

Gas hydrate was inferred from the LWD data at Site NGHP-01-10 (Figure 18) and recovered in numerous cores on the catwalk (identified through IR images and photographed in the cores) within the depth interval from ~25 to ~160 mbsf (Figure 19). The observed gas hydrate existed as solid nodules, high-angle and sub-horizontal veins, and as fracture fill. Gas hydrate is also inferred to occur as minor pore-fill or possible grain-displacement material disseminated in the recovered pressure cores (as reviewed by Collett et al., this issue). The pressure-core degassing and X-ray core scans, as well as the semi-continuous cold spots in the IR data, confirm that fracture-filling gas hydrate is common throughout the gas hydrate occurrence zone at this site. Upon examination of the APC/XCB and pressure cores, no obvious lithologic control on gas hydrate occurrence (in terms of grain size) was observed. The split cores from Sites NGHP-01-10 and NGHP-01-12 often exhibited moussey and soupy textures which commonly result from the dissociation of gas hydrate and is consistent with the widespread observation of gas hydrate in the cores and well logs at these sites. At Site NGHP-01-10, interstitial water Cl^- concentrations (Figure 19) vary widely between ~26 and ~160 mbsf—this can be attributed to the decomposition of gas hydrate after core recovery. The analysis of pressure cores at this site yielded gas hydrate saturations ranging from near 2% to over 31%. The high LWD derived resistivities measured in Hole NGHP-01-10A have been attributed to the presence of gas hydrate (Figure 18). The gas hydrate saturations computed from resistivity well logs again appear to overestimate the gas hydrate saturations at

this site because of fractured nature of the gas hydrate reservoir system as reviewed by Collett et al., (this issue).

The appearance of near-surface, fracture-filling gas hydrate at Site NGHP-01-10 is very similar to the physical occurrence of gas hydrate cored at several cold-vent sites along the Cascadia margin. One of the best examples is the Bullseye vent area cored at Site U1328 on IODP Expedition 311 (Riedel et al., 2006), where beds containing massive forms of gas hydrate occurred within the uppermost ~40 mbsf, with gas hydrate concentrations exceeding 80% of pore space. At Site NGHP-01-10, however, the zone of high gas hydrate concentrations does not extend to the surface. It is also interesting that the depth to the sulfate-methane interface (SMI) is at about 17.2 mbsf at Site NGHP-01-10, which is much deeper than measured around most cold-vent sites and indicative of much less active vertical methane flux. The top of the apparent gas hydrate interval (at ~25 mbsf) appears to coincide with the occurrence of a fossil chemosynthetic community at Site NGHP-01-10, which may have been buried by the seismically imaged debris flow along the SW margin of the drill site. A debris flow covering the apparent cold vent at Site NGHP-01-10 would account for the lack of gas hydrate in the near-surface sediments and the relatively deep SMI.

Site NGHP-01-11

Site NGHP-01-11 (Prospectus Site GDGH12-A) is located in central part the Krishna-Godavari Basin near Site NGHP-01-04 (Figure 1). The water depth at this site is ~1,007m. This site was not selected as a primary coring site and only LWD data were obtained from Hole NGHP-01-11A.

The BSR at Site NGHP-01-11 is widespread and especially well defined where it cross-cuts sedimentary strata (Figure 20). The depth of the BSR at Site NGHP-01-11 is estimated at ~150 mbsf. As expected, the BSR depth becomes shallower towards the northwest as water depth decreases. A series of bright seismic reflectors between seafloor and the BSR may indicate gas hydrate, while the bright reflectors immediately below the BSR probably indicate the presence of free-gas.

Resistivities logged in Hole NGHP-01-11A (Figure 21) show a general negative correlation with porosity, except in the intervals 95–113 mbsf and 144–146 mbsf, where high resistivities suggest that gas hydrate is present. The strongest evidence for gas hydrate is in the interval 95–113 mbsf, where the Archie-computed gas hydrate saturation reaches a maximum of about 35%. The thin high-resistivity interval at 144–146 mbsf does not coincide with a density high and shows a maximum Archie computed gas hydrate saturation of 35%. Outside of these intervals, there is no strong evidence for gas hydrate. The downhole-log-inferred gas hydrate occurrence at 95–113 mbsf appears to correlate to a prominent seismic reflector above the BSR.

Site NGHP-01-12

Site NGHP-01-12 (Prospectus Site KGGH03-A; 1st New Site) was established during the course of NGHP-01 to further delineate the gas hydrate occurrence identified at Site NGHP-01-10 (Figures 1 and 17). Site NGHP-01-12 was placed 500 m towards the southeast of the industry well GD-3-1. This site is located within the seismically-disturbed section as described around Site NGHP-01-10. The water depth at this site is ~1,038 m.

Hole NGHP-01-12A included limited APC coring through the SMI, followed by a series of two XCB and pressure coring packages to a total depth of 150.9 mbsf. As discussed above in the summary for Site NGHP-01-10, gas hydrate was inferred from the LWD data at Site NGHP-01-10 (Figure 18) and recovered in cores (Figure 19) from both Sites NGHP-01-10 and NGHP-01-12 within the depth interval

from ~25 to about the TD of Hole NGHP-01-12A (150.9 mbsf). At Site NGHP-01-10, interstitial water Cl^- concentrations varied widely between ~26 and ~160 mbsf, whereas at Hole NGHP-01-12A, Cl^- concentrations were generally higher and relatively more uniform with depth, indicating that in-situ gas hydrate concentrations were probably lower.

Site NGHP-01-13

As with Site NGHP-01-12, Site NGHP-01-13 (Prospectus Site KGGH03-A; 2nd New Site) was established to further delineate the gas hydrate occurrence identified at Site NGHP-01-10 (Figures 1 and 17). Site NGHP-01-13, the third site in this area, was located 150 m northwest of Site NGHP-01-12 (closer to Site GD-3-1). This site was located within the seismically-disturbed section as described around Sites NGHP-01-10 and Site NGHP-01-12. The water depth at this site is ~1,038 m.

Hole NGHP-01-13A was drilled for wireline logging to a TD of 200 mbsf. Analysis of the downhole resistvity log data collected from Hole NGHP-01-13A (Figure 18) yielded uniformly high gas hydrate saturations (higher than ~40%) over the entire logged interval. These estimates are slightly lower but similar to the saturations derived from the LWD logs in Hole NGHP-01-10A.

Site NGHP-01-14

Site NGHP-01-14 (Prospectus Site GDGH14-A) is located in the northern part of the Krishna-Godavari Basin (Figure 1). This site was selected as an alternate location in the program and was not part of the pre-coring LWD program. The water depth at this site is ~895 m.

Seismic data from this site shows the typical sediment sequence of basin and ridge observed throughout the Krishna-Godavari Basin (Figure 22), with each ridge associated with a deep-rooted fault and the basin sequence developed on the down-thrown side of the fault towards the SE. The basins are characterized by seafloor-parallel to sub-parallel sedimentary beds, whereas the ridge flanks are dominated by beds with larger northwesterly-dips and somewhat brighter reflection amplitudes, especially below the BSR. The depth of the BSR is estimated at 109 mbsf at Site NGHP-01-14.

At Site NGHP-01-14, one hole (NGHP-01-14A) was drilled, cored, and wireline logged to a total depth of 180 mbsf (Figures 23 and 24). The lithostratigraphy recovered at Site NGHP-01-14 is similar to the lithostratigraphy previously drilled at the other sites throughout the Krishna-Godavari Basin. Site NGHP-01-14 is located between Sites NGHP-01-05 and NGHP-01-15, and all three sites are located at similar water depths (~900–950 m). The lithostratigraphy at all three sites was generally described as nannofossil-bearing clay; however, there are thicker sands at Sites NGHP-01-14 and Site NGHP-01-15 than at Site NGHP-01-05.

The occurrence of gas hydrate at Site NGHP-01-14 was inferred from slightly elevated and uniform downhole measured wireline resistivities in the sedimentary section from 65 to 105 mbsf (Figure 23). Two intervals in particular (67–72 mbsf and 82–87 mbsf) show higher resistivity values that might reflect higher concentrations of gas hydrate. Archie analysis of the wireline resistivity data indicates that gas hydrate saturations could be as high as ~20 % in these two intervals. Interstitial water analysis below ~20 mbsf reveals highly variable chloride concentrations that are also slightly shifted to lower values (Figure 24). This suggests that the majority of the gas hydrate at Site NGHP-01-14 is most likely disseminated within the sediments at low concentrations. Overprinted on this "diffuse" distribution of gas hydrate are two zones where Cl^- concentrations are depleted by as much as 12% relative to modern seawater values, which appears to correlate to the downhole log inferred gas hydrate occurrences in the interval from about 65 to 105 mbsf. Gas hydrate was observed in some of the interstitial water samples prior to squeezing.

In addition, IR anomalies were also observed throughout this same interval when imaged on the catwalk and six gas hydrate samples were collected in the interval from 103.3 to 106.2 mbsf. One pressure core from a depth of 101 mbsf, which is within the well log inferred hydrate-bearing interval, yielded a gas hydrate saturation of 10.7%.

Site NGHP-01-15

Site NGHP-01-15 (Prospectus Site GDGH11) is located in the Krishna-Godavari Basin (Figure 1). Site NGHP-01-15 is one of the northern sites drilled in the Krishna-Godavari Basin during this expedition. This site was selected as an alternate location in the program and was not part of the pre-coring LWD program. The water depth at this site is ~926 m.

Similar to Site NGHP-01-14, the seismic data from Site NGHP-01-15 show a typical Krishna-Godavari Basin sequence of ridges and basins with a well-developed BSR at depth of 126 mbsf (Figure 25). This site does not show the steeply dipping, high-reflectivity layers below the BSR that characterize other Krishna-Godavari Basin sites drilled during this expedition; rather, the sediments are more flat lying.

At Site NGHP-01-15, one hole (NGHP-01-15A) was drilled, cored, and wireline logged to a total depth of 200 mbsf (Figures 26 and 27). As noted above, the lithostratigraphy recovered at Site NGHP-01-15 is similar to that drilled at other sites throughout the Krishna-Godavari Basin: nannofossil-bearing clay with relatively thick sand laminae and beds of various thicknesses.

Interstitial water analysis of cores from Hole NGHP-01-15A indicates the presence of localized beds containing concentrated gas hydrate within the depth interval from ~60 to 90 mbsf (Figures 27). Gas hydrate was observed and sampled from one core at depths of 78.63–79.13 mbsf in Hole NGHP-01-15A, which also exhibited a relatively continuous IR anomaly (~9 m in length) when imaged on the catwalk. Moussey sediment textures (formed during gas hydrate dissociation) were also observed within the cores recovered from Hole NGHP-01-15A. Physical observations of the core on the catwalk confirmed that the IR-imaged and sampled gas hydrate in the interval of 78.63–79.13 mbsf occurred in a prominent sand bed (Figures 26 and 27). Gas hydrate, associated with clean sand and woody debris, was also recovered in a pressure core from a depth of 86.7 mbsf in Hole NGHP-01-15A.

Relatively high resistivity values measured during the wireline logging program in Hole NGHP-01-15A above ~110 mbsf suggest that some gas hydrate is present above this depth. The highest resistivity values between ~75 and 81 mbsf correspond to the section in which the strong temperature anomalies were measured on the catwalk and gas hydrate samples were recovered. Archie analysis of the wireline recorded resistivity data indicates that gas hydrate could occupy as much as ~25 % of the pore space in some intervals between ~90 and ~110 mbsf and could locally occupy almost 50% around 80 mbsf.

Site NGHP-01-16

Site NGHP-01-16 (Prospectus "Stepout Site") is located in the northern part of the Krishna-Godavari Basin study area (Figure 1). The water depth at this site is ~1,253 m. Site NGHP-01-16 is located within the Reliance Industry Ltd. D6 exploration block and is ~8 km N of Site NGHP-01-07. This site was selected as an alternate location in the program and was not part of the pre-coring LWD program.

The stratigraphy at this site is characterized by two distinct seismic facies (Figure 28). The upper package extends to a depth of ~80 mbsf and consists of a series of almost seafloor-parallel layers with relatively high seismic reflectivity and is marked by an unconformity at its base. The lower section is

characterized by reduced reflectivity and inclined bedding. Within this low-reflectivity package, the BSR is clearly visible at a depth of ~170 mbsf.

At Site NGHP-01-16, one hole (NGHP-01-16A) was continuously cored to a depth of 217.0 mbsf and then wireline logged (Figures 29 and 30). The recovered cores consist primarily of clays with limited silt, nannofossils, and foraminifera. Sand/silt laminae and beds occur as frequently at Site NGHP-01-16 as they do at Site NGHP-01-07, but sand beds are rarer at Site NGHP-01-16. Coring at Site NGHP-01-07 probably penetrated sediments deposited closer to a channel on the continental slope, whereas the thinner sands at Site NGHP-01-16 suggest a more distal position relative to slope channels.

Interstitial water chemistry data (Figure 30) did not indicate any significant gas hydrate occurrences at Site NGHP-01-16 in the depth interval above ~85 mbsf; however, from this depth to the depth of the BSR (~170 mbsf), the Cl^- concentrations become progressively depleted with respect to modern seawater. The lower Cl^- values within this depth interval probably reflect minor dilution of the interstitial water Cl^- by gas hydrate dissociation induced during the core recovery process. The minimum Cl^- concentrations at 162.5 mbsf indicate somewhat higher amounts of gas hydrate in the vicinity of the seismically-inferred BSR. In addition, IR thermal anomalies were also observed in several cores above the BSR (from ~110 to ~170 mbsf). A small amount of gas hydrate was also inferred in a pressure core from a depth of 163.1 mbsf. Gas hydrate was also inferred from the downhole wireline logging data (Figure 29); the high resistivities measured in the interval between 90 and 155 mbsf are clearly associated with gas hydrate occurrences. Archie analysis of the wireline resistivity log data from Site NGHP-01-16 indicates that gas hydrate could occupy as much as ~50 % of the pore space in some intervals between ~120 and 155 mbsf. Despite the low core recovery in most of this interval, some of the highest resistivity values coincide with low temperature anomalies measured in the recovered core, in particular between 126 and 133 mbsf and between 135 and 140 mbsf.

Site NGHP-01-20

Site NGHP-01-20 (Prospectus Site KGGH05) is located at the far southwestern end of the Krishna-Godavari Basin study area (Figure 1). The water depth is ~1,146 m. This site was added to test for the occurrence of gas hydrate in one of the more structurally-complex sites occupied during the expedition.

Site NGHP-01-20 is located on a small structural high ~75 m above the adjacent seafloor (Figure 31). Seismic lines crossing the site show a strong event at the drill site at an estimated depth of ~220 mbsf, which may represent a BSR. However, this event is not laterally extensive and is restricted to a few hundred meters around the drill site and may not be a BSR. However, the increase in reflection amplitude may be the effect of free gas trapped below the gas hydrate stability zone.

Two holes (NGHP-01-20A and NGHP-01-20B) were drilled and cored at this site (Figure 32); Hole NGHP-01-20A was cored to 148.8 mbsf and Hole NGHP-01-20B was drilled to 148.8 mbsf, then cored to 187.3 mbsf. Pressure coring and wireline logging were not attempted due to poor hole conditions experienced in both NGHP-01-20A and NGHP-01-20B. Site NGHP-01-20 was not part of the pre-coring LWD program.

Core recovery at Site NGHP-01-20 was extremely low; we also experienced poor hole conditions, and "packing-off" of the drill string during connections. As inferred from the porewater chemistry and sedimentological data collected at Hole NGHP-01-20A, core recovery was likely limited due to the presence of coarse lithologies or abundant gas hydrate. However, most of the sediments recovered at this

site were composed of a variety of nannofossil-bearing clay, volcanic glass-bearing clay, pyrite-bearing clay, and authigenic carbonate-bearing clay.

Several thin IR thermal anomalies and interstitial water Cl^- anomalies were observed in the cores (Figure 32) from Site NGHP-01-20, which probably indicate the presence of gas hydrate. The shallowest IR anomaly was recorded at ~43 mbsf and occurred within a nannofossil-rich clayey silt containing several coarser-grained silt and sand beds and laminae. A second IR anomaly, detected between 115 mbsf to 125 mbsf, occurred within a fine-grained clay section. The IR anomaly at this interval appears to be broader and more diffuse than the more discrete anomaly observed at ~43 mbsf and may reflect a more disseminated accumulation of gas hydrate in this finer-grained material.

In general, the Cl^- depth profile shows a steady decrease to the bottom of Hole NGHP-01-20A, probably caused by dissociation of small amounts of finely-dispersed gas hydrate. The absence of IR anomalies in the deeper portion of the holes drilled at this site may be a product of the sparse core recovery. Better constraints on the relationship between the lithologic, porewater chemistry, and IR thermal data are not easily resolved as no pressure cores or wireline logging data were collected at Site NGHP-01-20.

Site NGHP-01-21

Site NGHP-01-21 (Prospectus Site KGGH03-A; New FR1) was established to further delineate the gas hydrate occurrence identified at Site NGHP-01-10 (Figures 1 and 17) to obtain additional gas-hydrate-bearing pressure-core samples for post-NGHP Expedition 01 study. This site was located 20 m southeast of Hole NGHP-01-10A on a bearing of 136°. This site was also located within the seismically disturbed section as described around Site NGHP-01-10 (Riedel et al., 2010). The water depth at this site is ~1,049 m.

A total of three holes were drilled at Site NGHP-01-21. Hole NGHP-01-21A was partially drilled, XCB cored and pressure cored to a depth of 91.5 mbsf (Figure 19). Hole NGHP-01-21B included only two pressure core deployments and was drilled to a total depth of 200 mbsf for wireline logging (no useful well log data was collected). Hole NGHP-01-21C was dedicated to pressure-core gas hydrate sampling to a total depth of 78 mbsf. Evidence of gas hydrate was observed in four pressure cores from Hole NGHP-01-21A, one pressure core from Hole NGHP-01-21B, and four pressure cores from Hole NGHP-01-21C (Figure 19). Much like the pressure core observations from Site NGHP-01-10, X-ray images of pressure cores from Site NGHP-01-21 showed gas hydrate in thin, sediment-displacing structures (layers and veins); in massive lumps; and possibly as finely disseminated pore-filling particles. Post expedition, high-resolution CT X-ray scanning indicated that what was originally thought to be disseminated pore-filling gas hydrate was actually a network of fine veins, the bulk of which were invisible on the two-dimensional X-rays acquired on the ship.

3.2. Mahanadi Basin

Site NGHP-01-08

Site NGHP-01-08 (Prospectus Site MNGH01-1-A) is located in the central part of the Mahanadi Basin along the northeast coast of India (Figure 33). The water depth at this site is ~1,689 m. The site is located within the Reliance Industry Ltd. D10 exploration block. This site was not selected as a coring site after the LWD campaign was completed.

The seismic stratigraphy at this site is characterized by three distinct seismic facies (Figure 34). The top ~100 mbsf is characterized by low-amplitude, constant-frequency reflections which suggest a series of

thinly-bedded layers. Below this sequence, a layer approximately 25 m thick can be identified, which lacks internal seismic reflectivity. Below this sequence, the seismic data shows signs of minor deformation and unconformable contacts. The sequence extends to well below 350 mbsf (total depth (TD) of Hole NGHP-01-08A). Hole NGHP-01-08A was designed to target a distinct seismic reflection within the gas hydrate stability field at a depth of ~190 mbsf (Figure 34). A strong BSR occurs at a depth of ~257 mbsf. The section below the BSR occasionally shows increased amplitudes; this is likely due to the presence of gas.

Porosity and resistivity curves in Hole NGHP-01-08A (acquired by LWD) generally mirror each other, suggesting that little or no gas hydrate is present (Figure 35). Below a depth of ~220 mbsf, however, Archie-derived gas hydrate saturations suggest that as much as 10% of the pore space could be occupied by either gas hydrate above the BSR or by free gas below.

Site NGHP-01-09

Site NGHP-01-09 (Prospectus Site MNGH-01-2) is located in the Mahanadi Basin off the northeast coast of India (Figure 33). The site is located within the Reliance Industry Ltd. D10 exploration block. The water depth at this site is ~1,935 m. This site was not selected for coring and only LWD data were obtained from Hole NGHP-01-09A.

As imaged on the available seismic data, the sediments around this site are highly faulted, which contrasts with Site NGHP-01-08 (Figure 36). The faults extend from the base of the imaged section to near the seafloor. No clear BSR can be identified; however, at a depth of ~290 mbsf, unusually high seismic reflectivity is identified, which could mark the occurrence of free gas associated with gas hydrate above.

The LWD-acquired resistivity logs in Hole NGHP-01-09A (Figure 37) show a general negative correlation with the log-derived porosity curve, suggesting that little or no gas hydrate is present. Much like Site NGHP-01-08, however, below a depth ~190 mbsf in Hole NGHP-01-09A, the Archie-derived gas hydrate saturations suggest that as much as 10 percent of the pore space could be occupied by gas hydrate above the BSR or by free gas below.

Site NGHP-01-18

Site NGHP-01-18 (Prospectus Site MNGH-REL 5) is located in the central part of the Mahanadi Basin along the northeast coast of India (Figure 33). The water depth at this site is ~1,374 m. The site is located within the Reliance Industry Ltd. D10 exploration block.

The seismic data from this site are characterized by relatively uniform, almost seafloor-parallel reflectors with little seismic amplitude variation (Figure 38). The seismic events below ~210 mbsf show a sharp increase in reflectivity. This high reflectivity interval is only about 150 m thick and is limited laterally to less than 1 km in width. Below this high-reflectivity zone, the reflection amplitudes again appear relatively uniform. Although no strong, isolated BSR can be identified at this site, the top of the high-reflectivity zone is interpreted to represent the base of the gas hydrate stability zone (BGHSZ) with free gas accumulations below, causing the bright reflectivity. In general, the seismic data at this site shows complex structures and geometries suggestive of channelized deposition.

Site NGHP-01-18 was the first of two sites cored and drilled in the Mahanadi Basin after the LWD drilling program at Sites NGHP-01-08 and NGHP-01-09. Sites NGHP-01-18 and NGHP-10-19 were designed as linked sites with Site NGHP-01-18 to test the sedimentary section overlying the apparent channelized free-gas accumulation. Site NGHP-01-18 was not part of the pre-coring LWD program. At Site

NGHP-01-18, one hole (NGHP-01-18A) was drilled and cored to a depth of 190 mbsf (Figure 39); pressure coring and wireline logging were not attempted due to severe weather conditions. Also because of safety reasons, Hole NGHP-01-18A was stopped 20 m above the top of the seismically-inferred free-gas-bearing section at ~210 mbsf.

The sediments at Site NGHP-01-18 are composed of a variety of calcareous and siliceous biogenic-bearing clays and volcanic glass-bearing clays. Several small IR thermal anomalies were observed in the cores and may indicate that disseminated gas hydrate was present within clay sediments at 55 mbsf to 65 mbsf, at 115 mbsf, and at 180 mbsf (Figure 39). Porewater geochemistry data also showed subtle porewater freshening coincident with the IR anomalies at 115 mbsf and 180 mbsf. In addition, the Cl^- concentrations from ~100 mbsf to the bottom of the hole are slightly freshening with depth. The IR-measured core temperatures also show a minor but distinct shift to colder values below ~115 mbsf. These two observations may reflect the presence of minor quantities of disseminated gas hydrate throughout this depth interval. It appears that the sedimentary section directly overlying the apparent channelized free-gas accumulation at Site NGHP-01-18 contains gas hydrate at relatively low concentrations within a mostly clay-to-silt dominated section.

Site NGHP-01-19

Site NGHP-01-19 (Prospectus Site MNGH-Gap) is located in the central part of the Mahanadi Basin along the northeast coast of India (Figure 33Error! Reference source not found.). The water depth at this site is ~1,422 m. The site is located within the Reliance Industry Ltd. D10 exploration block.

Site NGHP-01-19 was the second of two sites cored and drilled in the Mahanadi Basin after the LWD drilling program at Sites NGHP-01-08 and NGHP-01-09. Site NGHP-01-19 was not part of the pre-coring LWD program. As noted above, Sites NGHP-01-18 and NGHP-10-19 were designed as linked sites (Figures 38 and 40), with Site NGHP-01-19 being drilled in a gap between two similar channelized free-gas accumulations in order to safely obtain core and downhole log data from both above and below the expected base of the gas hydrate stability zone in this region.

The BSR near Site NGHP-01-19, at a depth of 205 mbsf, marks the top of the high-amplitude, channelized (cut-and-fill) free-gas accumulations bounding this gap site (Figure 40). Inside the gap, however, the sediments are of similar reflection strength above and below the projected depth of the BSR.

Hole NGHP-01-19A was cored to a depth of 305 mbsf (with conventional and pressure cores) and Hole NGHP-01-19B was drilled (partially cored) and wireline logged to 280 mbsf (including a VSP survey) (Figures 41 and 42). The sediments at Hole NGHP-01-19A are dominated by clays (with varying amounts of volcanic glass, pyrite, authigenic carbonate and aragonite, plant debris, nannofossils, and foraminifera) that alternate with diminished amounts of oozes. The oozes are rarely pure and commonly contain clay, volcanic glass, and/or foraminifera.

At Site NGHP-01-19, a general decrease in core temperature was observed in the IR data from the cores above the depth of the BSR, from ~170 mbsf to ~205 mbsf and again within the interval from ~125 mbsf to ~130 mbsf (Figure 42). The observed IR response is generally indicative of low-concentrations diffuse gas hydrate. In addition, interstitial water samples taken from the intervals with IR anomalies also showed porewater freshening (Figure 42). Two pressure cores from 128.0 mbsf and 195.3 mbsf also yielded evidence of gas hydrate in the two IR and Cl^- inferred gas hydrate intervals described above (Figure 42).

Archie analysis of the wireline recorded resistivity data from Hole NGHP-01-19B indicates that gas hydrate could occupy ~15% of the pore space in the ~25-m-thick section immediately above the BSR (Figure 41). This coincides with the interval with the lowest measured IR temperatures. The apparent high saturation values (ranging from 5-15%) below the BSR could be associated with the presence of free gas, which is also suggested by low well log measured acoustic velocities between ~205 and ~225 mbsf.

3.3. Andaman Sea

Site NGHP-01-17

Site NGHP-01-17 (Prospectus Site ANGH01) is located in the Andaman Sea along the eastern coast of the Andaman Islands (Figure 43). The water depth at this site is at ~1,344 m. There has been no record of drilling/coring in this area, and the preliminary investigation of the seismic data showed a seismic reflection at a depth of ~608 mbsf that possess many of the features of a BSR (Figure 44). However, this would suggest a much deeper BGHSZ than observed elsewhere during the expedition. Log data subsequently confirmed that this event is very likely a gas-hydrate-associated BSR.

Site NGHP-01-17 was the only site established during this expedition offshore of the Andaman Islands. Hole NGHP-01-17A was cored to a total depth of 691.6 mbsf. An offset well (NGHP-01-17B) was subsequently drilled to 718 mbsf and wireline logged (including a VSP survey) (Figures 45 and 46). This site was not part of the pre-coring LWD program.

At Site NGHP-01-17, a remarkably uniform 691.6-m-thick sediment sequence of predominantly nannofossil ooze was deposited at an estimated sedimentation rate of ~5.6 cm/ky. The terrigenous sediment contribution is low at this site, indicating that both suspended material from the Irrawaddy River to the north and from the Andaman Islands to the west and northwest are not major sources of sediment at this location. The sediment sequence drilled at Site NGHP-01-17 also contains a remarkable record of the volcanic activity in Andaman region since the Miocene. The sequence contains 382 horizons of pyroclastic materials, including layers and patches of white, gray and black ash, white pumice fragments, and dispersed black ash and rare scoria of lapilli size.

Gas hydrate was inferred and detected from numerous core IR and porewater Cl^- anomalies at Site NGHP-01-17 (Figure 46). These anomalies were first observed at a depth of ~250 mbsf and are present sporadically from the ash beds and ash-rich zones to the depth of the BSR (608 mbsf). However, the gas hydrate occurred as only pore-filling material and was not physically observed in the cores on the catwalk. There is good correlation between the IR thermal anomalies and high wireline log measured P-wave velocities and resistivities within the gas-hydrate-bearing volcanic ashes at this site. These data help confirm that gas hydrate was present in these intervals. No ash beds or ash-rich zones were observed in the pressure cores recovered from this site (Figure 46). However, abundant methane was recovered in a pressure core from a depth of 586.3 mbsf (just above the depth of the predicted BSR). An additional pressure core from a depth of 672.3 mbsf, which is below the BSR, contained abundant methane and is interpreted to indicate the presence of free gas. Also of interest in the analysis of core gas samples from Site NGHP-01-17, an apparent reduction of the C_1/C_2 ratio below 565 mbsf signals the presence of thermogenic hydrocarbon gas input that has likely mixed with in-situ microbial methane.

Archie analysis of the wireline measured resistivity log data indicates that gas hydrate could occupy as much as ~20 % of the pore space in fine layers occurring in the entire section logged above the BSR (Figure 45). Most of the highest saturation values coincide with IR-inferred, gas-hydrate-bearing,

ash-rich units with peak saturation values exceeding 50%. High saturation values below the BSR could be associated with the presence of free gas as predicted by pressure coring (Figure 46).

As previously noted, the BSR at this site (~600 mbsf) is unusually deep. Downhole temperature measurements confirmed that the geothermal gradient at this site is very low, which accounts for the anomalously deep BSR and base of the assumed methane hydrate stability zone.

3.4. Kerala-Konkan Basin

Site NGHP-01-01

Site NGHP-01-01 (Prospectus Site KKGH01) is the only site drilled during NGHP Expedition 01 on the western continental margin of India in the Arabian Sea (Kerala-Konkan Basin) (Figure 47). The water depth at this site is ~2,663 m. Compared to the holes drilled on the eastern continental slope of India, Site NGHP-01-01 stands out as a carbonate-rich pelagic record characterized by low organic matter content, rather than by a typical hemipelagic continental margin lithology. Hole NGHP-01-01A was cored to 290 mbsf; wire-line logging was performed after coring (no LWD logging was conducted at this site).

The seismic data from Site NGHP-01-01 shows a widespread but low-amplitude event that was interpreted as a potential BSR (Figure 48); however, this event is the same polarity as the seafloor and fully concordant with the interval stratigraphy and therefore unlikely to be a BSR or otherwise indicative of gas hydrate.

No evidence of, or proxies for, gas hydrate was observed at this site (Figures 49 and 50). In fact, organic geochemical studies at Site NGHP-01-01 were unable to detect the presence of any hydrocarbon gases. Coring at Site NGHP-01-01 recovered a remarkably homogenous sequence of oozes. Formation densities measured in the borehole suggests that the BSR at 217 ± 5 mbsf might be the result of subtle changes in formation density that we ascribe to changes in clay content in otherwise carbonate-rich sediment.

4. NGHP-01 scientific reporting

NGHP-01 provided the data and information needed to characterize the lithostratigraphic controls on the occurrence of gas hydrate, physical properties of gas hydrate-bearing sediments, interstitial-water and gas geochemistry, and microbiology of the gas hydrate systems in the Krishna-Godavari Basin, the Mahanadi Basin, the Andaman Sea, and the Kerala-Konkan Basin. NGHP-01 also yielded important information on the well log and geophysical properties of hydrate-bearing sediments in each basin visited during the expedition.

Initial scientific results obtained from NGHP-01 and associated expedition data were first reported in the NGHP Expedition 01 Initial Reports (Collett et al., 2008a) and the NGHP Expedition 01 Downhole Log Data Report (Collett et al., 2008b). As discussed in the introduction to this report and listed in Tables 2A and 2B, the scientific results associated with NGHP-01 gas hydrate research efforts have been previously published in a growing list of scientific journal articles, conference proceedings, and in this special issue of the Journal of Marine and Petroleum Geology, which includes the most complete compilation of the scientific results from both the shipboard and post-expedition shore based research activities as reviewed in the following section of this report.

Tables 2A and 2B, provide the complete literature reference for all of the journal articles and conference proceedings that have reported on data and scientific results from NGHP-01. The entries in Tables 2A

and 2B also include short technical synopsis of each published report. For organizational purposes, each entry in Tables 2A and 2B has been grouped into the following topical categories:

1. *NGHP-01 project summaries*
2. *Lithostratigraphic controls on the occurrence of gas hydrate*
3. *Physical properties of gas hydrate-bearing sediments*
4. *Interstitial-water and gas geochemistry*
5. *Microbiologic systems*
6. *Well log analysis*
7. *Geophysical analysis*
8. *Basin and system analysis*
9. *Gas hydrate production and energy assessment*

5. Gas hydrate petroleum systems analysis

In recent years, significant progress has been made in addressing key issues on the formation, occurrence, and stability of gas hydrate in nature. The concept of a gas hydrate petroleum system, similar to the concept that guides conventional oil and gas exploration, has been developed to systematically assess the geologic controls on the occurrence of gas hydrate in nature (Collett et al., 2009). In a gas hydrate petroleum system, the individual factors that contribute to the formation of gas hydrate can be identified and assessed; the most important include (1) gas hydrate pressure-temperature stability conditions, (2) gas charge – the combination of gas source and migration, and (3) the nature of the host sediment or "reservoir". In the following discussion, the geologic controls on the stability and formation of gas hydrates are reviewed and assessed for the drill sites established during NGHP-01.

5.1. Gas hydrate stability

Gas hydrates exist under a limited range of temperature and pressure conditions such that the depth and thickness of the zone of potential gas hydrate stability can be calculated given information on temperature and pressure gradients with depth, and gas and formation water chemistry. Gas hydrate phase-boundary information (Figure 51) coupled with subsurface temperature conditions indicate that in oceanic sediment, gas hydrates can occur where the bottom-water temperature approaches 0°C and water depths exceed about 300 m. The vertical extent of the gas hydrate stability zone is determined mostly by the geothermal gradient.

To understand the geologic controls on the distribution of the gas (methane) hydrate stability zone (GHSZ) in the offshore of India, NGHP-01 featured 76 temperature tool deployments in an attempt to characterize the thermal regime of the sites occupied during the expedition (Table 1). The downhole temperature data collected during the expedition was used to calculate the depth to the base of the GHSZ at most of the sites that were continuously cored (Table 1). Most gas hydrate stability studies assume that the pore pressure gradient is hydrostatic (9.795 kPa/m). However, the seafloor temperature and geothermal gradient for any given site can be highly variable. Most gas hydrate studies also assume that methane is the only gas occupying the clathrate structure; however, it is well established that the addition of other hydrocarbon gases such as ethane or propane to the pure methane gas system shifts the phase

boundary to the right in Figure 51, thus deepening the zone of potential gas hydrate stability. Pore-water dissolved salt, however, such as NaCl lowers the temperature at which methane hydrate forms.

In the analysis of gas hydrate stability conditions in the offshore of India as reviewed in Collett et al., (2008a), the temperature data acquired during NGHP-01 was first used to estimate the geothermal gradient, a hydrostatic pore pressure gradient and a pure methane hydrate gas chemistry were assumed and a pore water salinity of 35 ppt were used to estimate the depth to the base of the GHSZ at 11 sites established during NGHP-01 (Table 1). For the most part, the calculated depth to the base of the GHSZ for each site falls near the estimated depth of the BSR (when present) as inferred from seismic data, which indicates that the assumption of hydrostatic pressure conditions and pure methane gas chemistry and a pore water chemistry similar to sea water is generally valid for the gas hydrate stability conditions in the offshore of India.

During the post-drilling phase of the NGHP-01 effort, additional studies of the acquired subsurface temperature data and information on seismic inferred BSR depths were used to refine the subsurface heat flow model for the Krishna–Godavari Basin (Shankar and Riedel, 2010; Shanker et al., 2010; Mandal et al., this volume). These studies generally indicate that the gas hydrate stability zone in the Krishna–Godavari Basin is impacted by local variations in heat flow associated with topographic focusing and defocusing effects and local faulting and fluid flux. But for the most part the predicted gas hydrate stability zone depths as derived from the NGHP-01 acquired subsurface temperature data closely matches the model derived gas hydrate stability conditions predicted from the seismic inferred BSR depths.

5.2. Gas charge – gas source and migration

The availability of large quantities of hydrocarbon gas from either microbial or thermogenic sources or both is an important factor controlling the formation and distribution of gas hydrates in nature. Stable carbon isotope analyses indicate that the methane in most oceanic methane hydrate is derived from microbial sources, which appears to be also true for most if not all of the methane hydrate occurrences discovered on NGHP-01 based on the analyses of gas molecular and isotopic compositions (Collett et al., 2008a).

The gas geochemistry preformed during drilling at Site NGHP-01-1 in the Kerala-Konkan Basin showed no evidence for hydrocarbons through the entire 290 m cored section. It was concluded that the BSR at this site had no relationship to the occurrence of free gas or gas hydrate, furthermore there was no direct evidence for an active petroleum system at this site.

The analyses of hydrocarbon gas concentrations and isotopic compositions of the gases collected from the NGHP-01 core sites in the Krishna-Godavari Basin revealed the presence of almost only microbial methane with additional incidental amounts of microbial ethane. However, the questions remain unanswered about how such prodigious quantities of microbial gas could have formed and been preserved in the basin especially when the volume of conventional microbial gas reserves are included in this consideration. Kundu et al., (2008) and other researchers have suggested that the formation of gas hydrates in the basin may have provided a mechanism to "retain" microbial gas within the shallow sedimentary section. In their model they proposed that with continued sedimentation and subsidence, hydrate accumulations that had formed in the GHSZ would have exited the base of the GHSZ, destabilized, and charged conventional traps and hydrate reservoirs in the overlying GHSZ; which over time would have led to the accumulation of a relatively large volume of microbial gas within the Krishna-Godavari Basin petroleum system.

Analyses of the hydrocarbon gas concentrations and isotopic composition at Sites NGHP-01-18 and NGHP-01-19 reveal that the principal hydrocarbon gas within the near-surface sedimentary section of the Mahanadi Basin is microbial methane with additional incidental amounts of microbial ethane. Traces of other hydrocarbon gases through pentane are present below 110 mbsf, however there is no indication that these gases represent any significant presence of a thermogenic sourced gas. Gas has been encountered by industry wells below about 2,000 mbsf that has been interpreted as a mixture of microbial and thermogenic gas. As with the Krishna-Godavari Basin, there is no clear explanation for the high abundance of microbially-sourced gas in the Mahanadi Basin.

The analyses of the hydrocarbon gas concentrations and isotopic composition at Site NGHP-01-17 along the convergent margin setting in the Andaman Sea revealed the presence of mostly microbial methane with additional incidental amounts of microbial ethane. Other hydrocarbon gases up through pentane are present below 590 mbsf. One analysis of propane carbon isotopic composition from 672 mbsf indicates a thermogenic origin. It appears that from a depth of 0 to 575 mbsf only microbially-sourced methane is present, but below this section there is evidence of minor amounts thermogenic gas, where a lower than expected methane/ethane ratio with respect to the geothermal gradient indicates that there are anomalous hydrocarbons and the potential for thermogenic gas at depth.

As established by Sloan and Koh (2008), highly concentrated gas hydrate accumulations contain a substantial volume of gas, which is potentially derived from microbial and/or thermogenic sources. Typically, not enough microbial methane is generated internally within the methane-hydrate stability zone alone to account for the gas content of most methane hydrate accumulations (Kvenvolden, 1993). In addition, most methane hydrate accumulations are in sediments that have not been deeply buried or subjected to temperatures high enough to form thermogenic gas. Thus, the gas within most hydrate accumulations is likely concentrated in the hydrate stability zone by a potential combination of processes — one of which, gas migration, would appear to be a critical component within most gas hydrate petroleum systems.

Geologic controls on fluid migration limit the availability of gas and water for the formation of gas hydrate and is an important factor that needs to be assessed when considering the controls on the occurrence of gas hydrate. Deeply-buried conventional microbial-derived gas accumulations discovered by industry exploration drilling along the east coast of India (Bastia, 2006) have raised many questions on the origin of microbial gas in marine sediments. At a regional scale, especially in the Krishna-Godavari Basin, the occurrence of methane hydrate appears to be closely associated with large scale structural features. For example, as discussed above in the site summaries, the fracture-controlled methane hydrate accumulation at Site NGHP-01-10 (Figure 1; Table 1) is found at the crest of a relatively large, tightly folded, ridge structure and the occurrence of gas hydrate appears to be controlled by gas flux through the local fault and fracture system generated by the regional stress.

The analysis of IR thermal images of conventional cores, X-ray scans of pressure cores, downhole LWD-derived resistivity images, and visual observations of cores upon recovery reveal the occurrence of gas hydrate in the offshore of India in a wide range of conditions. In general, most of the recovered gas hydrate was characterized as fracture-filling material in clay-dominated sediments and in some cases pore-filling grains or particles disseminated in coarser grained sediments. These observations further indicate the apparent need for effective migration conduits, such a fractures and stratigraphically-controlled carrier beds, to deliver and concentrate the gas required for the formation of the observed gas hydrate occurrences.

5.3. Reservoir – host sediment

The study of gas hydrate samples indicates that the physical nature of in-situ gas hydrates is highly variable (reviewed by Sloan and Koh, 2008). Gas hydrates are observed (1) occupying pores of coarse or fine-grained sediment; (2) grain-displacing nodules disseminated within fine-grained sediment; (3), filling fractures, most commonly within fine-grained sediments; or (4) a massive unit near the sea-floor composed mainly of solid gas hydrate with minor amounts of sediment. Most gas hydrate field expeditions, however, have shown that the occurrence of concentrated gas hydrate is mostly controlled by the presence of fractures and/or coarser grained sediments in which gas hydrate fills fractures or is disseminated in the pores of sand-rich reservoirs (Collett, 1993; Dallimore and Collett, 2005; Riedel et al., 2006; Collett et al., 2008a, 2008b; Fujii et al., 2009; Park et al., 2008; Yang et al., 2008; Lee et al., 2011; Yamamoto et al., 2012a, 2012b). Torres et al., (2008) concluded that hydrate grows preferentially in coarse-grained sediments because lower capillary pressures in these sediments that permit the migration of gas and nucleation of hydrate. The growth of gas hydrate in clay-rich sediments, however, is less understood. But Torres et al., (2008) further concluded that in smaller pores, capillary forces will preclude the exsolution of methane from pore fluids, thus limiting the amount of gas available for the formation of gas hydrate. Cook and Goldberg (2008) also proposed that in cases where the concentration of gas in water exceeds solubility within clay-rich sedimentary sections, hydrate forms in pore-segregated fracture planes that propagate in the direction of the maximum principal stress ― in most cases, near vertical fractures. This proposed model appears to account for the occurrences of apparent "strata-bound" fracture-filling gas hydrate occurrences as observed in the Gulf of Mexico (Cook et al., 2012) and in the Krishna-Godavari Basin (Cook and Goldberg, 2008; Cook et al., this volume).

To further understand the formation of gas hydrate in sediments, Jain and Juanes (2009) presented a physical model that couples multiphase fluid flow with sediment mechanics to permit the investigation of the upward migration of gas through a water-filled sediment column. Jain and Juanes (2009) report that grain size is the main factor controlling the mode of gas transport in the sediment, and they show that coarse-grain sediments favor capillary invasion, while fracturing dominates in fine-grain media. Their results predict that in fine-grained sediments, hydrate will likely form in veins following a fracture network pattern, and the hydrate concentration will likely be quite low. In coarse sediments, the buoyant methane gas likely invades the pore space more uniformly, in a process akin to invasion percolation, and the overall pore occupancy is likely to be much higher than in a fracture-dominated regime. These results are consistent with laboratory experiments and field observations of gas hydrate in the offshore of India.

For the most part, the integrated analyses of downhole logging data and linked IR core thermal imaging, interstitial water analyses, and pressure core X-ray imaging from the sites drilled during NGHP-01 indicate that the occurrence of concentrated gas hydrate is mostly controlled by the presence of fractures and/or coarser grained (mostly silt- and limited sand-rich and ash-rich beds) sediments.

As reviewed in Table 1, the gas hydrate at most of the sites occupied during NGHP-01 appear to range from mostly fracture-filling to pore-filling within relatively fine-grained sedimentary units of variable thickness. Only one site in the Krishna-Godavari Basin exhibited pore-filling gas hydrate within discrete coarser grained sedimentary units at high gas hydrate saturations (Site NGHP-01-15). High concentrations of gas hydrate was also found in porous ash beds at the site cored and logged in the Andaman Sea (Site NGHP-01-17). The majority of marine gas hydrate systems that have been studied to date are fine-grained, clay-dominated, and are often associated with surficial gas seeps. The discovery of the 130-m-thick fracture-controlled gas hydrate accumulation at Site NGHP-01-10 in the Krishna-Godavari Basin appears to be within a fractured clay-dominated system in which gas hydrate is

concentrated in vertical and sub-vertical gas conduits that at one time were connected to a seafloor seep. Further analysis of the downhole-acquired borehole RAB resistivity images from other sites (including Sites NGHP-01-2, -3, -4, -5, -6, -7, and -11) indicate that many of the individual, apparently stratigraphically-controlled disseminated gas hydrate deposits, are likely fracture-filling type gas hydrate occurrences in which vertical to sub-vertical fractures provide the void space required for gas hydrate nucleation. Recent field studies, including NGHP-01, have shown that localized, deeply buried, fracture dominated gas hydrate deposits are likely more common than previously considered (Riedel et al., 2006; Collett et al., 2008a, 2008b; Park et al., 2008; Cook et al., 2012).

5.4. Summary note

In terms of gas hydrate as a potential energy resource, the concept of a gas hydrate petroleum system has been shown to be a useful tool to systematically assess the geologic controls on the occurrence of gas hydrates. In this study, the petroleum system concept has been used to assess geologic variables, such as "reservoir conditions" and "gas charge" (as related to gas source and migration), to better understand how they impact the occurrence and physical nature of gas hydrate at various scales in the offshore of India. For the sites drilled in the Krishna-Godavari Basin, the Mahanadi Basin and in the Andaman Sea area, the availability of gas does not appear to be a significant limiting factor with most of available reservoir systems in all of these settings containing significant volumes of either gas hydrate above the base of the GHSZ or free-gas below the GHSZ. At Site NGHP-01-1 in the Kerala-Konkan Basin, however, the supply of gas to the GHSZ appears to be limiting factor for the occurrence of gas hydrate.

The study of gas hydrate-bearing cores and downhole well log data acquired during NGHP-01 has documented the highly-variable physical nature of in-situ gas hydrate occurrences in the offshore of India. The observation that the occurrence of gas hydrate in fine-grained sediment is mostly controlled by the presence of excess gas that generates fractures that are subsequently filled with gas hydrate is an important advancement in our understanding of gas hydrate formation in nature. However, the formation of highly concentrated gas hydrate accumulations, more suitable for energy extraction, appears to require the presence of relatively coarse-grained sediments with porosity needed to support the migration and accumulation of gas, and the nucleation of gas hydrate. The interdependence of gas hydrate stability conditions, gas charge, and the presence of suitable reservoirs on the occurrence of gas hydrates in the offshore of India has been well documented with the lithostratigraphic, physical property, geochemical, microbiological, and downhole log data collected during NGHP-01.

6. Conclusion

The Indian National Gas Hydrate Program Expedition 01 (NGHP-01) was designed to study the gas hydrate occurrences off the Indian Peninsula and along the Andaman convergent margin with special emphasis on understanding the geologic and geochemical controls on the occurrence of gas hydrate. Drilling of both a passive and convergent continental margin on the same expedition also allowed for the comparison of the geologic factors believed to control the occurrence of gas hydrate in these two distinct geologic settings.

NGHP-01 discovered gas hydrate in numerous complex geologic settings. As we consider the nature of the geologic and geochemical controls on the occurrence of gas hydrate in the offshore of India (i.e., the gas hydrate petroleum system, which includes hydrate stability conditions, gas charge, and reservoir conditions), it is important to first note that the calculated depth to the base of the methane hydrate stability zone, as derived from downhole temperature measurements obtained during NGHP-01, closely

matches the depth of the seismically-identified bottom simulating reflectors (BSRs) at most of the sites established during the expedition.

When considering the macroscopic and microscopic reservoir controls on the occurrence of gas hydrate in the offshore of India, the analysis of NGHP-01 acquired IR images of cores, X-ray images of pressure cores, downhole well log data, and visual observations of cores upon recovery reveal the occurrence of gas hydrate in a wide range of conditions; with the recovered gas hydrate characterized as either fracture-filling or pore-filling material. At a regional scale, especially in the Krishna-Godavari Basin, the occurrence of gas hydrate appears to be closely associated with large scale structural features that serve to focus gas migration.

For most of areas examined during NGHP-01, the gas included within the recovered gas hydrate samples appears to have been almost all methane, which appears to have been sourced by mostly microbial degradation of organic material. In several cases, however, there appears to be close spatial association of some gas hydrates with the deeper conventional microbial gas accumulations. For example, the fracture controlled gas hydrate accumulation in the Krishna-Godavari Basin at Site NGHP-01-10 is found at the crest of a relatively tightly folded ridge structure and the occurrence of gas hydrate appears to be controlled by gas flux through the local fracture system generated by the regional stress regime.

Our understanding of how gas hydrates occur and behave in nature is still growing and evolving—we do not yet know if gas hydrates can be economically produced. Certainly, international cooperative projects, such as NGHP-01, have contributed greatly to our understanding of hydrates in nature and will continue to be a critical source of the information to advance our understanding of gas hydrates.

Acknowledgement

The editors wish to thank those that contributed to the success of the National Gas Hydrate Program Expedition 01 (NGHP-01). NGHP-01 was planned and managed through collaboration between the Directorate General of Hydrocarbons (DGH) under the Ministry of Petroleum and Natural Gas (India), the U.S. Geological Survey (USGS), and the Consortium for Scientific Methane Hydrate Investigations (CSMHI) led by Overseas Drilling Limited (ODL) and FUGRO McClelland Marine Geosciences (FUGRO). The platform for the drilling operation was the research *D/V JOIDES Resolution*, operated by ODL. Much of the drilling/coring equipment used was provided by the Integrated Ocean Drilling Program (IODP) through a loan agreement with the US National Science Foundation. Wireline pressure coring systems and supporting laboratories were provided by IODP/Texas A&M University (TAMU), FUGRO, USGS, U.S. Department of Energy (USDOE) and HYACINTH/GeoTek. Downhole logging operational and technical support was provided by Lamont-Doherty Earth Observatory (LDEO) of Columbia University. The financial support for the NGHP-01, from the Oil Industry Development Board, Oil and Natural Gas Corporation Ltd., GAIL (India) Ltd. and Oil India Ltd. is gratefully acknowledged. We also acknowledge the support extended by all the participating organizations of the NGHP: MoP&NG, DGH, ONGC, GAIL, OIL, NIO, NIOT, and RIL. The authors and editors are thankful to the Management of the National Gas Hydrate Program, DGH and ONGC for permission to publish this report in the Journal of Marine and Petroleum Geology.

This contribution was funded in part by the U.S. Geological Survey Energy Resources Program and the U.S. Department of Energy under Interagency Agreement No. DE-AI21-92MC29214. Any use of trade, product, or firm names is for descriptive purposes only and does not imply endorsement by the U.S. Government.

References

Alam, M., Alam, M.M., Curray, J.R., Chowdhury, M., and Gani, M., 2003, An overview of the sedimentary history of the Bengal Basin in relation to the regional tectonic framework and basin fill history: Sedimentary Geology, v. 155, p. 179-208.

Bastia, R., 2006, An overview of Indian sedimentary basins with special focus on emerging east coast deepwater frontiers: The Leading Edge, v. 25, p. 818-829.

Biksham, G., and Subrahmanyam, V., 1988, Sediment transport of the Godavari River Basin and its controlling factors: Journal of Hydrology, v. 101, p. 275-290.

Clift, P.D., Shimizu, N., Layne, G.D., Blusztajn, J.S., Gaedicke, C., Schluter, H.-U., Clark, M.K., and Amjad, S., 2001, Development of the Indus Fan and its significance for the erosional history of the western Himalaya and Karakoram: Geological Society of America Bulletin, v. 113, p. 1039-1051.

Colin, C., Kissel, C., Blamart, D., and Turpin, L., 1998, Magnetic properties of sediments in the Bay of Bengal and the Andaman Sea—Impact of rapid North Atlantic Ocean climatic events on the strength of the Indian monsoon: Earth and Planetary Science Letters, v. 155, p. 623-635.

Collett, T.S., 1993, Natural gas hydrates of the Prudhoe Bay and Kuparuk River area, North Slope, Alaska: American Association of Petroleum Geologists Bulletin, v. 77, no. 5, p. 793-812.

Collett, T.S., Johnson, A., Knapp, C., Boswell, R., 2009, Natural Gas Hydrates – A Review, in Collett, T., Johnson, A., Knapp, C., Boswell, R., eds., Natural Gas Hydrates -- Energy Resource Potential and Associated Geologic Hazards: American Association of Petroleum Geologists Memoir 89, 68 p.

Collett, T.S., and Lee, M.W., 2012, Well log characterization of natural gas hydrates: Petrophysics, v. 53, no. 5 (October 2012), p. 348-367.

Collett, T.S., Boswell, R., Cochran, J.R., Kumar, P., Lall, M., Mazumdar, A., Ramana, M.V., Ramprasad, T., Riedel, M., Sain, K., Sathe, A.V., Vishwanath, K., and the NGHP Expedition 01 Scientific Party, (this issue), Geologic implications of gas hydrates in the offshore of India: Results of the National Gas Hydrate Program Expedition 01: Journal of Marine and Petroleum Geology.

Collett, T., Riedel, M., Cochran, J., Boswell, R., Presley, J., Kumar, P., Sathe, A., Sethi, A., Lall, M., Siball, V., and the NGHP Expedition 01 Scientific Party, 2008a, Indian National Gas Hydrate Program Expedition 01 Initial Reports: Prepared by the U.S. Geological Survey and Published by the Directorate General of Hydrocarbons, Ministry of Petroleum & Natural Gas (India), 1 DVD.

Collett, T., Riedel, M., Cochran, J., Boswell, R., Presley, J., Kumar, P., Sathe, A., Sethi, A., Lall, M., Siball, V., Guerin, G., Malinerno, A., Mrozewski, S., Cook, A., Sarker, G., Broglia, C., Goldberg, D., and the NGHP Expedition 01 Scientific Party, 2008b, Indian National Gas Hydrate Program Expedition 01 Downhole Log Data Report: Prepared by the U.S. Geological Survey and Published by the Directorate General of Hydrocarbons, Ministry of Petroleum & Natural Gas (India), 2 DVD set.

Cook, A.E., Anderson, B., Rasmus, J., Sun, K., Li, Q., Collett, T., Goldberg, D., 2012, Electrical anisotropy of gas hydrate-bearing sand reservoirs in the Gulf of Mexico: Journal of Marine and Petroleum Geology, v. 34, p. 72–84.

Cook, A.E., and Goldberg, D., 2008, Extent of gas hydrate filled fracture planes: Implications for in situ methanogenesis and resource potential: Geophysical Research Letters, v. 35, L15302.

Cook, A.E., Goldberg, D.S., and Malinverno, A., (this issue), Natural gas hydrates occupying fractures: a focus on non-vent sites on the Indian continental margin and the northern Gulf of Mexico: Journal of Marine and Petroleum Geology.

Curray, J.R., 1991, Possible greenschist metamorphism at the base of a 22-km sedimentary section, Bay of Bengal: Geology, v. 19, p. 1097–1100.

Curray, J.R., Emmel, F.J., Moore, D.G., and Raitt, R.W., 1982, Structure, Tectonics and Geological History of the Northeastern Indian Ocean, in Nairn, A.E.M., and Stehli, F.G., eds., The Ocean Basins and Margins, New York, Plenum Press, 1982, 6, p. 399–450.

Dallimore, S.R., and Collett, T.S., eds., 2005, Scientific results from the Mallik 2002 gas hydrate production research well program, Mackenzie Delta, Northwest Territories, Canada: Geological Survey of Canada Bulletin 585, two CD-ROM set.

Duncan, R.A., 1990, The volcanic record of the Reunion hotspot, Proceedings of the Ocean Drilling Program—Scientific Results, v. 115, p. 3–10.

Duncan, R.A., and Pyle, D.G., 1988, Rapid eruption of the Deccan flood basalts at the Cretaceaous/Tertiary boundary: Nature, v. 333, p. 841–843.

Dyment, J., 1991, Structure et évolution de la lithosphere océanique dans l'océan Indien—Apport des anomalies magnétiques: Strasbourg, France, Universite Louis Pasteur de Strasbourg, Ph.D. thesis, 374 p.

Federov, L.V., Ravich, M.G., and Hofmann, J., 1982, Geologic comparison of southeastern peninsular India and Sri Lanka with a part of Antarctica, in Antarctic Geology and Geophysics, Craddock, C., ed.: Madison, Wisc. University of Wisconsin Press, p. 157–171.

Fujii, T., Namikawa, T., Okui, T., Kawasaki, M., Ochiai, K., Nakamizu, M., Nishimura, M., Takano, O., and Tsuji, Y., 2009, Methane hydrate occurrence and saturation confirmed from core samples, eastern Nankai Trough, Japan, in Collett, T., Johnson, A., Knapp, C., Boswell, R., eds., Natural Gas Hydrates -- Energy Resource Potential and Associated Geologic Hazards: American Association of Petroleum Geologists Memoir 89, p. 385-400.

Jain, A.K., and Juanes, R., 2009, Preferential Mode of gas invasion in sediments: Grain-scale mechanistic model of coupled multiphase fluid flow and sediment mechanics: Journal of Geophysical Research, v. 114, B08101, 19 p.

Kumar, P., Collett, T.S., Boswell, R., Cochran, J.R., Lall, M., Mazumdar, A., Ramana, M.V., Ramprasad, T., Riedel, M., Sain, K., Sathe, A.V., Vishwanath, K., and the NGHP Expedition 01 Scientific Party, (this

issue), Geologic implications of gas hydrates in the offshore of India: Krishna-Godavari Basin, Mahanadi Basin, Andaman Sea, Kerala-Konkan Basin: Journal of Marine and Petroleum Geology.

Kundu, N., Pal, N., Sinha, N., and Budhiraja, I., 2008, Palo hydrate and its role in deep water Plio-Pleistocene gas reservoir in Krishna-Godavari Basin, India: Proceedings of the 6th International Conference on Gas Hydrates (ICGH 2008), July 6-10, 2008, Vancouver, British Columbia, Canada, 8 p.

Kvenvolden, K.A., 1988, Methane hydrate—A major reservoir of carbon in the shallow geosphere? Chemical Geology, v. 71, p. 41-51.

Kvenvolden, 1993, A primer in gas hydrates, in Howell, D.G., ed., The Future of Energy Gases: U.S. Geological Survey Professional Paper 1570, p. 279-292.

Lee, Sung-Rock, Ryu, Byong-Jae, Bahk, Jang-Jun, Yoo, Dong-G., Lee, Joo-Y., Yi, Jun-Seog, Collett, T.S., Riedel, M., Torres, M.E., and UBGH2 Science Party, 2011, Recent developments of gas hydrate program in the Ulleung Basin gas hydrate drilling expedition 2: Proceedings of the 7th International Conference on Gas Hydrates (ICGH 2011), July 17-21, 2011, Edinburg, Scotland, 7 p.

Mandal, R., Dewangan, P., Ramprasad, T., Kumar, B.J.P, and Vishwanath, K., (this issue), Effect of thermal non-equilibrium, seafloor topography and fluid advection on BSR-derived geothermal gradient: Journal of Marine and Petroleum Geology.

Park, Keun-Pil, Bahk, Jang-Jun, Kwon, Youngin, Kim, Gil-Young, Riedel, M., Holland, M., Schultheiss, P., Rose, K., and the UBGH-1 Scientific Party, 2008, Korean National Program Expedition confirm rich gas hydrate deposits in the Ulleung Basin, East Sea, in DOE-NETL Fire In the Ice Methane Hydrate Newsletter, Spring, 2008, p. 6-9. http://www.netl.doe.gov/technologies/oil-gas/publications/Hydrates/Newsletter/HMNewsSpring08.pdf#page=6

Powell, C.M., Roots, S.R., and Veevers, J.J., 1988, Pre-breakup continental extension in East Gondwanaland and the early opening of the eastern Indian Ocean: Tectonophysics, v. 155, p. 261-183.

Raju, K.A., Ramprasad, T., Rao, P.S., Rao, R.R., and Varghese, J., 2004, New insights into the tectonic evolution of the Andaman basin, northeast Indian Ocean: Earth and Planetary Science Letters, 221, p. 145-163.

Ramana, M.V., Ramprasad, T., Desa, M., Sathe, A.V., and Sethi, A.K., 2006, Gas hydrate-related proxies inferred from multidisciplinary investigations in the Indian offshore areas: Current Science, v. 91, p. 183-189.

Ramana, M.V., Ramprasad, T, Paropkari, A.L., Borole, D.V., Rao, B.R., Karisiddaiah, S.M., Desam M., Kocherla, M., Joao, H.M., Lokabharati, P., Gonsalves, M.J., Pattan, J.N., Khadge, N.H., Babu, C.P., A.V., Kumar, P., and Sethi, A.K., 2009, Multidisciplinary investigations exploring indicators of gas hydrate occurrence in the Krishna–Godavari Basin offshore, east coast of India: Geo-Marine Letters, v. 29, p. 25-38.

Ramaswamy, V., Nair, R.R., Manganini, S., Haake, B., and Ittekkot, V., 1991, Lithonic fluxes to the deep Arabian Sea measured by sediment traps: Deep Sea Research, v. 38, p. 169-184.

Rao, Y.H., 2001, Gas hydrate investigations along the continental margins of India: Ph.D. Dissertation, Osmania University, Hyderabad, India, 234 p.

Riedel, M., Collett, T.S., Malone, M.J., and the Expedition 311 Scientists, 2006, Cascadia Margin Gas Hydrates, Expedition 311, Sites U1325 - U1329, 28 August - 28 October, 2005: Integrated Ocean Drilling Program Management International, Inc., for the Integrated Ocean Drilling Program, v. 311. 247 p. http://iodp.tamu.edu/ publications/exp311/311title.htm

Riedel, M., Collett, T.S., Kumar, P., Sathe, A.V., and Cook, A., 2010, Seismic imaging of a fractured gas hydrate system in the Krishna-Godavari Basin offshore India: Journal of Marine and Petroleum Geology, v. 27, p. 1,476-1,493.

Sastri, V.V., Venkatachala, B.S., and Narayanan, V., 1981, The evolution of the east coast of India: Paleogeography, Paleoclimatology, Paleoecology, v. 36, p. 23-54.

Scotese, C.R., Gahagan, L.M., and Larson, R.L., 1988, Plate tectonic reconstruction of the Cretaceous and Cenozoic ocean basins: Tectonophysics, v. 155, p. 27-48.

Shankar, U., and Riedel, M., 2010, Seismic and heat flow constraints from the gas hydrate system in the Krishna–Godavari Basin, India: Marine Geology, v. 276, P. 1-13.

Shankar, U., Riedel, M., and Sathe, A.V., 2010, Geothermal modeling of the gas hydrate stability zone along the Krishna Godavari Basin: Marine Geophysics Research, v. 31, p. 17-28.

Sloan, E.D., and Koh, C.A., 2008, Clathrate hydrates of natural gases, Third Edition: CRC Press, Taylor and Francis Group, Publishers, New York, New York, 721 p.

Subrahmanyam, V., Rao, D.G., Ramprasad, T., Kamesh Raju, K.A., and Gangadhura Rao, M., 1991, Gravity anomalies and crustal structure of the western continental margin off Goa and Mulki, India: Marine Geology, v. 99, p. 247-256.

Torres, M.E., Tréhu, A.M., Cespedes, N., Kastner, M., Wortmann, U.G., Kim, J.H., Long, P., Malinverno, A., Pohlman, J.W., Riedel, M., and Collett, T.S., 2008, Methane hydrate formation in turbidite sediments of northern Cascadia, IODP Expedition 311: Earth and Planetary Science Letters, v. 271, p. 170-180.

Yang, S., Zhang, H., Wu, N., Su, X., Schultheiss, P., Holland, M., Zhang, G., Liang, J., Lu, J., and Rose, K., 2008, High concentration hydrate in disseminated forms obtained in Shenhu area, North Slope of South China Sea: Proceedings of the 6th International Conference on Gas Hydrates (ICGH 2008), July 6-10, 2008, Vancouver, British Columbia, Canada, 10 p.

Yamamoto, Koji, Fujii, Tetsuya, Satoshi, Noguchi, and Nagao, Jiro, 2012a, The scientific objectives and program of the Japanese offshore methane hydrate production test: Proceedings of the American Geophysical Union Fall Meeting, December 3-7, 2012, San Francisco, California, 1 p.

Yamamoto, Koji, Inada, Norihito, Kubo, Satoshi, Fujii, Tetsuya, Suzuki, Kiyofumi, Konno, Yoshihiro, and Shipboard Scientists for the Methane Hydrate Offshore Production Test, 2012b, Pressure core sampling in the Eastern Nankai Trough, in DOE-NETL Fire In the Ice Methane Hydrate Newsletter, v. 12, issue 2, Summer, 2012, p. 1-6.

Figure and Table Captions

Figure 1. (A) National Gas Hydrate Program Expedition 01 (NGHP-01) drill site map depicting the location of the drill sites established during the expedition in the Krishna-Godavari Basin. (B) Insert bathymetric map depicting the location of the research drill sites established in the Krishna-Godavari Basin.

Figure 2. National Gas Hydrate Program Expedition 01 (NGHP-01) Site NGHP-01-02. (A) Section of 2D seismic line AD-94-13 around Site NGHP-01-02 (Prospectus Site KGGH03-A) showing overall structure of the setting and regional BSR occurrence. (B) Enlarged portion of seismic line AD-94-13 around Site NGHP-01-02 showing predicted formation tops and BSR depth (170 mbsf) based on a uniform seismic velocity of 1580 m/s. (C) Map showing location of seismic line AD-94-13 and Sites NGHP-01-02A and NGHP-01-02B. BSR = bottom simulating reflector

Figure 3. Summary of logging-while-drilling (LWD) data from Holes NGHP-01-02A and NGHP-01-02B (modified from Collett et al., 2008a). Including gas hydrate saturations (S_h) from Archie's equation and LWD porosity and resistivity logs in Hole NGHP-01-02B (Note that Archie analyses are known to overestimate gas hydrate saturations in fracture dominated reservoirs; Collett and Lee, 2012). LWD resistivity-at-bit (RAB) image data from Hole NGHP-01-02B. The red data quality flag indicates degraded data quality. gAPI = American Petroleum Institute gamma ray units, IDRO = Image-derived density (EcoScope), RHOB = Bulk density (EcoScope), neutron = Thermal neutron porosity (EcoScope), corrected porosity = density porosity with core derived grain densities (EcoScope), RING = Ring resistivity (GeoVISION), BIT = Bit resistivity (GeoVISION), Deep Button avg. = Button deep resistivity (GeoVISION), A40L = Attenuation resistivity measured at 400 kHz and a transmitter-receiver spacing of 40 in (EcoScope) and P16H = Phase-shift resistivity at 2 MHZ and a transmitter-receiver spacing of 16 in (EcoScope). BSR = bottom simulating reflector

Figure 4. National Gas Hydrate Program Expedition 01 (NGHP-01) Site NGHP-01-03. (A) Section of 2D seismic line AD-94-17 in the vicinity of Site NGHP-01-03 (Prospectus Site GDGH05-A) showing predicted formation tops and BSR depth (209 mbsf) based on a uniform seismic velocity of 1580 m/s. (B) Section of seismic line AD-94-16 around Site NGHP-01-03 (Prospectus Site GDGH05-A) showing predicted formation tops and BSR depth (209 mbsf) based on a uniform seismic velocity of 1580 m/s. (C) Map showing all holes occupied at Site NGHP-01-03 (GDGH05-A) and location of seismic lines AD-94-17 and AD-94-16. BSR = bottom simulating reflector

Figure 5. Summary of logging-while-drilling (LWD) data from Hole NGHP-01-03A (modified from Collett et al., 2008a). Including gas hydrate saturations (S_h) from Archie's equation, LWD porosity and resistivity-at-bit (RAB) image data from Hole NGHP-01-03A, and core derived porosity data (Note that Archie analyses are known to overestimate gas hydrate saturations in fracture dominated reservoirs; Collett and Lee, 2012). The red data quality flag indicates degraded data quality. gAPI = American Petroleum Institute gamma ray units, IDRO = Image-derived density (EcoScope), RHOB = Bulk density (EcoScope), neutron porosity = Thermal neutron porosity (EcoScope), corrected density porosity = density porosity with core derived grain densities (EcoScope), RING = Ring resistivity (GeoVISION), BIT = Bit resistivity (GeoVISION), Deep Button avg. = Button deep resistivity (GeoVISION), A40L = Attenuation resistivity measured at 400 kHz and a transmitter-receiver spacing of 40 in (EcoScope) and P16H = Phase-shift resistivity at 2 MHZ and a transmitter-receiver spacing of 16 in (EcoScope). BSR = bottom simulating reflector

Figure 6. Summary of core data from Site NGHP-01-03 (modified from Collett et al., 2008a). Methane phase diagram for Site NGHP-01-03, with total methane concentration measured from successful pressure

cores at Site NGHP-01-03. Concentration-depth profile of interstitial pore-water chlorinity in Hole NGHP-01-03B. Catwalk infrared core scan for Hole NGHP-01-03B. BSR = bottom simulating reflector

Figure 7. National Gas Hydrate Program Expedition 01 (NGHP-01) Site NGHP-01-04. (A) Section of 2D seismic line AD-94-25 around Site NGHP-01-04 (Prospectus Site KGGH01) showing a broad basin and an extensive BSR occurrence. (B) Section of seismic line AD-94-25 around Site NGHP-01-04 (Prospectus Site KGGH01) showing predicted formation tops and BSR depth (~182 mbsf) based on a uniform seismic velocity of 1580 m/s. (C) Map showing the hole occupied at Site NGHP-01-04 (KGGH01-A) and location of seismic line AD-94-25. BSR = bottom simulating reflector

Figure 8. Summary of logging-while-drilling (LWD) data from Hole NGHP-01-04A (modified from Collett et al., 2008a). Including gas hydrate saturations (S_h) from Archie's equation, LWD porosity and resistivity-at-bit (RAB) image data from Hole NGHP-01-04A (Note that Archie analyses are known to overestimate gas hydrate saturations in fracture dominated reservoirs; Collett and Lee, 2012). The red data quality flag indicates degraded data quality. gAPI = American Petroleum Institute gamma ray units, IDRO = Image-derived density (EcoScope), RHOB = Bulk density (EcoScope), neutron porosity = Thermal neutron porosity (EcoScope), corrected density porosity = density porosity with core derived grain densities (EcoScope), RING = Ring resistivity (GeoVISION), BIT = Bit resistivity (GeoVISION), Deep Button avg. = Button deep resistivity (GeoVISION), A40L = Attenuation resistivity measured at 400 kHz and a transmitter-receiver spacing of 40 in (EcoScope) and P16H = Phase-shift resistivity at 2 MHZ and a transmitter-receiver spacing of 16 in (EcoScope). BSR = bottom simulating reflector

Figure 9. National Gas Hydrate Program Expedition 01 (NGHP-01) Site NGHP-01-05. (A) Seismic line AD-94-33 (oriented NW-SE) intersecting with Site NGHP-01-05 (Prospectus Site KGGH02-A). (B) Section of seismic line AD-94-33 around Site NGHP-01-05 (Prospectus Site KGGH02-A) showing estimated depth of formation depth and BSR using a uniform velocity of 1580 m/s for the entire sediment column. (C) Map showing the holes occupied at Site NGHP-01-05 (KGGH02-A) and location of seismic line AD-94-33. BSR = bottom simulating reflector

Figure 10. Summary of logging-while-drilling (LWD) data from Hole NGHP-01-05B (modified from Collett et al., 2008a). Including gas hydrate saturations (S_h) from Archie's equation, LWD porosity and resistivity-at-bit (RAB) image data from Hole NGHP-01-05B, and core derived porosity data (Note that Archie analyses are known to overestimate gas hydrate saturations in fracture dominated reservoirs; Collett and Lee, 2012). The red data quality flag indicates degraded data quality. gAPI = American Petroleum Institute gamma ray units, IDRO = Image-derived density (EcoScope), RHOB = Bulk density (EcoScope), neutron porosity = Thermal neutron porosity (EcoScope), corrected density porosity = density porosity with core derived grain densities (EcoScope), RING = Ring resistivity (GeoVISION), BIT = Bit resistivity (GeoVISION), Deep Button avg. = Button deep resistivity (GeoVISION), A40L = Attenuation resistivity measured at 400 kHz and a transmitter-receiver spacing of 40 in (EcoScope) and P16H = Phase-shift resistivity at 2 MHZ and a transmitter-receiver spacing of 16 in (EcoScope). BSR = bottom simulating reflector

Figure 11. Summary of core data from Site NGHP-01-05 (modified from Collett et al., 2008a). Methane phase diagram for Site NGHP-01-05, with total methane concentration measured from successful pressure cores at Site NGHP-01-05. Concentration-depth profile of interstitial pore-water chlorinity in Hole NGHP-01-05C. Catwalk infrared core scan for Hole NGHP-01-05C. BSR = bottom simulating reflector

Figure 12. National Gas Hydrate Program Expedition 01 (NGHP-01) Site NGHP-01-06. (A) Section of 2D seismic line AD-94-39 around Site NGHP-01-06 (Prospectus Site KGGH04) showing a broad basin and an extensive BSR occurrence. (B) Section of seismic line AD-94-39 around Site NGHP-01-06

(Prospectus Site KGGH04) showing predicted formation depths and BSR depth (~210 mbsf) based on a uniform seismic velocity of 1580 m/s. (C) Map showing the hole occupied at Site NGHP-01-06 (KGGH01-A) and location of seismic line AD-94-39. BSR = bottom simulating reflector

Figure 13. Summary of logging-while-drilling (LWD) data from Hole NGHP-01-06A (modified from Collett et al., 2008a). Including gas hydrate saturations (S_h) from Archie's equation, LWD porosity and resistivity-at-bit (RAB) image data from Hole NGHP-01-06A (Note that Archie analyses are known to overestimate gas hydrate saturations in fracture dominated reservoirs; Collett and Lee, 2012). The red data quality flag indicates degraded data quality. gAPI = American Petroleum Institute gamma ray units, IDRO = Image-derived density (EcoScope), RHOB = Bulk density (EcoScope), neutron porosity = Thermal neutron porosity (EcoScope), corrected density porosity = density porosity with core derived grain densities (EcoScope), RING = Ring resistivity (GeoVISION), BIT = Bit resistivity (GeoVISION), Deep Button avg. = Button deep resistivity (GeoVISION), A40L = Attenuation resistivity measured at 400 kHz and a transmitter-receiver spacing of 40 in (EcoScope) and P16H = Phase-shift resistivity at 2 MHZ and a transmitter-receiver spacing of 16 in (EcoScope). BSR = bottom simulating reflector

Figure 14. National Gas Hydrate Program Expedition 01 (NGHP-01) Site NGHP-01-07. (A) Seismic inline 1539 (oriented NW-SE) intersecting with Site NGHP-01-07 (Prospectus Site KGGH06-A). Formation and BSR depths were estimated using a constant velocity of 1600 m/s for the entire sediment column. (B) Section of seismic crossline 3900 near Site NGHP-01-07 (Prospectus Site KGGH06-A). Formation and BSR depths were estimated using a constant velocity of 1600 m/s for the entire sediment column. (C) Map showing all holes occupied at Site NGHP-01-07 (KGGH06-A) and location of seismic inline 1539. BSR = bottom simulating reflector

Figure 15. Summary of logging-while-drilling (LWD) data from Hole NGHP-01-07A (modified from Collett et al., 2008a). Including gas hydrate saturations (S_h) from Archie's equation, LWD porosity and resistivity-at-bit (RAB) image data from Hole NGHP-01-07A, and core derived porosity data (Note that Archie analyses are known to overestimate gas hydrate saturations in fracture dominated reservoirs; Collett and Lee, 2012). The red data quality flag indicates degraded data quality. gAPI = American Petroleum Institute gamma ray units, IDRO = Image-derived density (EcoScope), RHOB = Bulk density (EcoScope), neutron porosity = Thermal neutron porosity (EcoScope), corrected density porosity = density porosity with core derived grain densities (EcoScope), RING = Ring resistivity (GeoVISION), BIT = Bit resistivity (GeoVISION), Deep Button avg. = Button deep resistivity (GeoVISION), A40L = Attenuation resistivity measured at 400 kHz and a transmitter-receiver spacing of 40 in (EcoScope) and P16H = Phase-shift resistivity at 2 MHZ and a transmitter-receiver spacing of 16 in (EcoScope). BSR = bottom simulating reflector

Figure 16. Summary of core data from Site NGHP-01-07 (modified from Collett et al., 2008a). Methane phase diagram for Site NGHP-01-07, with total methane concentration measured from successful pressure cores at Site NGHP-01-07. Concentration-depth profile of interstitial pore-water chlorinity at Site NGHP-01-07 (red circles, Hole NGHP-01-07B; blue circles, Hole NGHP-01-07D). Catwalk infrared core scan for Hole NGHP-01-07B. BSR = bottom simulating reflector

Figure 17. National Gas Hydrate Program Expedition 01 (NGHP-01) Sites NGHP-01-10, -12, -13, and -21. (A) Seismic line GDSW-16 (orientation is NW-SE) crossing drill Sites NGHP-01-10, -12, -13 and -21; note the occurrence of deepseated free gas brightening seismic reflectivity. (B) Enlargement of seismic line GDSW-16 showing the location of Sites NGHP-01-10, -12, -13, and -21. (C) Map showing all holes occupied at Sites NGHP-01-10, -12, -13, and -21 (GD-3-1).

Figure 18. Summary of logging-while-drilling (LWD) data from Hole NGHP-01-10A (modified from Collett et al., 2008a). Including gas hydrate saturations (S_h) from Archie's equation, LWD porosity and resistivity-at-bit (RAB) image data from Hole NGHP-01-10A, and core derived porosity data. The Archie derived gas hydrate saturations depicted in this display are higher than the true in situ saturations because of the fracture nature of the gas hydrate accumulation at Site NGHP-01-10 (Note that Archie analyses are known to overestimate gas hydrate saturations in fracture dominated reservoirs; Collett and Lee, 2012). The red data quality flag indicates degraded data quality. gAPI = American Petroleum Institute gamma ray units, IDRO = Image-derived density (EcoScope), RHOB = Bulk density (EcoScope), neutron porosity = Thermal neutron porosity (EcoScope), corrected density porosity = density porosity with core derived grain densities (EcoScope), RING = Ring resistivity (GeoVISION), BIT = Bit resistivity (GeoVISION), Deep Button avg. = Button deep resistivity (GeoVISION), A40L = Attenuation resistivity measured at 400 kHz and a transmitter-receiver spacing of 40 in (EcoScope) and P16H = Phase-shift resistivity at 2 MHZ and a transmitter-receiver spacing of 16 in (EcoScope). BSR = bottom simulating reflector

Figure 19. Summary of core data from Sites NGHP-01-10, -12, and -21. (modified from Collett et al., 2008a). Methane phase diagram for Site NGHP-01-10, with total methane concentration measured from successful pressure cores at Holes NGHP-01-10B, -10D, -12A, and -21A. Concentration-depth profile of interstitial pore-water chlorinity at Holes NGHP-01-10B, -10D, -12A, and -21A. Catwalk infrared core scans for Holes NGHP-01-10D and -21A. BSR = bottom simulating reflector

Figure 20. National Gas Hydrate Program Expedition 01 (NGHP-01) Site NGHP-01-11. (A) Section of 2D seismic line AD-94-27 around Site NGHP-01-11 (Prospectus Site GDGH12-A) showing a broad basin and an extensive BSR occurrence. (B) Section of seismic line AD-94-27 around Site NGHP-01-11 (Prospectus Site GDGH12-A) showing predicted formation tops and BSR depth (~150 mbsf) based on a uniform seismic velocity of 1580 m/s. (C) Map showing the hole occupied at Site NGHP-01-11 (GDGH12-A) and location of seismic line AD-94-27. BSR = bottom simulating reflector

Figure 21. Summary of logging-while-drilling (LWD) data from Hole NGHP-01-11A (modified from Collett et al., 2008a). Including gas hydrate saturations (S_h) from Archie's equation, LWD porosity and resistivity-at-bit (RAB) image data from Hole NGHP-01-11A (Note that Archie analyses are known to overestimate gas hydrate saturations in fracture dominated reservoirs; Collett and Lee, 2012). The red data quality flag indicates degraded data quality. gAPI = American Petroleum Institute gamma ray units, IDRO = Image-derived density (EcoScope), RHOB = Bulk density (EcoScope), neutron porosity = Thermal neutron porosity (EcoScope), corrected density porosity = density porosity with core derived grain densities (EcoScope), RING = Ring resistivity (GeoVISION), BIT = Bit resistivity (GeoVISION), Deep Button avg. = Button deep resistivity (GeoVISION), A40L = Attenuation resistivity measured at 400 kHz and a transmitter-receiver spacing of 40 in (EcoScope) and P16H = Phase-shift resistivity at 2 MHZ and a transmitter-receiver spacing of 16 in (EcoScope). BSR = bottom simulating reflector

Figure 22. National Gas Hydrate Program Expedition 01 (NGHP-01) Site NGHP-01-14. (A) Seismic inline AD-94-39 (oriented NW-SE) intersecting with Site NGHP-01-14 (Prospectus Site GDGH14-A). (B) Close-up of seismic line AD-94-39 (oriented NW-SE) intersecting with Site NGHP-01-14 (Prospectus Site GDGH14-A). Formation and BSR depths were estimated using a constant velocity of 1580 m/s for the entire sediment column. (C) Map showing the hole occupied at Site NGHP-01-14 (GDGH14-A) and location of seismic line AD-94-39. BSR = bottom simulating reflector

Figure 23. Summary of the wireline logs recorded in Hole NGHP-01-14A (modified from Collett et al., 2008a). The hole size is calculated from the Hostile Litho Density Sonde (HLDS) caliper. The density and porosity measurements made on core samples from Hole NGHP-01-14A are shown for comparison. Gas

hydrate saturations (S_h) from Archie's equation and wireline porosity and resistivity logs (ILD = Deep induction resistivity log) in Hole NGHP-01-14A. The red data quality flag indicates degraded data quality. SFLU = Spherically focused unaveraged resistivity, BSR = bottom simulating reflector

Figure 24. Summary of core data from Site NGHP-01-14 (modified from Collett et al., 2008a). Methane phase diagram for Site NGHP-01-14, with total methane concentration measured from a successful pressure core at Site NGHP-01-14. Concentration-depth profile of interstitial pore-water chlorinity at Site NGHP-01-14. Catwalk infrared core scan for Hole NGHP-01-14A. BSR = bottom simulating reflector

Figure 25. National Gas Hydrate Program Expedition 01 (NGHP-01) Site NGHP-01-15. (A) Seismic line AD-94-45 crossing drill Site NGHP-01-15 (Prospectus Site GDGH11). (B) Close up of seismic line AD-94-45 in the vicinity of Site NGHP-01-15 (Prospectus Site GDGH11). Formation and BSR depths were estimated using a constant velocity of 1580 m/s for the entire sediment column. (C) Map showing the hole occupied at Site NGHP-01-15 (GDGH11) and location of seismic line AD-94-45. BSR = bottom simulating reflector

Figure 26. Summary of the wireline logs recorded in Hole NGHP-01-15A (modified from Collett et al., 2008a). The hole size is calculated from the Hostile Litho Density Sonde (HLDS) caliper. The density and porosity measurements made on core samples from Hole NGHP-01-15A are shown for comparison. Gas hydrate saturations (S_h) from Archie's equation and wireline porosity and resistivity logs (ILD = Deep induction resistivity log) in Hole NGHP-01-15A. The red data quality flag indicates degraded data quality. SFLU = Spherically focused unaveraged resistivity, BSR = bottom simulating reflector

Figure 27. Summary of core data from Site NGHP-01-15 (modified from Collett et al., 2008a). Methane phase diagram for Site NGHP-01-15, with total methane concentration measured from the successful pressure cores at Site NGHP-01-15. Concentration-depth profile of interstitial pore-water chlorinity at Site NGHP-01-15. Catwalk infrared core scan for Hole NGHP-01-15A. BSR = bottom simulating reflector

Figure 28. National Gas Hydrate Program Expedition 01 (NGHP-01) Site NGHP-01-16. (A) Seismic inline 1315 from a 3D volume across Site NGHP-01-16. (B) Seismic crossline 3516 from 3D volume across Site NGHP-01-16. (C) Map showing the hole occupied at Site NGHP-01-16 (Step-out Site from Site NGHP-01-07) and location of seismic crossline 3516 and inline 1315. BSR = bottom simulating reflector

Figure 29. Summary of the wireline logs recorded in Hole NGHP-01-16A (modified from Collett et al., 2008a). The hole size is calculated from the Hostile Litho Density Sonde (HLDS) caliper. The density and porosity measurements made on core samples from Hole NGHP-01-16A are shown for comparison. Gas hydrate saturations (S_h) from Archie's equation and wireline porosity and resistivity logs (ILD = Deep induction resistivity log) in Hole NGHP-01-16A. The red data quality flag indicates degraded data quality. SFLU = Spherically focused unaveraged resistivity, BSR = bottom simulating reflector

Figure 30. Summary of core data from Site NGHP-01-16 (modified from Collett et al., 2008a). Methane phase diagram for Site NGHP-01-16, with total methane concentration measured from the successful pressure cores at Site NGHP-01-16. Concentration-depth profile of interstitial pore-water chlorinity at Site NGHP-01-16. Catwalk infrared core scan for Hole NGHP-01-16A. BSR = bottom simulating reflector

Figure 31. National Gas Hydrate Program Expedition 01 (NGHP-01) Site NGHP-01-20. (A) Seismic line AD-94-11 (NW-SE oriented) crossing Site NGHP-01-20. Depth of formation tops were estimates using a

constant velocity of 1,580 m/s. (B) Map showing all holes occupied at Site NGHP-01-20 (KGGH05) and location of seismic line AD-94-11. BSR = bottom simulating reflector

Figure 32. Summary of core data from Site NGHP-01-20 (modified from Collett et al., 2008a). Concentration-depth profile of interstitial pore-water chlorinity at Site NGHP-01-20. Catwalk infrared core scan for Holes NGHP-01-20A and -20B. BSR = bottom simulating reflector

Figure 33. (A) National Gas Hydrate Program Expedition 01 (NGHP-01) drill site map depicting the location of the drill sites established during the expedition in the Mahanadi Basin. (B) Insert bathymetric map depicting the location of the research drill sites established in the Mahanadi Basin.

Figure 34. National Gas Hydrate Program Expedition 01 (NGHP-01) Site NGHP-01-08. (A) Section of seismic inline 2148 from a 3D volume over Site NGHP-01-08 (Prospectus Site MNGH01-1-A) showing a widespread BSR associated with high-amplitude reflectors below. (B) Close up of seismic inline 2148 over Site NGHP-01-08 (Prospectus Site MNGH01-1-A) with predicted formation tops and BSR depth (~257mbsf) based on a uniform seismic velocity of 1,610 m/s. (C) Map of the Mahanadi Basin showing the location of available seismic data and Holes NGHP-01-08, -18, and -19. (D) Map showing the location of Hole NGHP-01-08A (MNGH01-1-A) and seismic inline 2148. BSR = bottom simulating reflector

Figure 35. Summary of logging-while-drilling (LWD) data from Hole NGHP-01-08A (modified from Collett et al., 2008a). Including gas hydrate saturations (S_h) from Archie's equation, LWD porosity and resistivity-at-bit (RAB) image data from Hole NGHP-01-08A. The red data quality flag indicates degraded data quality. gAPI = American Petroleum Institute gamma ray units, IDRO = Image-derived density (EcoScope), RHOB = Bulk density (EcoScope), neutron porosity = Thermal neutron porosity (EcoScope), corrected density porosity = density porosity with core derived grain densities (EcoScope), RING = Ring resistivity (GeoVISION), BIT = Bit resistivity (GeoVISION), Deep Button avg. = Button deep resistivity (GeoVISION), A40L = Attenuation resistivity measured at 400 kHz and a transmitter-receiver spacing of 40 in (EcoScope) and P16H = Phase-shift resistivity at 2 MHZ and a transmitter-receiver spacing of 16 in (EcoScope). BSR = bottom simulating reflector

Figure 36. National Gas Hydrate Program Expedition 01 (NGHP-01) Site NGHP-01-09. (A) Section of seismic inline 3014 from a 3D volume over Site NGHP-01-09 (Prospectus Site MNGH01-2) showing widespread faulting; no clear BSR can be identified. (B) Close up of seismic inline 3014 from a 3D volume over Site NGHP-01-09 (Prospectus Site MNGH01-2) with predicted formation depths based on a uniform seismic velocity of 1,610 m/s. (C) Map showing the location of Hole NGHP-01-09A (Prospectus Site MNGH01-2) and seismic inline 3014. BSR = bottom simulating reflector

Figure 37. Summary of logging-while-drilling (LWD) data from Hole NGHP-01-09A (modified from Collett et al., 2008a). Including gas hydrate saturations (S_h) from Archie's equation, LWD porosity and resistivity-at-bit (RAB) image data from Hole NGHP-01-09A. The red data quality flag indicates degraded data quality. gAPI = American Petroleum Institute gamma ray units, IDRO = Image-derived density (EcoScope), RHOB = Bulk density (EcoScope), neutron porosity = Thermal neutron porosity (EcoScope), corrected density porosity = density porosity with core derived grain densities (EcoScope), RING = Ring resistivity (GeoVISION), BIT = Bit resistivity (GeoVISION), Deep Button avg. = Button deep resistivity (GeoVISION), A40L = Attenuation resistivity measured at 400 kHz and a transmitter-receiver spacing of 40 in (EcoScope) and P16H = Phase-shift resistivity at 2 MHZ and a transmitter-receiver spacing of 16 in (EcoScope). BSR = bottom simulating reflector

Figure 38. National Gas Hydrate Program Expedition 01 (NGHP-01) Site NGHP-01-18. (A) NW-SE oriented seismic line ("Line 1") extracted from a 3D volume crossing Site NGHP-01-18 at trace 330. (B)

SW-NE oriented seismic line ("Line 2") extracted from a 3D volume crossing Site NGHP-01-18 at trace 115. (C) Map of the Mahanadi Basin showing the location of available seismic data and Holes NGHP-01-08, -18, and -19. (D) Close-up map of Site NGHP-01-18 with the location of two key-seismic lines shown: "Line 1" and "Line 2".

Figure 39. Summary of core data from Site NGHP-01-18 (modified from Collett et al., 2008a). Concentration-depth profile of interstitial pore-water chlorinity at Site NGHP-01-18. Catwalk infrared core scan for Hole NGHP-01-18A.

Figure 40. National Gas Hydrate Program Expedition 01 (NGHP-01) Site NGHP-01-19. (A) Seismic line (SW-NE oriented) crossing Site NGHP-01-19 ("Line-3"). The site is located at around trace 190 within a gap between two prominent highly-reflective channelized canyon-like features. The depth of the formation tops was estimated using a uniform velocity of 1,600 m/s. (B) Map of the Mahanadi Basin showing the location of available seismic data and Holes NGHP-01-08, -18, and -19. (C) Close-up map of Site NGHP-01-19 with the location of key-seismic line shown: "Line 3".

Figure 41. Summary of the wireline logs recorded during the two triple combination tool runs in Hole NGHP-01-19B (modified from Collett et al., 2008a). The hole size is calculated from the Hostile Litho Density Sonde (HLDS) caliper. The density and porosity measurements made on core samples from Hole NGHP-01-19A are shown for comparison. Gas hydrate saturations (S_h) from Archie's equation and wireline porosity and resistivity logs (ILD = Deep induction resistivity log) in Hole NGHP-01-19B. The red data quality flag indicates degraded data quality. SFLU = Spherically focused unaveraged resistivity, BSR = bottom simulating reflector

Figure 42. Summary of core data from Site NGHP-01-19 (modified from Collett et al., 2008a). Methane phase diagram for Site NGHP-01-19, with total methane concentration measured from the successful pressure cores at Site NGHP-01-19. Concentration-depth profile of interstitial pore-water chlorinity at Site NGHP-01-19. Catwalk infrared core scan for Hole NGHP-01-19A. BSR = bottom simulating reflector

Figure 43. (A) National Gas Hydrate Program Expedition 01 (NGHP-01) drill site map depicting the location of the Site NGHP-01-17 in the Andaman Sea. (B) Insert bathymetric map showing Site NGHP-01-17 in the Andaman area (Prospectus Site ANGH01).

Figure 44. (A) Seismic line AN-01-34 crossing Site NGHP-01-17. Most of the sediments appear to be seafloor parallel with some small inclination. Depths of bottom simulating reflector (BSR) and formation tops were estimated using a uniform velocity of 1600 m/s. (B) Seismic line AN-01-27 crossing north of Site NGHP-01-17. This line shows prominent ridges with Site NGHP-01-17 located within the saddle between the two ridges. (C) Detailed map of the area in the Andaman Islands showing Site NGHP-01-17 and location of key seismic lines.

Figure 45. Summary of the wireline logs recorded during the two triple combo runs in Hole NGHP-01-17B (modified from Collett et al., 2008a). The hole size is calculated from the Hostile Litho Density Sonde (HLDS) caliper. The density and porosity measurements made on core samples from Hole NGHP-01-17A are shown for comparison. Gas hydrate saturations (S_h) from Archie's equation and wireline porosity and resistivity logs in Hole NGHP-01-17B. The red data quality flag indicates degraded data quality. SFLU = Spherically focused unaveraged resistivity, BSR = bottom simulating reflector

Figure 46. Summary of core data from Site NGHP-01-17 (modified from Collett et al., 2008a). Methane phase diagram for Site NGHP-01-17, with total methane concentration measured from successful pressure cores at Site NGHP-01-17. Concentration-depth profiles of interstitial pore-water chlorinity in Hole

NGHP-01-17A, at depths below 180 mbsf influenced by dilution of the fluids by gas hydrate dissociation. Catwalk infrared core scan for Hole NGHP-01-17A showing potential cold cores associated with gas hydrate dissociation. BSR = bottom simulating reflector

Figure 47. (A) National Gas Hydrate Program Expedition 01 (NGHP-01) drill site map depicting the location of the Site NGHP-01-01 in the Kerala-Konkan Basin. (B) Insert bathymetric map showing Site NGHP-01-01 in the Kerala-Konkan Basin (Prospectus Site KKGH01).

Figure 48. National Gas Hydrate Program Expedition 01 (NGHP-01) Site NGHP-01-01. (A) Seismic line K-95-8B crossing Site NGHP-01-01. A bottom-simulating reflector (BSR?) appears throughout most of the section but was shown not to be gas hydrate related (see discussion in the text). (B). Close-up of seismic line K-95-8B showing the detailed sedimentary structures around Site NGHP-01-01. Depths were estimated using a uniform seismic velocity of 1,560 m/s. (B) Map showing location of Hole NGHP-01-01A (KKGH01) and location of seismic line K-95-8B. BSR = bottom simulating reflector

Figure 49. Summary of the wireline logs recorded in Hole NGHP-01-01A (modified from Collett et al., 2008a). The hole size is calculated from the Hostile Litho Density Sonde (HLDS) caliper. The density and porosity measurements made on core samples from Hole NGHP-01-01A are shown for comparison. Gas hydrate saturations (S_h) from Archie's equation and wireline porosity and resistivity logs (ILD = Deep induction resistivity log) in Hole NGHP-01-01A. The red data quality flag indicates degraded data quality. SFLU = Spherically focused unaveraged resistivity, BSR = bottom simulating reflector

Figure 50. Summary of core data from Site NGHP-01-01 (modified from Collett et al., 2008a). Concentration-depth profile of interstitial pore-water chlorinity at Site NGHP-01-01.

Figure 51. Arbitrary example of the depth-temperature zone in which gas (methane) hydrate is stable in an outer continental margin marine setting (modified from Kvenvolden, 1988).

Table 1. National Gas Hydrate Program Expedition 01 drill site data and summary information on the occurrence of gas hydrate at each site established during the expedition, including listing of site number, hole designation, water depth as determined by drilling or coring, device or measurement used to indicate the presence of gas hydrate, description of the evidence for the occurrence of gas hydrate, dominant sediment type at each site as determined by coring or inferred from downhole log data, gas hydrate reservoir type as determined from various data sources, predicted gas source, and depth to the base of the gas hydrate stability zone (BGHSZ) (modified from Collett et al., 2008a). See Explanation at the end of the table for definition of terms, acronyms, and measurement units used in this table.

Table 2A. Listing of scientific journal articles in this special issue of the Journal of Marine and Petroleum Geology that deal with the scientific results of the Indian National Gas Hydrate Program Expedition 01 (NGHP-01). Each citation includes a short technical synopsis of the published report.

Table 2B. Listing of previously published scientific journal articles that deal with scientific results of the Indian National Gas Hydrate Program Expedition 01 (NGHP-01). Each citation includes a short technical synopsis of the published report.

Table 1

Site	Hole	Depth (mbsf)	Indicator	Description	Dominant sediment type	Gas hydrate reservoir type	Gas source	BGHSZ (mbsf)
Krishna-Godavari Basin								
NGHP-01-02					No core	Possible fracture-filling and/or pore-filling	No core	NA
	-	170	BSR					
	A	70-170	Well logs (resistivity)	Slightly elevated resistivity (1-2 ohm-m) over background; Archie Sh <10%				
NGHP-01-03					Clay with limited silt/sand beds	Possible fracture-filling and/or pore-filling	Microbial	203
	-	209	BSR					
	B	60-209	Core water chemistry (Cl^-)	Slightly depleted Cl^- concentrations				
	B	176	Core (pressure core) gas volume	<1.0% Sh				
	C	184	Core (pressure core) gas volume	<1.0% Sh				
	A	0-209	Well logs (resistivity)	Thinly bedded, slightly elevated resistivity (~0.5 ohm-m) over background; *Archie Sh <20%				
NGHP-01-04					No core	Fracture-filling with possible pore-filling	No core	NA
	-	182	BSR					
	A	80-100	Well logs (resistivity)	Fracture, slightly elevated resistivity (~0.5 ohm-m) over background; *Archie Sh <25%				
NGHP-01-05					Clay with limited silt/sand beds	Fracture-filling with possible pore-filling	Microbial	130
	-	125	BSR					
	C/D	70-125	IR associated core water chemistry (Cl^-) anomaly	Depleted Cl^- concentrations with depth to the BSR				
	D	114.9, 124.9	Core (pressure core) gas volume	<1.0% Sh				
	C/D	76.9, 78.3, 84.9, 86.0	Core (pressure core) gas volume	0.6-9.4% Sh				
	A	55-94	Well logs (resistivity)	Series of gas hydrate filled fractures, elevated resistivity (2.0-5.0 ohm-m) over background; *Archie Sh ranging from 20-70%				
	B	53-90	Well logs (resistivity)	Series of gas hydrate filled fractures, elevated resistivity (2.0-5.0 ohm-m) over background; *Archie Sh ranging from 20-70%				
NGHP-01-06					No core	Fracture-filling with possible pore-filling	No core	NA
	-	210	BSR					

	A	137-148	Well logs (resistivity)	Series of gas hydrate filled fractures, slightly elevated resistivity (0.5-1.0 ohm-m) over background; *Archie Sh <25%				
NGHP-01-07					Clay with limited silt/sand beds	Fracture-filling with possible pore-filling	Microbial	198
	-	188	BSR					
	-	70, 130	High amplitude seismic reflector above BGHSZ					
	B/D	15-188	IR associated core water chemistry (Cl^-) anomaly	Depleted and elevated Cl^- concentrations with depth to the BSR				
	B	148.2	Core (pressure core) gas volume	1.1 % Sh				
	A	70-90	Well logs (resistivity)	Series of gas hydrate filled fractures, elevated resistivity (0.5-2.0 ohm-m) over background; *Archie Sh <25%				
	A	130-150	Well logs (resistivity)	Series of gas hydrate filled fractures, elevated resistivity (0.5-2.0 ohm-m) over background; *Archie Sh <25%				
NGHP-01-10 NGHP-01-12 NGHP-01-13 NGHP-01-21					Clay with limited silt/sand beds	Fracture-filling with possible pore-filling	Microbial	160
	-	160	BSR					
	10B/10D/12A/21A	26-160	IR associated core water chemistry (Cl^-) anomaly	Depleted and elevated Cl^- concentrations with depth to the BSR				
	10B/10D/12A/21A	46.7, 47.4, 70.0, 77.8, 93.3, 98.2, 117.4, 145.1, 164.4	Core (pressure core) gas volume	2.0-31.5% Sh				
	10A	27-160	Well logs (resistivity)	Thick gas hydrate filled fracture system from near the seafloor to the depth of the BSR, elevated resistivity (1.0-100.0 ohm-m) over background; *Archie Sh ranging from 50-85%				
NGHP-01-11					No core	Fracture-filling with possible pore-filling	No core	NA
	-	150	BSR					
	A	95-113	Well logs (resistivity)	Series of gas hydrate filled fractures, elevated resistivity (0.5-1.5 ohm-m) over background; *Archie Sh <35%				
	A	144-146	Well logs (resistivity)	Gas hydrate filled fracture, elevated resistivity (0.5-3.5 ohm-m) over background; *Archie Sh <35%				
NGHP-01-14					Clay with slightly more abundant silt/sand beds	Possible pore-filling (highly disseminated gas hydrate)	Microbial	150
	-	109	BSR					

	A	20-109	IR associated core water chemistry (Cl^-) anomaly	Depleted Cl^- concentrations with depth to the BSR				
	A	101	Core (pressure core) gas volume	10.7% Sh				
	A	67-72	Well logs (resistivity)	Thinly bedded, slightly elevated resistivity (0.5-1.0 ohm-m) over background; Archie Sh <20%				
	10A	82-87	Well logs (resistivity)	Thinly bedded, slightly elevated resistivity (~0.5 ohm-m) over background; Archie Sh <20%				
NGHP-01-15					Clay with more abundant silt/sand beds	Pore-filling (ranging from disseminated to one highly saturated gas hydrate sand bed)	Microbial	126
	-	126	BSR					
	A	60-90	IR associated core water chemistry (Cl^-) anomaly	Depleted Cl^- concentrations associated with disseminated gas hydrate and one distinct sand bed (78.63-79.13 mbsf)				
	A	86.7	Core (pressure core) gas volume	16.1% Sh				
	A	75-81	Well logs (resistivity)	Interbedded clay/silt/sand section, elevated resistivity (0.5-5.0 ohm-m) over background; Archie Sh ranging from 25-50%				
	A	90-110	Well logs (resistivity)	Interbedded clay/silt/sand section , elevated resistivity (0.5-1.0 ohm-m) over background; Archie Sh ranging from 25-50%				
NGHP-01-16					Clay with more abundant silt/sand beds	Possible pore-filling (disseminated gas hydrate)	Microbial	178
	-	170	BSR					
	A	85-170	IR associated core water chemistry (Cl^-) anomaly	Depleted Cl^- concentrations with depth to the BSR				
	A	163.1	Core (pressure core) gas volume	1.1% Sh				
	A	90-155	Well logs (resistivity)	Thinly bedded, slightly elevated resistivity (0.5-3.0 ohm-m) over background; Archie Sh ranging from 10-50%				
NGHP-01-20					Clay with possibly abundant sand-rich reservoirs (incomplete data to evaluate)	Possible pore-filling (disseminated gas hydrate)	Microbial	NA
	-	220	BSR	Local, discontinuous BSR?				
	A/B	43-187.3 depth of deepest core	IR associated core water chemistry (Cl^-) anomaly	Depleted Cl^- concentrations with depth to the bottom of the B hole. Possible significant sand reservoirs based on core recovery problems.				

Mahanadi Basin								
NGHP-01-08					**No core**	**Possible pore-filling and/or fracture-filling**	**No core**	**NA**
	-	**257**	**BSR**					
	A	**220-257**	**Well logs (resistivity)**	**Slightly elevated resistivity (~0.2 ohm-m) over background; Archie Sh <10%**				
NGHP-01-09					**No core**	**Possible pore-filling and/or fracture-filling**	**No core**	**NA**
	-	**290**	**BSR**					
	A	**190-290**	**Well logs (resistivity)**	**Slightly elevated resistivity (~0.5 ohm-m) over background; Archie Sh <10%**				
NGHP-01-18					**Clay with limited silt/sand beds**	**Possible pore-filling**	**Microbial**	**210**
	-	**210**	**BSR (top of high-reflectivity zone)**					
	A	**115-190 depth of deepest core**	**IR associated core water chemistry (Cl^-) anomaly**	**Depleted Cl^- concentrations with depth to the bottom of the hole**				
NGHP-01-19					**Clay with limited silt/sand beds**	**Possible pore-filling**	**Microbial**	**220**
	-	**205**	**BSR (top of high-reflectivity zone)**					
	A	**125-130**	**IR associated core water chemistry (Cl^-) anomaly**	**Depleted Cl^- concentrations**				
	A	**170-205**	**IR associated core water chemistry (Cl^-) anomaly**	**Depleted Cl^- concentrations above BSR**				
	A	**128.0, 195.3**	**Core (pressure core) gas volume**	**0.5-2.4% Sh**				
	A	**105-120**	**Well logs (resistivity)**	**Thinly bedded, slightly elevated resistivity (0.5-1.0 ohm-m) over background; Archie Sh ranging from 5-20%**				
	A	**180-205**	**Well logs (resistivity)**	**Thinly bedded, slightly elevated resistivity (0.5-1.0 ohm-m) over background; Archie Sh <20%**				
Andaman Sea								
NGHP-01-17					**Clay/silt (nannofossil ooze) with volcanic ash beds**	**Pore-filling (ranging from disseminated to highly saturated gas hydrate in ash beds)**	**Microbial + Thermogenic**	**620**
	-	**608**	**BSR (uncertain phase)**					
	A	**250-608**	**IR associated core water chemistry (Cl^-)**	**Depleted Cl^- concentrations associated with ash beds**				

	A	328.0, 412.7	Core (pressure core) gas volume	0.1-0.6% Sh				
	A	586.3	Core (pressure core) gas volume	7.6 % Sh				
	B	250-608	Well logs (resistivity)	Slightly elevated resistivity (0.5-2.0 ohm-m) over background; Archie Sh ranging from 5-40%				
Kerala-Konkan Basin								
NGHP-01-01					Carbonate-rich pelagic sediments	No evidence of gas hydrate	Below detection	360
	-	217	BSR (uncertain phase)	Result of subtle changes in formation density associated with changes in lithology (not related to the occurrence of gas hydrate)				
	A	-	No log or core evidence of gas hydrate					

TABLE EXPLANATION

Gas hydrate indicators
Seismic: Bottom simulator reflectors (BSR)
Seismic: Direct indicators ("peak" leading high amplitude reflectors
Core: Direct observations

Core: Temperature from inferred scanning (IR)
Core: Interstitial water chemistry (Cl^-)
Core: Gas volume from pressure cores
Well logs: Elevated resistivities and acoustic velocities

*Archie analyses are known to overestimate gas hydrate saturations in fracture dominated reservoirs.

Gas hydrate reservoir forms
Pore-filling or grain-displacement
Fracture-filling

Reservoir sediment types
Clay-silt-sand (ash)

Sh = Gas hydrate saturation
mbsf = meters below seafloor
BGHSZ = base gas hydrate stability zone
NA = not available

Table 2A

Reference	Synopsis
1. NGHP-01 project summaries	
Collett, T.S., Boswell, R., Cochran, J.R., Kumar, P., Lall, M., Mazumdar, A., Ramana, M.V., Ramprasad, T., Riedel, M., Sain, K., Sathe, A.V., Vishwanath, K., and the NGHP Expedition 01 Scientific Party, (this issue), Geologic implications of gas hydrates in the offshore of India: Results of the National Gas Hydrate Program Expedition 01: Journal of Marine and Petroleum Geology.	This report is intended to provide an overview of the occurrence of gas hydrates in the offshore of India and summarize the operational and technical results of the NGHP01 expedition. This report includes a review of the earlier gas hydrate research efforts in India that led to formation of the NGHP. The main body of the report reviews planning and operational phases of the NGHP01 expedition; which is followed by detailed descriptions of the NGHP01 drilling results and the evidence for the occurrence of gas hydrates in the Krishna-Godavari Basin, the Mahanadi Basin, the Andaman Sea, and in the Kerala-Konkan Basin.
Kumar, P., Collett, T.S., Boswell, R., Cochran, J.R., Lall, M., Mazumdar, A., Ramana, M.V., Ramprasad, T., Riedel, M., Sain, K., Sathe, A.V., Vishwanath, K., and the NGHP Expedition 01 Scientific Party, (this issue), Geologic implications of gas hydrates in the offshore of India: Krishna-Godavari Basin, Mahanadi Basin, Andaman Sea, Kerala-Konkan Basin: Journal of Marine and Petroleum Geology.	This report provides a technical review of the occurrence of gas hydrate in the Krishna-Godavari Basin, the Mahanadi Basin, the Andaman Sea, and in the Kerala-Konkan Basin, including a hole-by-hole synopsis of the evidence for gas hydrates at each of the NGHP-01 drill sites established during the expedition. This report also summarizes the operational and scientific results of the NGHP-01 expedition efforts as presented in the technical reports that make up the special issue of the Journal of Marine and Petroleum Geology on gas hydrates in the offshore of India. Additional studies of data and samples obtained through the NGHP-01 expedition has led to the publication additional journal articles and reports not included special issue of the Journal of Marine and Petroleum Geology; the scientific results associated with these additional contributions have been summarized in this report. This report concludes with a systematic review of the gas hydrate petroleum systems that control the occurrence of gas hydrate in the offshore of India.
Wegner, S.A., and Campbell, K.J., (this issue), Drilling hazard assessment for hydrate bearing sediments including drilling through the BSRs: Journal of Marine and Petroleum Geology. JMPG-D-14-00201	As part of the NGHP-01 pre-drill site evaluation process, a geohazard review was conducted for 19 potential drill sites in the Krishna-Godavari Basin, the Kerala-Konkan Basin, the Mahanadi Basin, and the Andaman Islands. This site review identified several potential drilling hazards, including, but not limited to, seafloor slopes and failure conditions, complex seafloor topography, anomalous seismic amplitude responses, shallow gas hydrates, shallow free gas, shallow water-flow, and faults/fractures. In some cases the location of a proposed site were moved to a more favorable location and/or the planned depth of drilling was reduced, or the proposed site was removed from consideration. No significant drilling problems were encountered during the execution of NGHP-01.
2. Lithostratigraphic controls on the occurrence of gas hydrate	
Phillips, S.C., Johnson, J.E., Underwood, M.B., Guo, J., Giosan, L., and Rose, K., (this issue), Bulk and clay mineral composition of sediments in the Bay of Bengal, Andaman Sea, and Arabian Sea recovered during NGHP Expedition 01: Journal of Marine and Petroleum Geology. JMPG-D-14-00087	This report presents results of bulk and clay mineralogy from X-ray diffraction analysis of sediments from 12 sites drilled during NGHP-01, which documented major changes in sediment source in the Krishna-Godavari Basin (Plio-Pleistocene to recent), Mahanadi Basin (Late Miocene to recent), Andaman Sea (Late Miocene to recent), and Kerala-Konkan Basin (Early Oligocene to recent). It was also concluded that the higher abundance of fully hydrated smectite in the Krishna-Godavari Basin may play a role in gas hydrate formation by sustaining higher permeabilities at any given value of porosity.
Rose, K.K., Johnson, J.E., Torres, M.E., Hong, W.L., Giosan, L., Solomon, E.A., Kastner, M., Cawthern, T., Long, P.E., and Schaef, H.T., (this issue), Anomalous porosity preservation and preferential accumulation of gas hydrate in the Andaman Accretionary Wedge, NGHP-01 Site 17A: Journal of Marine and Petroleum Geology. JMPG-D-13-00448	This report integrates and analyzes sediment core datasets from NGHP-01, with a focus on assessing the geologic controls on the occurrence of gas hydrate at Site NGHP-01-17 in the Andaman Sea. Using sedimentology data, physical property data, geochemical analyses from scanning electron microscopy, grain size measurements, and ion activity analysis of samples from Site NGHP-01-17, the authors concluded that secondary authigenic carbonate mineral (grains) growth enhanced both sediment porosity and permeability in the deeper half of the cored sedimentary section at this site. This study finds that grain-scale features such as the identified authigenic carbonates can have a substantial impact on the occurrence and saturation of gas hydrate in reservoir lithofacies. Such phenomena likely has broad implications for hydrate resource evaluation and identification in a variety of systems.
3. Physical properties of gas hydrate-bearing sediments	
Dai, S., and Santamarina, J.C., (this issue), Sampling natural hydrate-bearing sediments: pressure core technology used in the Krishna-Godavari Basin: Journal of Marine and Petroleum Geology. JMPG-D-14-00059	This report examines the causes and impact of changes in stress and strain during drilling, core recovery, transportation, handling, and testing on the physical nature of hydrate-bearing cores that have been obtained with pressure core systems. Pressure core technology allows the recovery and characterization hydrate-bearing sediments while preserving the hydrate mass under in situ pressure conditions. This study examins core disturbance due to mechanical extension, negative pore pressure generation during unloading (Mandel-Cryer effect), secondary hydrate formation, changes in hydrate mass as a function of changes in pressure and temperature all within the stability field. This work suggests that pressure drops associated with the activity of cutting the core itself may couple with coring induced heating to trigger transient hydrate dissociation followed by secondary hydrate formation in pressure cores recovered during NGHP-01.
Eswari, V.V., Raju, B., Chari, V.D., Prasad, P.S.R., and Sain, Kalachand, (this issue), Laboratory study of methane hydrate formation kinetics and structural stability in sediments: Journal of Marine and Petroleum Geology. JMPG-D-14-00080	The authors report on a series of laboratory experiments to assess the effect of various sediment properties on methane hydrate formation kinetics and the growth of gas hydrates in natural systems. Methane hydrate formation was studied in a stirred reactor filled with a suspension of silica (1-50 µm diameter grain-size) and naturally occurring sediments from the Krishna-Godavari Basin to compare hydrate formation kinetics. The results of these experiments document a particle grain-size effect on the formation of gas hydrate, in this case the addition of silica decreased the gas to hydrate conversion efficiency by 20-30% but the formation of gas hydrate was more rapid in the sediment mixture (relative to a system without sediment).
Holland, M., and Schultheiss, P.J., (this issue), Comparison of methane mass balance and X-ray computed tomography for calculation of gas hydrate content of pressure cores: Journal of Marine and Petroleum Geology. JMPG-D-14-00101	This reports deals with the analysis of 12 pressure cores recovered from the Krishna-Godavari Basin during NGHP-01. Two methods were used to calculate gas hydrate saturation: (1) methane mass balance after depressurization and gas collection, and (2) voxel intensity analysis of X-ray computed tomographic (CT) core reconstructions. All pressure core derived gas hydrate saturations were similar to independent estimates of gas hydrate saturation from pore-water freshening. CT intensity analysis of pressure cores showed promise for calculation of the saturation of vein hydrate in natural samples. Theoretical examination of the CT intensity method showed that this method would be unable to detect pore-filling gas hydrate.
Priest, J.A., Clayton, C.R.I., and Rees, E.V.L., (this issue), Potential impact of gas hydrate dissociation on the strength of host sediment in the Krishna-Godavari Basin: Journal of Marine and Petroleum Geology. JMPG-D-13-00397	The authors of this report review the analysis of two hydrate-bearing pressure cores collected from the Krishna-Godavari Basin during NGHP-01. Detailed analysis of the cores included high-resolution 3-D X-ray computer tomographic scanning, particle size analysis, water content analysis, and interstitial water salinity analysis. Additional core test included specific gravity and strength tests, including liquid and plastic limit and undrained triaxial compression tests. The results of these tests showed the sediment to be a high plasticity clay with a relatively high water content, and low shear strength leading to a significant under-consolidation of the in situ sediment. The authors concluded that the presence of hydrate in veins and related enhancing sediment strength were the main contributing factors to the apparent under-consolidation. Hydrate dissociation within this under-consolidated sedimentary section may potentially lead to seafloor instability.
Stern, L.A., and Lorenson, T.D., (this issue), Grain-scale imaging and compositional characterization of select India NGHP Expedition-01 gas-hydrate-bearing cores, and comparison to other natural gas hydrates: Journal of Marine and Petroleum Geology. JMPG-D-14-00127	This report deals with the grain-scale characteristics and gas analyses of hydrate-bearing samples retrieved during NGHP-01. This laboratory study used cryogenic scanning electron microscopy, X-ray spectroscopy, and gas chromatography to investigate gas hydrate grain morphology and distribution within sediments, gas hydrate composition, and methane isotopic composition of samples from Krishna-Godavari Basin and Andaman Sea drill sites. The hydrate-forming gas was determined to be predominantly methane with trace quantities of higher molecular weight hydrocarbons of primarily microbial origin. Gas hydrate in the Krishna-Godavari Basin samples commonly occurred as nodules or coarse veins. Gas hydrate also occurred as highly faceted crystals lining the interiors of cavities. Other samples exhibit gas hydrate grains rimmed by NaCl-bearing material, presumably produced by salt exclusion during hydrate formation. Well-preserved microfossil and other biogenic detritus was also found within several samples from the Andaman Sea.
Winters, W., Wilcox-Cline, R.W., Long, P., Dewri, S.K., Kumar, P., Stern, L., and Kerr, L., (this issue), Comparison of physical and geotechnical properties of sediment from offshore India and other hydrate reservoirs: Journal of Marine and Petroleum Geology. JMPG-D-13-00455	This report contains one of the largest and most complete reviews of the physical and geotechnical properties of hydrate-bearing sediments in nature. In this report, the authors compare both the inter- and intra-well variability of the sites established during NGHP-01, they also compare these sites to other marine and terrestrial permafrost-related hydrate core sites. These studies have shown that coarser-grained sediments (in both permafrost-related and marine environments) may contain high gas hydrate-pore saturations, while finer-grained sediments may contain low-saturation disseminated type hydrate or more complex forms, including nodules, layers, and high-angle planar and rotational veins. The comparison of index properties and more sophisticated test results show that standard geotechnical relationships can also be used to predict the controls on the occurrence of gas hydrate in other previously unexplored regions.
4. Interstitial-water and gas geochemistry	
Hong, W.L., Solomon, E.A., and Torres, M.E., (this issue), A kinetic-model approach to quantify the effect of mass transport deposits on pore water profiles in the Krishna-Godavari Basin, Bay of Bengal: Journal of Marine and Petroleum Geology. JMPG-D-14-00051	This report presents a model derived from interstitial-water chemistry data in seven NGHP-01 drill sites in the Krishna-Godavari Basin that simulates the interstitial-water profiles to quantify the magnitude and age of mass transport deposits (MTD) in the basin. The model successfully reproduced the S-shape pore water sulfate and ammonium profiles observed at these sites and provided estimates of the thickness of individual MTDs, time elapsed after the MTD event, rate of organic matter-fueled sulfate reduction in the MTD, and time required to reach a new steady state. The model results suggests that the MTDs at the seven core sites are 8 to 25 meters thick and are 300 to 1,600 years old.

Solomon, E.A., Spivack, A.J., Kastner, M., Torres, M.E., and Robertson, G., (this issue), Gas hydrate distribution and carbon sequestration through coupled microbial methanogenesis and silicate weathering in the Krishna-Godavari Basin, offshore India: Journal of Marine and Petroleum Geology. JMPG-D-14-00116	In this study of core data from NGHP-01, a comprehensive suite of pore water solute concentrations and isotope ratios were analyzed to investigate the distribution and concentration of gas hydrate along the Indian continental margin, in situ diagenetic and metabolic reactions, fluid migration and flow pathways, and fluid and gas sources. Gas hydrate was interpreted to be present at all of the sites cored, and in situ microbial methanogenesis has led to average gas hydrate saturations that are typically <5%. Deep-sourced fluid and gas migration produces gas hydrate saturations up to 68% along an isolated coarser-grained stratigraphic horizon at Site NGHP-01-15 and up to 41% within a fractured clay-dominated system at Site NGHP-01-10. This study also noted that dissolved inorganic carbon concentrations that are in equilibrium within in situ alkalinities, indicate that the CO_2 produced through methanogenesis is effectively neutralized by weathering of detrital silicate minerals producing alkalinity. Calcium is simultaneously released from detrital silicates and consumed through precipitation of authigenic carbonates. The continual neutralization of methanogenic CO_2 by silicate weathering and storage of the alkalinity produced in authigenic carbonates suggests that continental margin sediments may be capable of playing a significant role in modulating the global CO_2 budget over geologic time-scales.
Sujith, P.P., Gonsalves, Maria Judith B.D., Rajkumar, V., and Miriam Sheba, V., (this issue), Manganese cycling and its implication on methane related processes in the Andaman continental shelf sediments: Journal of Marine and Petroleum Geology. JMPG-D-13-00327	This report documented for the first time that in situ methane generation and oxidation in the Andaman Sea continental slope could be coupled with the cycling of Mn rich fluids. These results indicate that subsurface sediments harbor microorganisms that participate in the Mn cycling process, where the availability of organic carbon dictates the direction in which the reactions occur. Besides the aerobic oxidation of methane, Mn has been reported to occur under reducing conditions. The findings suggest that Mn redox changes affect the methane oxidation/production rates by serving either as an electron donor and/or an electron acceptor.
5. Microbiologic systems	
Fernandes, Christabelle E.G., Gonsalves, Maria Judith B.D., Nazareth, Delcy R., Nagarchi, Lubbnaz, and Kamaleson, Sam A., (this issue), Microbial iron reduction is coupled to methane oxidation in subsurface sediments of the Arabian Sea: Journal of Marine and Petroleum Geology. JMPG-D-14-00155	Through the study of a sediment core acquired from Site NGHP-01-01 in the Kerala-Konkan Basin, the authors examine the coupled relationship between microbial iron reduction and methane oxidation in subsurface sediments of the Arabian Sea. The authors conclude that iron reduction may possibly play an important role in the microbial composition of the sediments in the Kerala-Konkan Basin and may also control the generation and emission of methane from this system.
Sheba, V.M., Sujith, P.P., and Gonsalves, Maria Judith B.D., (this issue), Diversity and activity of methane oxidizing bacteria in subsurface sediments of the Krishna Godavari Basin: Journal of Marine and Petroleum Geology. JMPG-D-14-00144	This study attempts to look into the groups of organisms that may present in the NGHP-01 cored section of the Krishna Godavari Basin to characterize the ecology of a gas hydrate rich ecosystem, with a focus on identifying the groups of organisms present in these sediments, their characteristics, and activity. This study shows that methane oxidizing bacteria (MOB) are important in controlling the emission of greenhouse gas from methane hydrate systems. The distribution of MOB in the NGHP-01 sediments showed greater abundance at the surface than samples collected from previous marine expeditions in the basin. These results broaden our understanding of oceanic methanotrophs and how their activity controls the emission of methane from a gas hydrate rich ecosystems like the Krishna-Godavari Basin.
6. Well log analysis	
Cook, A.E., Goldberg, D.S., and Malinverno, A., (this issue), Natural gas hydrates occupying fractures: a focus on non-vent sites on the Indian continental margin and the northern Gulf of Mexico: Journal of Marine and Petroleum Geology. JMPG-D-13-00430	The authors of this contribution compare and contrast the characteristics of natural gas hydrates in fractures at non-vent/non-chimney sites from the NGHP-01 Expedition with those discovered in the U.S. Gulf of Mexico. This report concludes that in both settings, that the fractured dominated gas hydrate accumulations occur exclusively in fine-grained sediment and that the fractures are typically near-vertical and oriented in similar directions within each individual site. Overall, downhole well log measured electrical resistivity was the only physical property always affected by the presence of near-vertical gas hydrate filled fractures. In addition, the borehole encountered near-vertical fracture systems were restricted to the stratigraphic section within the gas hydrate stability zone and were not observed intersecting the base of the gas hydrate stability zone; thus indicating that the formation and growth of gas hydrate contributed directly to the formation of the fractures that host the well log imaged gas hydrate occurrences.
Jaiswal, P., Al-Bulushi, S., and Dewangan, P., (this issue), Logging-while-drilling and wireline velocities: Site NGHP-01-10, Krishna-Godavari Basin, India: Journal of Marine and Petroleum Geology. JMPG-D-13-00447	In this report, a new method for rock physics modeling of hydrate-filled fractures is developed and applied to compare the logging-while-drilling (LWD) and wireline conveyed downhole acoustic velocity log data from two holes at Site NGHP-01-10 in the Krishna-Godavari Basin. The authors shown that the differences in the measured velocities between the LWD and wireline logged holes could be due to changes in fracture conditions rather than changes in hydrate content. The authors suggests that frequently reported intra-site variability in hydrate saturations from LWD and wireline logged holes could be more related to interpretative methods than actual geologic variability.
Riedel, M., Guerin, G., and Goldberg, D., (this issue), Compressional and shear-wave velocities from gas hydrate bearing sediments: examples from the India and Cascadia margins as well as Arctic permafrost regions: Journal of Marine and Petroleum Geology. JMPG-D-14-00164	This report reviews downhole acquired acoustic velocity data from hydrate-bearing sediments as acquired during three marine gas hydrate drilling projects: NGHP-01, Ocean Drilling Program Leg 204, and the Integrated Ocean Drilling Program 311. This data is also compared to acoustic log data collected from two terrestrial permafrost-associated gas hydrate sites: the Ignik-Sikumi site in Alaska and the Mallik site in northern Canada. In this study, both shear-wave (Vs) and compressional-wave (Vp) acoustic log data are used to evaluate sediment grain-size control on the Vp and Vs properties of hydrate-bearing sediments. The comparison of data sets in this study show that in terrestrial Arctic settings, where thick sand-rich reservoirs are more prevalent, high gas hydrate saturations dominate the acoustic properties of the sediments. Data from the terrestrial Arctic settings show a strong linear relationship between Vp and Vs with depth. Data from the mostly clay-dominated marine sites off India and ODP Leg 204 suggest a different (shifted to lower Vp and Vs log values), but still a linear relationship with depth. Marine sites, however, with a higher percentage of silt- and sand occurrences (i.e. Site NGHP-01-17 in the Andaman Sea) exhibit intermediate Vp and Vs values.
Shankar, U., and Riedel, M., (this issue), Assessment of gas hydrate saturation in marine sediments from resistivity and compressional-wave velocity log measurements in the Mahanadi Basin, India: Journal of Marine and Petroleum Geology. JMPG-D-13-00214	In this study, pore-water chemistry data, electrical resistivity and sonic velocity logs, collected during NGHP-01, are used to estimate gas hydrate saturations at three sites in the Mahanadi Basin: Sites NGHP-01-08, -09, and -19. Gas hydrate saturations estimated from pore-water chloride concentrations shows values up to ~10% of the pore space at depths just above the base of the gas hydrate stability zone. Gas hydrate saturations estimated from electrical resistivity and acoustic velocity logs using standard empirical relations and modeling approaches are comparable, with gas hydrate saturations calculated at ~10-15% of the pore space. The occurrence of gas hydrate was shown to be associated with channel-levee sedimentary complexes based on the regional seismic data, but the cored/logged section lacked a significant sand fraction, which is required for the formation of higher gas hydrate saturations. The authors speculated, that significant sand deposition could occur further downslope in this setting where typical fan-type deposits can be inferred from the seismic data and thus higher accumulations of gas hydrate would be expected.
Sriram, G., Dewangan, P., and Ramprasad, T., (this issue), Modified effective medium model for gas hydrate bearing, clay dominated sediments in the Krishna-Godavari Basin: Journal of Marine and Petroleum Geology. JMPG-D-13-00344	In this study, NGHP-02 acquired well logs from the Krishna-Godavari Basin were used to examine the interaction between the sediment grains of unconsolidated marine sediments and gas hydrate. The authors of this report used the friction-dependent effective medium model (EMM) to estimate compressional- and shear-wave velocities of fluid saturated sediments at Site NGHP-01-03, which represent the “background fluid-saturated marine sediment site” and were compared with the downhole measured acoustic velocity well log data from this site. It was determined that the model derived shear-wave velocities are over estimated by the Hertz-Mindlin contact theory, which suggests that the background shear-wave velocity needs to be modeled without friction at the grain contact for unconsolidated marine sediments. The Site NGHP-01-07 a load-bearing gas hydrate deposit was also modeled, which showed that the derived gas hydrate saturation values were independent of frictional parameters under these conditions. The proposed EMM with zero friction and the mixed grain contact model is able to predict the velocities of fluid-saturated sediments as well as hydrate-bearing sediments in the Krishna-Godavari Basin.
7. Geophysical analysis	
Dewangan, P., Mandal, R., Jaiswal, P., Ramprasad, T., and Sriram, G., (this issue), Estimation of seismic attenuation of gas hydrate bearing sediments from multi-channel seismic data: A case study from Krishna-Godavari offshore basin: Journal of Marine and Petroleum Geology. JMPG-D-13-00386	The authors in this report estimate the magnitude of seismic attenuation from multi-channel seismic data acquired from the Krishna-Godavari Basin for a fracture dominated hydrate-bearing sedimentary section near Site NGHP-01-10. In this study, the authors calculate the seismic quality factor (Q), which is the inverse of seismic attenuation, by two methods: (1) the spectral ratio method, and (2) the peak frequency method. The estimated effective Q-values values are the product of several factors, such as gas hydrate and free gas content and the nature of faulting. The hydrate-bearing intervals as identified by increases in measured seismic velocities where shown to have elevated Q-values indicating that the presence of hydrate decreases attenuation in fine-grained, clay dominated marine sediments. It was also shown that the presence of free gas increases seismic attenuation. In contrast, a “blanked zone” on the recorded seismic section shows a decrease in seismic attenuation probably due to the presence of “load-bearing” gas hydrate.

Mandal, R., Dewangan, P., Ramprasad, T., Kumar, B.J.P, and Vishwanath, K., (this issue), Effect of thermal non-equilibrium, seafloor topography and fluid advection on BSR-derived geothermal gradient: Journal of Marine and Petroleum Geology. JMPG-D-13-00433	In this study 3D seismic data volumes from the Krishna-Godavari Basin in the vicinity of sites established during NGHP-01 was used to identify bottom simulating reflectors (BSRs). Geothermal gradients were estimated from the expected temperature at the seafloor as projected to the expected temperature at the depth of the seismic imaged BSR. The spatial variations in the BSR derived geothermal gradient show a strong correlation with seafloor topography in the Krishna-Godavari Basin. It was shown that the geothermal gradient decreases over the topographic mounds associated with inner toe-thrust faults and recent mass transport deposits. The temperature profile beneath the mapped mounds may not be in equilibrium with the surroundings stratigraphic section either due to recent uplift along the inner toe-thrust faults or rapid deposition of sediments due to slumping along the margin.
Ramana, M.V., Anitha, G., Desa, M., Ramprasad, T., and Dewangan, P., (this issue), Synthesis of deep multichannel seismic and high resolution sparker data: implications for the geological environment of KG offshore, Eastern Continental Margin of India: Journal of Marine and Petroleum Geology. JMPG-D-14-00126	This report presents an integrated study of deep multichannel and shallow high resolution seismic data from the Krishna-Godavari Basin, which focused on characterizing the geologic evolution of the shallow structural features in the basin. This study shows that the upper slope is mainly characterized by sediment subsidence, gas/fluid expulsion features and pathways, occasional diapiric intrusions and growth faulting, while the mid slope is associated with a minibasin containing low energy sediment deposits. The lower slope is characterized by intense faulting, thrusting, and diapiric intrusions. The multichannel seismic data was used to map six major sediment sequences in the basin from the Cretaceous to Recent. This study also revealed a direct link between the deeper and shallow structural features in the basin, inferring that the shallower thrust related gas release features may be the product of deep seated shale tectonism.
8. Basin and system analysis	
Cawthern, T., Johnson, J.E., Giosan, L., Flores, J.A., Rose, K., and Solomon, E., (this issue), A Late Miocene-Early Pliocene biogenic silica crash in the Andaman Sea and Bay of Bengal: Potential teleconnections to the Pacific: Journal of Marine and Petroleum Geology. JMPG-D-13-00450	This report integrates shipboard and downcore datasets from NGHP-02 with post-cruise analysis of biogenic silica mass accumulation rates from Sites NGHP-01-17 and -19. Theses analysis indicate that the biogenic silica (BSi) mass accumulation rates dramatically decreased nearly synchronously in the Andaman Sea and northern Bay of Bengal regions at approximately 6 Ma. This decrease in BSi primary productivity is coincident in time with diminished communication between Indian Ocean and Pacific Ocean water masses through the Indonesian through-flow. Subsequent recovery of BSi mass accumulation rates in the northern Bay of Bengal was likely supported through enhanced freshwater runoff from the Mahanadi River. This study provides, for the first time, surface water productivity analyses of Miocene-Recent sediments in the Andaman Sea and Northern Bay of Bengal regions. This study finds that Indian Ocean and Pacific Ocean water teleconnections have contributed to variations in surface water productivity in the Bay of Bengal and Andaman Sea regions; which provides novel insight into the long timescale interactions between Indian Ocean and Pacific Ocean water masses.
Flores, J.A., Johnson, J.E., Mejía-Molina, A.E., Álvarez, M.C., Sierro, F.J., Sing, S.D., Mahanti, S., and Goisan, L., (this issue), Sedimentation rates from calcareous nannofossil and planktonic foraminifera biostratigraphy in the Andaman Sea, northern Bay of Bengal, and eastern Arabian Sea: Journal of Marine and Petroleum Geology. JMPG-D-14-00085	In this study, the analysis of calcareous nannofossil and planktonic foraminifera in sediment cores collected during NGHP-01 allowed for the identification of several micropaleontological events that were astronomically calibrated to established chronological frameworks for six of the sites cored during NGHP-01. These results allowed the calculation sedimentation rates for representative sites in the Krishna-Godavari Basin, the Mahanadi Basin, the Andaman Sea, and the Kerala-Konkan Basin, as well as the identification of sedimentation hiatuses that were linked to the sedimentary history of each basin.
Joshi, R.K., Mazumdar, A., Peketi, A., Ramamurty, P.B., Naik, B.G., Kocherla, M., Carvalho, M.A., Mahalakshmi, P., Dewangan, P., and Ramana, M.V., (this issue), Gas hydrate destabilization and methane release events in the passive continental margin: A case study from the Krishna-Godavari basin, Bay of Bengal: Journal of Marine and Petroleum Geology. JMPG-D-14-00040	In this report, the investigators explorer the possible influence of methane emission on carbon isotope ratio of planktic and benthic foraminifera and further constrained the ages of the major methane expulsion events in the Krishna-Godavari Basin. This report presents the carbon-oxygen stable isotope ratios of planktic and benthic foraminifera and carbon isotope ratios of sediment organic matter and lipid extracts in a sediment core (MD161-8) from the Krishna-Godavari Basin. Based 14C and U/Th age dating of foraminiferal tests and authigenic carbonates respectively, a minimum age of 46 to 58 kyr was suggested for a significant methane expulsion event in the basin.
Kocherla, M., Pillai, S., Teichert, B.M.A., Satyanarayanan, M., Ramamurthy, P.B., Patil, D.J., and Rao, A.N., (this issue), Occurrence and genesis of gas-hydrate related authigenic carbonates from Krishna-Godavari offshore basin (Bay of Bengal): Journal of Marine and Petroleum Geology. JMPG-D-14-00090	This report presents the analysis of authigenic siderite and high-Mg calcite nodules/concretions from 17 long cores recovered from the Krishna-Godavari Basin. The cores were collected from the *R/V Marion Dufresne* in 2007. More than 100 carbonate nodules/concretions were recovered from the cores. The authors suggests that the abundant authigenic carbonate and the highly depleted carbon isotope ratios of the analyzed high-Mg calcite nodules, indicate that the carbon source for the formation of authigenic carbonates was from the flow of methane-enriched fluids from below through fracture network formed because of shale diapirism.
Phillips, S.C., Johnson, J.E., Giosan, L., and Rose, K., (this issue), Monsoon-influenced variation in productivity and lithogenic sediment flux since 110 ka in the offshore Mahanadi Basin, northern Bay of Bengal: Journal of Marine and Petroleum Geology. JMPG-D-13-00446	This report utilizes the cored sedimentary section recovered from the Mahanadi Basin during NGHP-01 to reconstruct biogenic and lithogenic sediment accumulation rates, organic carbon sources, and sources of magnetic susceptibility variation in the northern Bay of Bengal over the past 110,000 years. The authors use a multi-proxy approach to examine changes in productivity and terrigenous sedimentation on orbital timescales. The mass-accumulation rate of $CaCO_3$, a function of marine productivity, drastically increased between 10 and 70 ka and is correlated to previously-documented elevated Asian dust fluxes and increased Bay of Bengal salinity during a weakened southwest monsoon.
Teichert, B., Johnson, J.E., Giosan, L., Rose, K., Kocherla, M., Solomon, E.A., Connolly, E., and Torres, M.E., (this issue), Composition and origin of authigenic carbonates in the Krishna-Godavari and Mahanadi Basins, eastern continental margin of India: Journal of Marine and Petroleum Geology. JMPG-D-14-00083	Authigenic carbonate cements, (micro) nodules, bioturbation casts and tubes from 10 core locations drilled during NGHP-01 were investigated for this study. Three main processes responsible for authigenic carbonate precipitation were identified: organoclastic sulfate reduction, anaerobe methane oxidation, and methanogenesis. Evidence of vigorous methane seepage is indicated in the carbonates recovered at Sites NGHP-01-7, -10, and -12 in the Krishna-Godavari Basin and Site NGHP-01-19 in the Mahanadi Basin. Two separate horizons of methane seep carbonates were identified in the Krishna-Godavari Basin, with the upper horizon dated at 40,000-51,600 B.P., clearly indicating that methane seepage has been much more vigorous in the past possibly due to a glacial sea level lowstand.
Usapkar, A., Dewangan, P., Kocherla, M., Ramprasad, T., Mazumdar, A. and Ramana, M.V., (this issue), Neo methane flux event and sediment dispersal pattern in the Krishna-Godavari offshore basin: evidence from rock magnetic techniques: Journal of Marine and Petroleum Geology. JMPG-D-13-00360	In this study, detailed rock magnetic measurements such as susceptibility, susceptibility of anhysteric remnant magnetization, saturation isothermal remnant magnetization, and soft-isothermal remnant magnetization were carried out on samples collected from 73 near-surface gravity cores collected in the Krishna Godavari Basin to understand the distribution of sediment magnetic parameters and their relation to methane seepage. Core analysis at one of the core sites indicated a substantial loss in the concentration of magnetic minerals. Due to the close association of the dissolution of magnetic minerals with evidence of anaerobic methane oxidation, the reduced magnetization at the anomalous core site was attributed to a large release of HS_2. We believe that the methane flux was variable in the past which might have shifted the sulfate-methane transition zone (SMTZ) through time, with the release HS_2 facilitating the dissolution of magnetic minerals at the various paleo SMTZ depths.
9. Gas hydrate production and energy assessment	
Kneafsey, T., and Moridis, G.J., (this issue), X-Ray computed tomography examination and comparison of gas hydrate dissociation in NGHP-01 Expedition (India) and Mount Elbert (Alaska) sediment cores: experimental observations and numerical modeling: Experimental observations and numerical modeling: Journal of Marine and Petroleum Geology. JMPG-D-13-00462	Within this laboratory and modeling study, a total of 17 segments of pressure-core and non-pressurized-core samples collected during NGHP-01 were examined using X-ray computed tomography (CT) scanning. As part of this study, dissociation (depressurization and heating) test were also performed on a core from NGHP-01 and a core from the Mount Elbert Gas Hydrate Stratigraphic Test Well that was drilled in northern Alaska. The depressurization test of the Alaska hydrate-bearing core was also simulated using the TOUGH+HYDRATE computer code. The CT scans of the NGHP-01 core samples revealed the presence of hydrate in the form of veins, nodules, and disseminated in sedimentary layers. During the dissociation tests, changes were observed to the sample as the result of mechanical changes to the sediment matrix.
Ramesh, S., Vedachalam, N., Ramesh, R., Prasad, N.T., Ramadass, G.A., and Atmanand, M.A., (this issue), An approach for methane hydrates reservoir dissociation from the marine settings of Krishna Godhavari Basin, East Coast of India: Journal of Marine and Petroleum Geology. JMPG-D-14-00045	This report reviews the various techniques that might be used to produce gas from the clay-rich gas hydrate reservoirs in the Krishna-Godavari Basin. The authors present a new production concept in which an electrode placed in the gas hydrate reservoir is used to deliver heat energy to the formation and gas is produced to a well by sustained depressurization. The proposed production scheme was also modeled using a MATLAB program and simulated with the TOUGH+HYDRATE software code. The modeling results show that the calculated energy balance for the proposed production scheme is at a ratio of 1:4.

Table 2B

Reference	Synopsis
1. NGHP-01 project summaries	
Collett, T.S., Riedel, M., Boswell, R., Cochran, J.R., Kumar, P., Sethi, A.K., Sathe, A.V., and NGHP Expedition-01 Scientific Party, 2006, International team completes landmark gas hydrate expedition in the offshore of India: U.S. Department of Energy, National Energy Technology Laboratory, Fire-In-The-Ice Newsletter, v. 6, issue 3, 1-4.	This newsletter article summarized the operational and initial scientific results of the NGHP-01 Expedition. This article includes a review on the scientific goals of NGHP-01 and listed for the first time several of the key scientific findings.
Collett, T., Riedel, M., Cochran, J., Boswell, R., Kumar, P., Sathe, A., and the NGHP Expedition 01 Scientific Party, 2008, Indian continental margin gas hydrate prospects: results of the India National Gas Hydrate Program (NGHP) Expedition 01: Proceedings of the 6th International Conference on Gas Hydrates (ICGH 2008), Vancouver, British Columbia, Canada, July 6-10, 2008, p. 1-10.	This report provides a review of the operational and scientific results of NGHP-01. The report starts with a review of the planning phases of the NGHP-01 expedition, which is followed by a review of the NGHP-01 drilling results and the evidence for the occurrence of gas hydrates in the Krishna-Godavari Basin, the Mahanadi Basin, the Andaman Sea, and in the Kerala-Konkan Basin.
Collett, T., Riedel, M., Cochran, J., Boswell, R., Presley, J., Kumar, P., Sathe, A., Sethi, A., Lall, M., Siball, V., and the NGHP Expedition 01 Scientific Party, 2008, Indian National Gas Hydrate Program Expedition 01 Initial Reports: Prepared by the U.S. Geological Survey and Published by the Directorate General of Hydrocarbons, Ministry of Petroleum & Natural Gas (India), 1 DVD.	This was the NGHP-01 initial expedition report. This report contains the initial scientific results obtained from NGHP-01 and associated expedition data. This report includes a series of integrated drill site chapters describing the operational history and scientific data collected during the expedition. This report also contains a methods chapter, in which the procedures used to acquire and analyze sediment core and downhole log data have been described.
Collett, T., Riedel, M., Cochran, J., Boswell, R., Presley, J., Kumar, P., Sathe, A., Sethi, A., Lall, M., Siball, V., Guerin, G., Malinerno, A., Mrozewski, S., Cook, A., Sarker, G., Broglia, C., Goldberg, D., and the NGHP Expedition 01 Scientific Party, 2008b, Indian National Gas Hydrate Program Expedition 01 Downhole Log Data Report: Prepared by the U.S. Geological Survey and Published by the Directorate General of Hydrocarbons, Ministry of Petroleum & Natural Gas (India), 2 DVD set.	This was the NGHP Expedition 01 downhole log data report. This report includes the downhole logging-while-drilling and open-hole wireline tool coveyed well log data collected during NGHP-01.
Kumar, P., Collett, T.S., Sethi, A.K., Sathe, A.V., Sibal, V.K., Riedel, M., Boswell, R., Cochran, J.R., and NGHP Expedition-01 Scientific Party, 2007, Gas hydrate coring/drilling program in Indian Offshore – an overview of NGHP Expedition-01, 2006: Proceedings of the 7th International Oil and Gas Conference, PETROTECH-2007, New Delhi, India, January 15-19, 2007, p. 1-9.	This report provides an overview of the operational and scientific results of NGHP-01. This report includes a review of the planning and operational phases of the NGHP-01 expedition, which is followed by detailed descriptions of the NGHP01 drilling results and the evidence for the occurrence of gas hydrates in the Krishna-Godavari Basin, the Mahanadi Basin, the Andaman Sea, and in the Kerala-Konkan Basin.
2. Lithostratigraphic controls on the occurrence of gas hydrate	
Esteban, L., Enkin, R.J., and Hamilton, T., 2008, Gas hydrates and magnetism: comparative geological settings for diagenetic analysis: Proceedings of the 6th International Conference on Gas Hydrates (ICGH 2008), Vancouver, British Columbia, Canada, July 6-10, 2008, p. 1-9.	In this study, detailed magnetic investigation, complemented by petrological observations, were undertaken on sediment cores from the Mallik site in the Mackenzie Delta (Canada), and two marine settings, IODP Expedition 311 cores from the Cascadia margin and cores from NGHP-01 sites in the Krishna-Godavari Basin, the Mahanadi Basins, and the Andaman Sea. This report includes detailed stratigraphic profiles of fine scale variations in bulk magnetic measurements correspond to changes in lithology, grain size and pore fluid geochemistry. The lowest values of magnetic susceptibility were observed where iron has been reduced to paramagnetic pyrite, formed in settings with high methane and sulphate or sulphide flux, such as methane vent sites. High magnetic susceptibility values are observed in sediments which contain detrital magnetite, for example from glacial deposits, which has survived diagenesis. Other high magnetic susceptibility values were observed in sediments in which the ferrimagnetic iron-sulphide minerals greigite or smythite have been diagenetically introduced, which have been shown to be related to the occurrence of gas hydrate.
Phillips, S.C., Johnson, J.E., Miranda, E., and Disenhof, C., 2011, Improving CHN measurements in carbonate-rich marine sediments: Limnology and Oceanography: Methods, v. 9, p. 194-203.	In this report, the authors identify and describe three common problems related carbon, hydrogen, and nitrogen (CHN) elemental analysis and demonstrate these concerns with core samples collected during NGHP-01. For this study, total organic carbon (TOC), total carbon (TC), and total nitrogen (TN) contents were measured from core samples collected in the Krishna-Godavari Basin, Mahanadi Basin, Andaman Sea, and Kerala-Konkan Basin. The origin and evolution of the carbon and nitrogen content at these locations were integrated with the regional lithostratigraphic record for each site. The results of this study allowed for the development of sediment-specific protocols for accurate CHN measurements in carbonate-rich marine sediments.
Riedel, M., Collett, T.S., and Shankar, U., 2010, Documenting channel features associated with gas hydrates in the Krishna–Godavari Basin, offshore India: Marine Geology, v. 279, P. 1-11.	The main objective of this study was to show that the occurrence of gas hydrate is controlled by elements of the gas hydrate petroleum system: trap, seal, migration pathway, location relative to the base of gas hydrate stability zone. Evidence for a sand-dominated gas hydrate reservoir were recovered in cores and downhole log data from Site NGHP-01-15 in the Krishna–Godavari Basin. This study showed that the gas hydrate-bearing sand-rich reservoir section at Site NGHP-01-15 was linked to a prominent seismic reflection mapped on 3D seismic images along a 1-km long trend south of the drill site. The authors conclude this seismic reflection feature represents a channel system, and that local changes in the seismic character of the channel feature reveals the presence of sand-rich levee deposits.
3. Physical properties of gas hydrate-bearing sediments	
Anders, E., and Muller, W.H., 2008, Compact multipurpose sub-sampling and processing of in-situ cores with PRESS (Pressurized Core Sub-Sampling and Extrusion System): Proceedings of the 6th International Conference on Gas Hydrates (ICGH 2008), Vancouver, British Columbia, Canada, July 6-10, 2008, p. 1-6.	This report describes the design and use of the Technische Universität Berlin (TUB) Pressurized Core Sub-Sampling and Extrusion System (PRESS), which enables well-defined sectioning and transfer of drilled pressure-cores. PRESS when coupled with DeepIsoBUG (University Cardiff), which allows sub-sampling and incubation of coaxial core-sections to examine high-pressure adapted bacteria or biogeochemical processes without depressurization. Successful PRESS deployments in the Gulf of Mexico, on IODP Expedition 311 and as part of the NGHP-01 expedition demonstrated the contribution of the PRESS and DeepIsoBUG pressure core processing systems.
Clayton, C., Kingston, E., Priest, J., Schultheiss, P., and the NGHP Expedition 01 Scientific Party, 2008, Testing of pressurized cores containing gas hydrate from deep ocean sediments: Proceedings of the 6th International Conference on Gas Hydrates (ICGH 2008), Vancouver, British Columbia, Canada, July 6-10, 2008, p. 1-9.	This report summarizes the techniques used at Southampton University to handle and process pressure core samples obtained during NGHP-01. Some of the pressure cores, once recovered from the seafloor, were subject to rapid depressurization and immersed in liquid nitrogen for use in subsequent laboratory testing programs. The original intention was to re-pressurize and unfreeze the material before testing in the Gas Hydrate Resonant Column (GHRC) apparatus at Southampton University. Initial X-ray CT scanning of the samples, however, showed that the sample quality was too poor for such testing. Instead a suite of geotechnical testing was carried out, the results of which are included in this report.
Holland, M., Schultheiss, P., Roberts, J., and Druce, M., 2008, Observed gas hydrate morphologies in marine sediments: Proceedings of the 6th International Conference on Gas Hydrates (ICGH 2008), Vancouver, British Columbia, Canada, July 6-10, 2008, p. 1-7.	This report reviews the preliminary results of the physical properties program on NGHP-01 with a focus on analyzing the morphology of gas hydrate samples recovered in pressurized cores during the expedition. Upon recovery, pressure cores are subjected to nondestructive analyses, including gamma density, comprssional-wave velocity, and X-ray imaging to examine the character of the gas hydrate relative to the structure of the surrounding sediment. In this report, gas hydrate morphology from pressure cores are summarized from the recent gas hydrate expeditions in India (NGHP-01), China, and Korea, as well as from the Ocean Drilling Program Leg 204, the Integrated Ocean Drilling Program Expedition 311, and the Gulf of Mexico Joint Industry Project. The most striking result is the variability of gas hydrate morphology in clay-rich sediments, ranging from complex vein structures to pore-filling.

Kumar, P., Das, H.C., Anbazhagan, K., Lu, H., and Ripmeester, J.A., 2008, Structural characterization of natural gas hydrates in core samples from offshore India: Proceedings of the 6th International Conference on Gas Hydrates (ICGH 2008), Vancouver, British Columbia, Canada, July 6-10, 2008, p. 1-6.	In this report, the authors review and describe the physical nature of the solid forms of gas hydrate as recovered in cores during NGHP-01. In addition, the results of Raman, NMR and XRD laboratory analysis of selected gas hydrate samples are reported. The sampled gas hydrates were shown to be “structure I hydrate” with methane as the dominant guest molecule. The occupancy of the included methane in the large cage of the structure I hydrate was shown to be almost complete, while the methane occupancy was more variable in the small cages. The “hydrate number” for most of the hydrates averaged 6.10 ± 0.15.
Priest, J., Kingston, E., Clayton, C., Schultheiss, P., Druce, M., and the NGHP Expedition 01 Scientific Party, 2008, The structure of hydrate bearing fine grained marine sediments: Proceedings of the 6th International Conference on Gas Hydrates (ICGH 2008), Vancouver, British Columbia, Canada, July 6-10, 2008, p. 1-8.	As documented in this report, recent advances in pressure coring technology, such as new pressure coring tools and transfer systems used on NGHP-01 enabled the recovery and analysis of fine grained sediments with intact gas hydrate, which has provided the opportunity to study the morphology of gas hydrates within fine grained sediments. Results have shown that in fine grained sediments gas hydrates grow along fractures and faults within the sediment. This effort has also shown that sample disturbance is still a major concern and further techniques are required to limit these effects.
Rees, E.V.L., Priest, J.A., and Clayton, C.R.I., 2011, The structure of methane gas hydrate bearing sediments from the Krishna-Godavari Basin as seen from micro-CT scanning: Journal of Marine and Petroleum Geology, v. 28, p. 1,283-1,293.	In this laboratory study, pressure cores (from Sites NGHP-01-10 and -21) recovered from the Krishna-Godavari Basin during NGHP-01 were examined shore based after the expedition. Once on shore, high resolution X-ray CT scanning was employed to obtain detailed three-dimensional images of the internal structure of each hydrate-bearing core, which yielded evidence of persistent gas hydrate vein like features. The majority of hydrate veins were found to be orientated between 50 and 80 degrees to the horizontal. Analysis of the strike of the veins suggested a slight preferential orientation in each individual section, which allowed the authors to concluded that hydraulic fracturing by upward advecting pore fluids was the main formation mechanism for the veined hydrate deposits at Sites NGHP-01-10 and -21.
Stern, L.A., and Kirby, S.H., 2008, Natural gas hydrates up close: a comparison of grain characteristics of sample from marine and permafrost environments as revealed by cryogenic SEM: Proceedings of the 6th International Conference on Gas Hydrates (ICGH 2008), Vancouver, British Columbia, Canada, July 6-10, 2008, p. 1-12.	The authors of this report used cryogenic SEM technology to investigate the physical nature of gas-hydrate-bearing samples recovered by drill core along the India margin (NGHP-01), Cascadia margin (IODP Leg 311), Gulf of Mexico (R/V Marion Dufresne in 2002), and Mackenzie River Delta (Mallik site). Preliminary assessment of India NGHP-01 samples and others indicate that gas hydrate often occurs as a dense substrate with a significant fraction of isolated mircopores. Other NGHP-01 samples revealed regions dominated by highly faceted gas hydrate crystals that line the walls of cavities where the hydrate appeared to have grown unimpeded.
Winters, W.J., 2011, Physical and geotechnical properties of gas-hydrate-bearing sediment from offshore India and the northern Cascadia Margin compared to other hydrate reservoirs: Proceedings of the 7th International Conference on Gas Hydrates (ICGH 2011), Edinburgh, Scotland, United Kingdom, July 17-21, 2011, p. 1-22.	In this summary report, the physical and geotechnical properties of gas-hydrate-bearing sediment from a number of different geologic settings have been presented and compared. It was shown that coarser-grained sediments in the Arctic (e.g., North Slope of Alaska; Mackenzie Delta, Northwest Territories) can contain gas-hydrate at high pore saturations, while finer-grained sediments in numerous offshore marine settings (e.g., offshore India) tend to have more complex gas-hydrate morphologies, including nodules, layers, and high-angle planar and rotational veins.
Winters, W.J., Waite, W.F., and Mason, D.H., 2008, Physical properties of pressurized samples recovered during the 2006 National Gas Hydrate Program Expedition offshore India: Proceedings of the 6th International Conference on Gas Hydrates (ICGH 2008), Vancouver, British Columbia, Canada, July 6-10, 2008, p. 1-10.	This report reviews the preliminary results of the physical properties program on NGHP-01 with a focus on analyzing pressurized core samples from the expedition. This report contains the index property, acoustic velocity, and triaxial shear test results for samples recovered from the Krishna-Godavari Basin. In addition, the authors discussed the effects of sample storage temperature, handling, and change in structure of fine-grained sediment.
Yun, Tae-Sup, Fratta, D., and Santamarina, J.C., 2010, Hydrate-bearing sediments from the Krishna-Godavari Basin: physical characterization, pressure core testing, and scaled production monitoring: Energy Fuels, v. 24, p. 5,972-5,983.	In this study, three pressure cores collected from the Krishna-Godavari Basin during NGHP-01 were tested at an onshore facility in Singapore after the expedition. The cores were maintained under ~13 MPa fluid pressure for 3 months before being tested. The test program included the measurement of elastic wave velocity, shear strength, and electrical conductivity, followed by fast depressurization of the sub-sampled core samples. A specially designed “instrumented pressure testing chamber” (IPTC) was used to characterize the cores. X-ray images showed horizontal layering, pronounced heterogeneity from milli- to centimeter scales, with the presence of high-density nodules and both horizontal and sub-vertical gas hydrate lenses. Regions of the cores with high P- and S-wave velocities, low electrical conductivity, and high undrained shear strength were identified as apparent hydrate-bearing portions of the tested specimens. Physical properties were also monitored during the depressurization of pressure cores.
4. Interstitial-water and gas geochemistry	
Kastner, M., Spivack, A.J., Torres, M., Solomon, E.A., Borole, D.V., Robertson, G., and Das, H.V., 2008, Gas hydrates in three Indian Ocean regions, a comparative study of occurrence and subsurface hydrology: Proceedings of the 6th International Conference on Gas Hydrates (ICGH 2008), Vancouver, British Columbia, Canada, July 6-10, 2008, p. 1-6.	This report reviews the preliminary results of the inorganic geochemistry program on NGHP-01 with a focus on characterizing the geologic controls on the occurrence of gas hydrate in the Krishna-Godavari Basin, the Mahanadi Basins, and the Andaman Sea. Only in the Krishna-Godavari Basin, at Site NGHP-01-10 were higher than seawater chloride concentrations observed. In the Andaman Sea and Mahanadi Basin, only lower than seawater chloride concentrations were measured. In the Krishna-Godavari Basin, the highest gas hydrate concentrations were associated with fracture zones in clay-rich sediments and/or in some coarser grained units. In the Andaman Sea, however, they are primarily associated with volcanic ash horizons. Overall, the percent pore gas hydrate volume occupancies based on pressure core methane concentrations and the chloride concentrations in conventional cores are similar. Isotopic analysis of dissolved inorganic carbon (DIC) indicate that anaerobic oxidation of methane (AOM) is an important reaction responsible for sulfate reduction at most of the NGHP-01 sites. At several sites in the Krishna-Godavari Basin, however, the DIC isotopic values indicate that organic matter oxidation is the dominant reaction.
Mazumdar, A., Dewangan, P., Joao, H.M., Peketi, A., Khosla, V.R., Kocherla, M., Badesab, F.K., Joshi, R.K., Roxanne, P., Ramamurty, P.B., Karisiddaiah, S.M., Patil, D.J., Dayal, A.M., Hawkesworth, C.J., and Avanzinelli, R., 2009, Evidence of paleo–cold seep activity from the Bay of Bengal, offshore India: Geochemistry, Geophyscis, Geosystems, v. 10, no. 6, p. 1-15.	This report examines evidence for paleo-cold seeps as preserved in the methane-derived carbonate record associated with chemosynthetic clams from sediment cores in the Krishna-Godavari Basin (closely associated with Site NGHP-01-10) as collected during a cruise of the *R/V Marion Dufresne* , which showed a zone with a sharp increase in carbonate content within 16-20 mbsf. The presence of high Mg calcite cement, and pyrite within this zone suggest the seepage of methane and sulfide-bearing fluid to the seafloor in the past. The observed carbonate deposition might have resulted from the flow of methane-enriched fluids through the fracture network formed because of shale diapirism about 46.2 to 53.0 ka.
Mazumdar, A., Joao, H.M., Peketi, A., Dewangan, P., Kocherla, M., Joshi, R.K., and Ramprasad, T., 2012, Geochemical and geological constraints on the composition of marine sediment pore fluid: possible link to gas hydrate deposits: Journal of Marine and Petroleum Geology, v. 38, p. 35-52.	Pore water sulfate consumption in marine sediments is in part controlled by microbially driven sulfate reduction via organo-clastic and methane oxidation processes. In this study, the authors presented sediment pore fluid compositions for 10 long piston cores from the Krishna-Godavari Basin. These results show occurrence of transient (S and kink types) and steady state (quasi-linear) sulfate concentration profiles which were attributed partly to the anaerobic oxidation of methane and organo-clastic sulfate reduction. The presence of authigenic carbonates in multiple layers, with highly depleted carbon isotope ratios, also suggested the marked fluctuation in vertical methane flux through time. The observed S or kinked sulfate profiles were interpreted as additional evidence of recent enhancement in vertical methane flux possibly driven by reactivation of fault/fracture systems which provide the conduits for fluid flow.
Mazumdar, A., Peketi, A., Joao, H.M., Dewangan, P., and Ramprasad, T., 2014, Pore-water chemistry of sediment cores off Mahanadi Basin, Bay of Bengal: Possible link to deep seated methane hydrate deposit: Journal of Marine and Petroleum Geology, v. 49, p. 162-175.	In this study, pore-fluid composition of three piston cores (36-39 m long), collected in close proximity to NGHP-01-18 and -19 in the Mahanadi Basin, were analyzed to characterize the influence of organoclastic degradation and anaerobic oxidation of methane on the in situ concentration of sulfate, methane, and bicarbonate. The reported pore-fluid compositions reveal markedly consistent pore-water sulfate, alkalinity, ammonium and methane concentration profiles with depth. These quasi-linear concentration profiles and a shallow sulfate-methane transition zone (SMTZ) suggests high diffusive methane flux likely originating from below the base of gas hydrate stability zone.

Solomon, E.A., Spivack, A.J., Kastner, M., Borole, D.V., Robertson, G., and Das, H.V., 2008, Hydrogeochemical and structural controls on heterogeneous gas hydrate distribution in the K-G Basin offshore SE India: Proceedings of the 6th International Conference on Gas Hydrates (ICGH 2008), Vancouver, British Columbia, Canada, July 6-10, 2008, p. 1-10.	This report reviews the preliminary results of the inorganic geochemistry program on NGHP-01 with a focus on characterizing the occurrence of gas hydrate in the Krishna-Godavari Basin. The geochemical composition of pore fluids recovered from pressurized and non-pressurized cores show that the occurrence and concentration of gas hydrate varies considerably between the NGHP-01 sites in the Krishna-Godavari Basin. In all but three sites cored, gas hydrate is mainly disseminated within the pore space with typical pore space occupancies being <2%. Massive occurrences of gas hydrate are controlled by high-angle fractures in clay/silt sediments at three sites, and locally by lithology (sand/silt) at the more "diffuse" sites with a maximum pore space occupancy of ~67%.
5. Microbiologic systems	
Briggs, B., Colwell, F., Carini, P., Torres, M., Hangsterfer, A., Kastner, M., Brodie, E., Daly, R., Holland, M., Long, P., Schaef, H., Delwiche, M., Winters, W., and Riedel, M., 2008, Distribution of the dominant microbial communities in marine sediments containing high concentrations of gas hydrates: Proceedings of the 6th International Conference on Gas Hydrates (ICGH 2008), Vancouver, British Columbia, Canada, July 6-10, 2008, p. 1-6.	This report reviews the preliminary results of the microbiological sampling program on NGHP-01. The primary objective of this effort was to determine the quantity, diversity, and distribution of microbial communities in the context of abiotic (e.g., grain size, presence/absence of hydrates) and geochemical (redox state, organic carbon content) properties in gas-rich marine sediments. Understanding the fine-scale distribution and factors that control the presence of sediment communities provides better parameters for computational models that describe carbon cycling in these systems.
Briggs, B.R., Inagaki, F., Morono, Y., Futagami, T., Huguet, C., Rosell-Mele, A., Lorenson, T.D., and Colwell, F.S., 2012, Bacterial dominance in subseafloor sediments characterized by methane hydrates: Federation of European Microbiological Societies, Microbiology Ecology, v. 81, no. 1, p. 88-98.	The objective of this study was to determine microbial abundance and diversity in sediments associated with the occurrence of gas hydrate in the Andaman Sea. In this study, Forty-three sediment samples were collected cores obtained from Site NGHP-01-17 at various depths that span the interval from 20–700 mbsf. Microscopic cell enumeration revealed that most sediment layers exhibited low microbial abundance. Statistical analysis of terminal restriction fragment length polymorphisms revealed distinct microbial communities from above, within, and below the zone of gas hydrate occurrence, which also correlated with a decrease in orgainic carbon.
6. Well log analysis	
Cook, A.E., Anderson, B.I., Malinverno, A., Mrozewski, S., and Goldberg, D.S., 2010, Electrical anisotropy due to gas hydrate-filled fractures: Geophysics, v. 75, no. 6, p. F173-F185.	In this study, downhole log data collected from the Krishna-Godavari Basin during NGHP-01 are used to characterize the nature of the gas hydrate filled fractures systems at two drill sites: NGHP-01-10 and NGHP-01-5. This study documented the fact that Archie derived resistivity log calculations will often over estimate gas hydrates saturations in gas hydrate filled fractures systems when compared to gas hydrate saturations obtained from other downhole logs and core data. The authors also note that intervals with near-vertical gas hydrate-filled fractures, there is considerable separation between phase shift and attenuation resistivity logs. Well log response modeling also showed that near-vertical hydrate-filled fractures can cause the abnormally high resistivity measurements in vertical holes due to electrical anisotropy.
Cook, A.E., and Goldberg, D., 2008, Extent of gas hydrate filled fracture planes: implications for in situ methanogenesis and resource potential: Geophysical Research Letters, v. 35, L15302, p. 1-5.	In this study, downhole logging-while-drilling borehole resesitivity images from two holes located 11 m apart drilled during NGHP-01 revealed high-angle gas hydrate filled fracture planes along a 31 m thick section in both holes. Monte Carlo simulations of hole locations, hole deviations, strike and dip, indicated that the fracture planes in the two holes are not the same feature. It was concluded that the gas hydrate filled fracture planes likely only extend a few meters laterally from each borehole and occur in an isolated horizontal interval, suggesting that the gas with these isolated fracture systems was formed by local microbial activity within the gas hydrate stability zone. The authors concluded that gas production from these reservoirs may be challenging.
Cook, A., and Goldberg, D., 2008, Stress and gas hydrate-filled fracture distribution, Krishna-Godavari Basin, India: Proceedings of the 6th International Conference on Gas Hydrates (ICGH 2008), Vancouver, British Columbia, Canada, July 6-10, 2008, p. 1-8.	In this report, the authors examine the high resistivity hydrate-bearing fractures found in unconsolidated clay sediments on logging-while-drilling borehole resistivity images from Sites NGHP-01-5, -6, -7,and -10 in the Krishna-Godavari Basin. The hydrate-filled fractures in these settings have aligned with the local stress regime. The authors also concluded, at Site NGHP-01-10, where 130 m thick section of gas hydrate-filled fractures were observed, fracturing is chaotic, likely associated with high gas flux rates.
Ghosh, R., Sain, K., and Ojha, M., 2010, Effective medium modeling of gas hydrate -filled fractures using the sonic log in the Krishna -Godavari basin, offshore eastern India: Journal of Geophysical Research, v. 114, B07102, p. 1-13.	In this report, it was shown by the analysis of logging-while-drilling resistivity-at-bit images and pressure cores collected during NGHP-01 in the Krishna-Godavari Basin that the morphology of gas hydrate occurrence in clay-rich sediment varies from complex vein structures (grain displacing) to invisible pore filling. Existing rock physics models, which relate acoustic data to in situ gas hydrate concentrations, generally assume an isotropic pore-filling gas hydrate nature, which yields misleading concentration estimates for fractured dominated gas hydrate occurrences in fine-grained sediments. In this study, the authors introduce and apply an unique effective medium theory to incorporate grain-displacing morphologies. The new model was used to estimate gas hydrate concentrations from sonic log velocities at Site NGHP-01-10 considering three basic gas hydrate morphologies: pore filling, grain displacing, and a combination of grain displacing and pore filling.
Lee, M.W., and Collett, T.S., 2009, Gas hydrate saturations estimated from fractured reservoir at Site NGHP-01-10, Krishna-Godavari Basin, India: Journal of Geophysical Research, v. 114, B07102, p. 1-13.	Recent studies show that gas-hydrate saturations estimated from resistivity- and acoustic-log data in near-vertical fracture systems (assuming isotropic reservoir conditions) are much higher than those estimated from pressure-core analysis. To reconcile this difference, the authors of this report presented an anisotropic gas-hydrate reservoir model. The analysis of logging-while-drilling and wireline resistivity-log data from Site NGHP-01-10 in India, yielded gas-hydrate saturations ranging from about 50 to 80% within an apparent fractured-dominated gas-hydrate system. Gas-hydrate saturations estimated from pressure cores in the same interval were less than about 25%. The primary cause for the difference in the resistivity-log- and pressure-core-derived gas hydrate saturations was attributed to the anisotropic nature of the reservoir due to the presence of gas hydrate in high-angle fractures. By using higher values for the Archie "cementation constant" m and the "saturation exponent" n in the resistivity analysis for fractured reservoirs, the authors of this report were able to significantly reduce the difference between the resistivity-log- and pressure core-derived saturation estimates.
Shankar, U., and Riedel, M., 2011, Gas hydrate saturation in the Krishna-Godavari Basin from p-wave velocity and electrical resistivity logs: Journal of Marine and Petroleum Geology, v. 28, no. 10, p. 1,768-1,778.	In this study, electrical resistivity logs from 10 sites drilled in the Krishna-Godavari Basin during NGHP-01 were used for gas hydrate saturation estimates using Archie's method. The authors also calculated gas hydrate saturation from sonic compressional-wave velocity logs assuming the gas hydrate in-frame effective medium rock-physics model for each site. For the most part, these combined well log evaluation techniques yielded relatively low (<5% of the pore space) gas hydrate saturations for the basin. However, several intervals of increased hydrate saturations were observed at Sites NGHP-01-03, -05 and -07. The well log calculate gas hydrate saturations and sediment porosities, were used along with gas hydrate stability modeling to estimate the total amount of gas hydrate within the Krishna-Godavari Basin, which was estimated to range from 5.7 to 32.1 trillion cubic feet of gas.
7. Geophysical analysis	
Prakash, A., Samanta, B.G., and Singh, N.P., 2010, A seismic study to investigate the prospect of gas hydrate in Mahanadi deep water basin, northeastern continental margin of India: Marine Geophysics Research, v. 31, p. 253-262.	In this study, a 3D seismic data volume covering 3,420 km^2 of the Mahanadi Basin was examined for seismic proxies related to the existence of gas hydrate. This examination revealed the presence of bottom simulating reflector (BSR) like features over a large areal portion of the basin. Coherency inversion of pre-stack time migration (PSTM) gathers shows an inversion of interval velocities across the BSR interfaces, which indicates hydrate bearing sediments overlying free gas bearing sediments.

Riedel, M., Collett, T.S., Kumar, P., Sathe, A.V., and Cook, A., 2010, Seismic imaging of a fractured gas hydrate system in the Krishna-Godavari Basin offshore India: Journal of Marine and Petroleum Geology, v. 27, p. 1,476-1,493.	In this study, logging-while-drilling (LWD), coring, and wire-line logging data from Site NGHP-01-10 in the Krishna-Godavari Basin was used to examine a thick, clay-rich, fracture-dominated gas hydrate system. Three-dimensional (3D) seismic data were also used in this study to image the fracture system and explain the occurrence of gas hydrate associated with the fractures. The LWD-derived fracture network at this site was mapped using seismic coherency attributes, which revealed a triangular-shaped fracture system cover an area of about 2.5 km^2. The authors concluded, that the occurrence of gas hydrate at Site NGHP-01-10 is the result of a specific combination of tectonic fault orientations and the migration of abundant of gas from a deeper source. It was also speculated that other similar features likely exist in the basin.
Sain, K., and Gupta, H., 2012, Gas hydrates in India: potential and development: Gondwana Research, v. 22, p. 645-657.	The authors of this report summarize the geologic and geophysical evidence for the occurrence of gas hydrate in the offshore of India. In this report the gas hydrates stability thickness map for offshore India has been updated and presented; the occurrence of seismic bottom simulating reflectors in the Krishna–Godavari, Mahanadi, Andaman, Kerala–Konkan, and Saurashtra regions have been described; seismic attenuation, reflection strength, instantaneous frequency and seismic blanking have been computed to characterize the sediments containing gas hydrate and free-gas. The authors have developed several approaches based on seismic travel-time tomography, full-waveform inversion, and amplitude versus offset (AVO) modeling to quantify gas hydrate concentrations in various expected gas hydrate accumulations. The authors of this report suggests "that free-gas lying below gas hydrate-bearing sediments can be produced economically in near future; however, it may take longer time to retrieve gas from gas hydrates."
8. Basin and system analysis	
Cochran, J.R., 2010, Morphology and tectonics of the Andaman Forearc, northeastern Indian Ocean: Geophysical Journal International, v. 182, p. 631-651.	This report summarizes the tectonic evolution of the Andaman Forearc in part from seismic and core data collected in support of the NGHP-01 Expedition. The stated purpose of this study was to assemble all available geophysical data to systematically define the morphology, structure and tectonics of the Andaman forearc region. As described in this report, the Andaman Sea has developed as the result of highly oblique subduction at the western Sunda Trench, leading to partitioning of convergence into trench-perpendicular and trench-parallel components and the formation of a northward-moving sliver plate to accommodate the trench parallel motion.
Mazumdar, A., Joshi, R.K., Peketi, A., and Kocherla, M., 2011, Occurrence of faecal pellet-filled simple and composite burrows in cold seep carbonates: a glimpse of a complex benthic ecosystem: Marine Geology, v. 289, P. 117-121.	In this study, the authors report on the occurrence of faecal pellet filled burrow casts associated with cold seep carbonate deposits located near Site NGHP-01-10 in the Krishna–Godavari Basin. This study provided additional evidence for seafloor methane expulsion that resulted in the development of a cold seep ecosystem in the basin.
Ponton, C., Giosan, L., Eglinton, T.I., Fuller, D.Q., Johnson, J.E., Kumar, P., and Collett, T.S., 2012, Holocene aridification of India: Geophysical Research Letters, v. 39, L03704, p. 1-6.	The authors of this study, reconstructed the Holocene paleoclimate of the "core monsoon zone" (CMZ) of the Indian peninsula using a sediment core recovered during NGHP-01 in the Krishna-Godavari Basin. Carbon isotopes of sedimentary leaf waxes documented a gradual increase in aridity-adapted vegetation from 4,000 until 1,700 years ago. The oxygen isotopic composition of planktonic foraminifer revealed unprecedented high salinity events in the Bay of Bengal over the last 3,000 years, which suggest that the CMZ aridification intensified in the late Holocene through a series of sub-millennial dry episodes.
Ramana, M.V., Ramprasad, T, Paropkari, A.L., Borole, D.V., Rao, B.R., Karisiddaiah, S.M., Desam M., Kocherla, M., Joao, H.M., Lokabharati, P., Gonsalves, M.J., Pattan, J.N., Khadge, N.H., Babu, C.P., A.V., Kumar, P., and Sethi, A.K., 2009, Multidisciplinary investigations exploring indicators of gas hydrate occurrence in the Krishna–Godavari Basin offshore, east coast of India: Geo-Marine Letters, v. 29, p. 25-38.	This reports deals with the results of a multidisciplinary investigation carried out within the framework of the Indian National Gas Hydrate Program in in the Krishna–Godavari Basin. This report summarizes the evidence for the occurrence of gas hydrate as indicated by the analysis of multi-channel seismic reflection data and estimates of gas hydrate stability zone thickness in the basin. Deep-tow digital side-scan sonar, multi-frequency chirp sonar, and sub-bottom profiler records were used to identify several surface and subsurface gas-escape features along the margin. Multi-channel seismic reflection data show the presence of bottom simulating reflections of continuous to discrete character. This study concluded that the geologic conditions in the Krishna–Godavari Basin were conducive for the occurrence of gas hydrate, which was confirmed with well log and core data collected during NGHP-01.
Shankar, U., and Riedel, M., 2010, Seismic and heat flow constraints from the gas hydrate system in the Krishna–Godavari Basin, India: Marine Geology, v. 276, P. 1-13.	The authors of this report re-interpreted 2D multi-channel seismic reflection profiles from the Krishna–Godavari Basin to further characterize the various seismic indicators for the presence of gas hydrate and associated free gas. This study was guided by new geothermal modeling of the gas hydrate stability conditions in the basin with borehole temperature data collected from NGHP-01 and bottom simulating reflector (BSR) depths interpreted from the available grid of 2D seismic data. The new thermal modeling effort provided a more complete view of the base of the gas hydrate stability zone across the basin. This study suggests that the gas hydrate stability zone in the Krishna–Godavari Basin is impacted by local variations in heat flow associated with topographic focusing and defocusing effects and local faulting and fluid flux. In general, the BSR-derived heat flow values increase towards the deeper water portion of the basin.
Shankar, U., Riedel, M., and Sathe, A.V., 2010, Geothermal modeling of the gas hydrate stability zone along the Krishna Godavari Basin: Marine Geophysics Research, v. 31, p. 17-28.	The aim of this study was to understand the detailed variation of heat flow estimated from the depth of mapped bottom simulating reflectors (BSRs) identified on a high resolution grid of seismic profiles across the Krishna–Godavari Basin. The thickness of the gas hydrate stability zone inferred from mapped BSR depths ranges up to 250 m. Downhole temperature data collected during NGHP-01 was also used to refine the subsurface heat flow model for the Krishna–Godavari Basin. The predicted gas hydrate stability zone depths as derived from the geothermal model closely matches the observed BSR depths.
Shukla, K.M., Tyagi, A.K., and Bhowmick, P.K., 2012, Geophysical studies for Natural gas Hydrate in East seacoast of India: Geohorizons, January, 2012, p. 73-81.	This report summarizes key developments in the history of gas hydrate geologic and geophysical studies globally and describes recent analysis of seismic data for the occurrence of gas hydrate in India. This report also describes the drill site review and selection process in support of the second expedition of National Gas Hydrate Program (NGHP-02) of India. Exploration activities have focused on the identification of sand-rich reservoir systems in the Krishna-Godavari Basin and Mahanadi Basin.

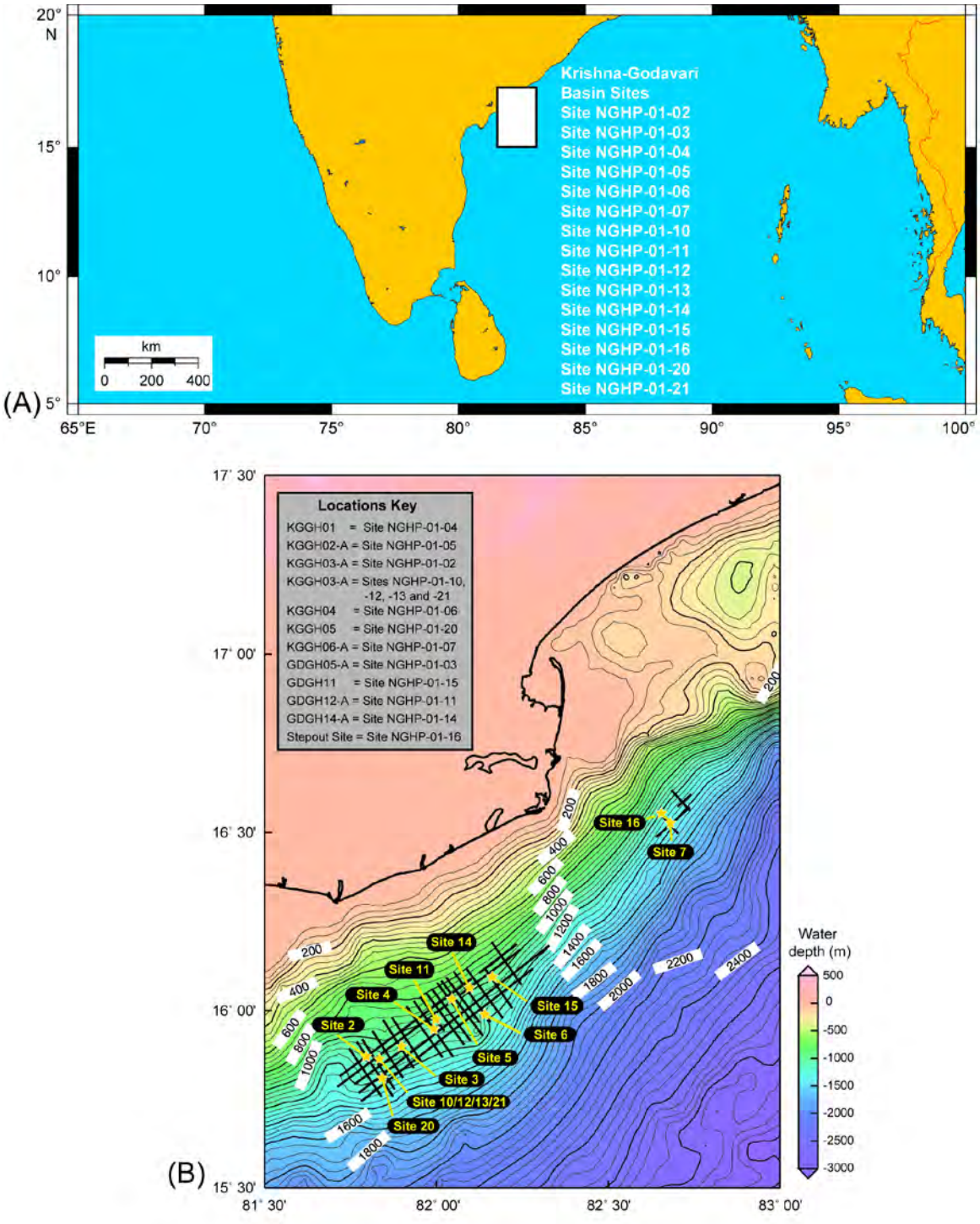
(A)
20° N
15°
10°
5°
65°E
70°
75°
80°
85°
90°
95°
100°
km
0 200 400
Krishna-Godavari Basin Sites
Site NGHP-01-02
Site NGHP-01-03
Site NGHP-01-04
Site NGHP-01-05
Site NGHP-01-06
Site NGHP-01-07
Site NGHP-01-10
Site NGHP-01-11
Site NGHP-01-12
Site NGHP-01-13
Site NGHP-01-14
Site NGHP-01-15
Site NGHP-01-16
Site NGHP-01-20
Site NGHP-01-21
(B)
17° 30'
17° 00'
16° 30'
16° 00'
15° 30'
81° 30'
82° 00'
82° 30'
83° 00'
Locations Key
KGGH01 = Site NGHP-01-04
KGGH02-A = Site NGHP-01-05
KGGH03-A = Site NGHP-01-02
KGGH03-A = Sites NGHP-01-10, -12, -13 and -21
KGGH04 = Site NGHP-01-06
KGGH05 = Site NGHP-01-20
KGGH06-A = Site NGHP-01-07
GDGH05-A = Site NGHP-01-03
GDGH11 = Site NGHP-01-15
GDGH12-A = Site NGHP-01-11
GDGH14-A = Site NGHP-01-14
Stepout Site = Site NGHP-01-16
Site 16
Site 7
Site 14
Site 11
Site 4
Site 2
Site 15
Site 6
Site 5
Site 3
Site 10/12/13/21
Site 20
200
400
600
800
1000
1200
1400
1600
1800
2000
2200
2400
Water depth (m)
500
0
-500
-1000
-1500
-2000
-2500
-3000

Figure 1

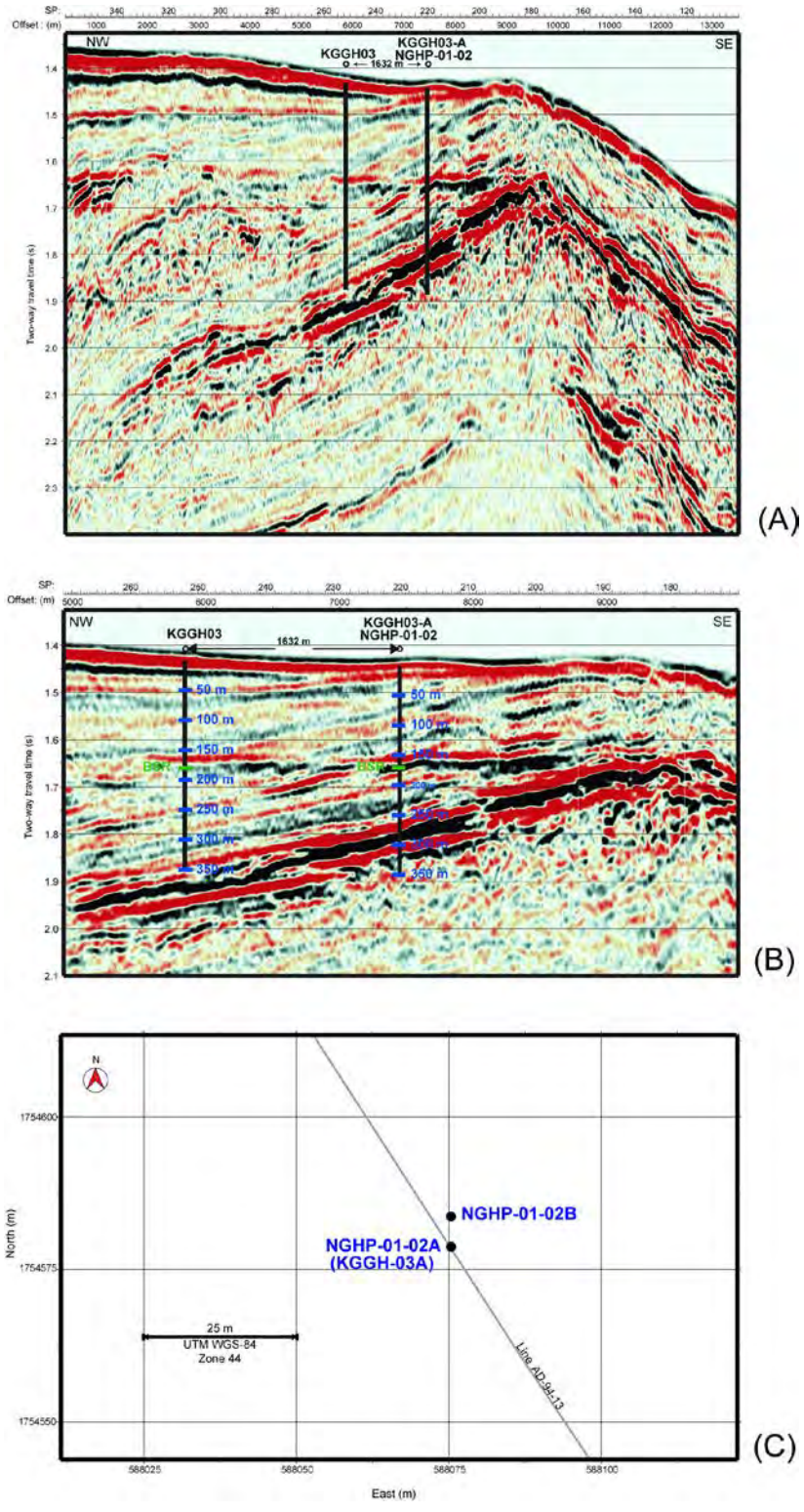
SP:
Offset : (m)
NW
SE
KGGH03
KGGH03-A
NGHP-01-02
1632 m
Two-way travel time (s)
(A)
50 m
100 m
150 m
200 m
250 m
300 m
350 m
BSR
Two-way travel time (s)
(B)
N
North (m)
East (m)
NGHP-01-02B
NGHP-01-02A
(KGGH-03A)
25 m
UTM WGS-84
Zone 44
Line AD94-13
1754600
1754575
1754550
588025
588050
588075
588100
(C)

Figure 2

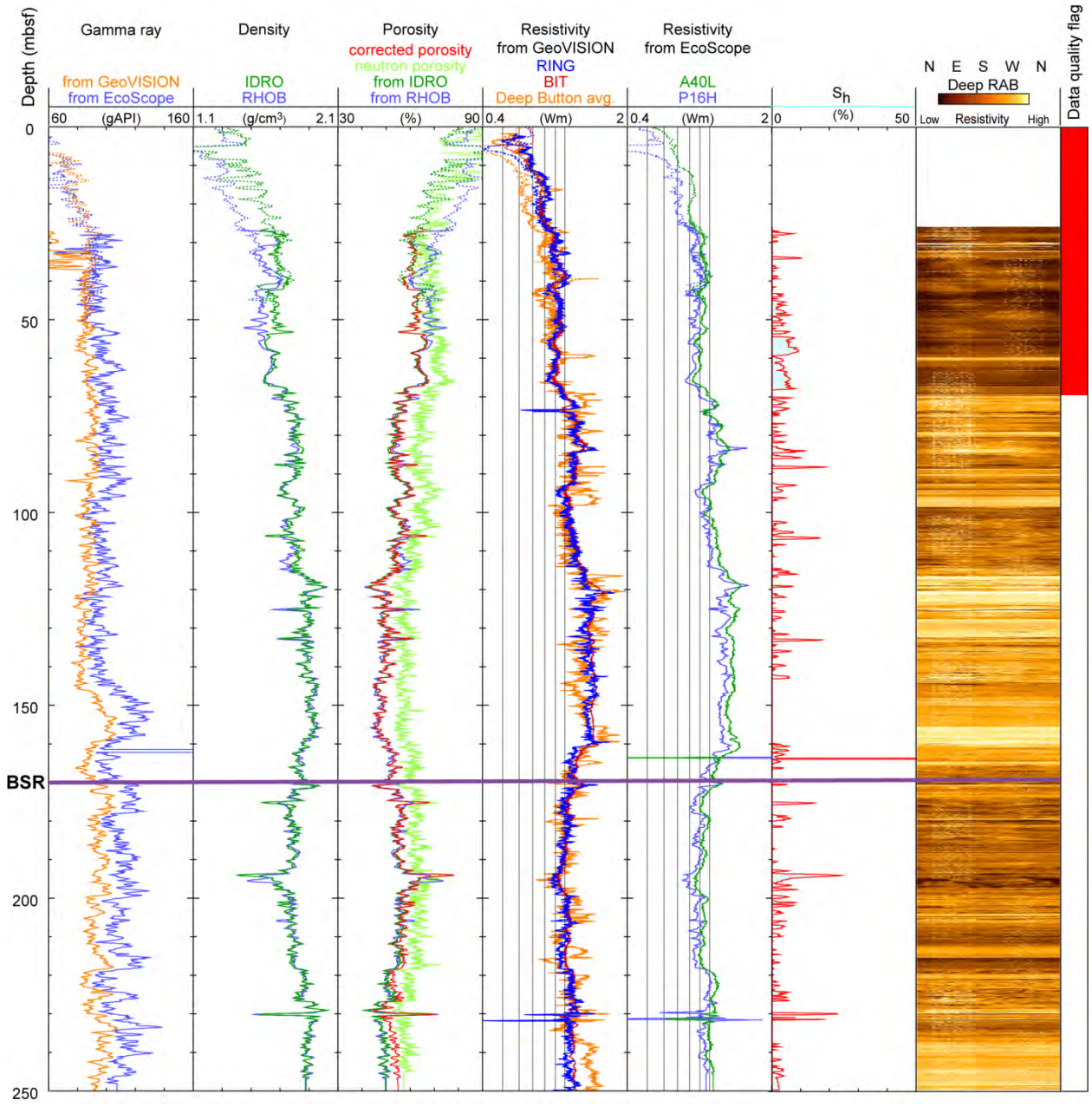
Depth (mbsf)
Gamma ray
from GeoVISION
from EcoScope
60 (gAPI) 160
Density
IDRO
RHOB
1.1 (g/cm3) 2.1
Porosity
corrected porosity
neutron porosity
from IDRO
from RHOB
30 (%) 90
Resistivity
from GeoVISION
RING
BIT
Deep Button avg.
0.4 (Wm) 2
Resistivity
from EcoScope
A40L
P16H
0.4 (Wm) 2
Sh
0 (%) 50
N E S W N
Deep RAB
Low Resistivity High
Data quality flag
0
50
100
150
BSR
200
250

Figure 3

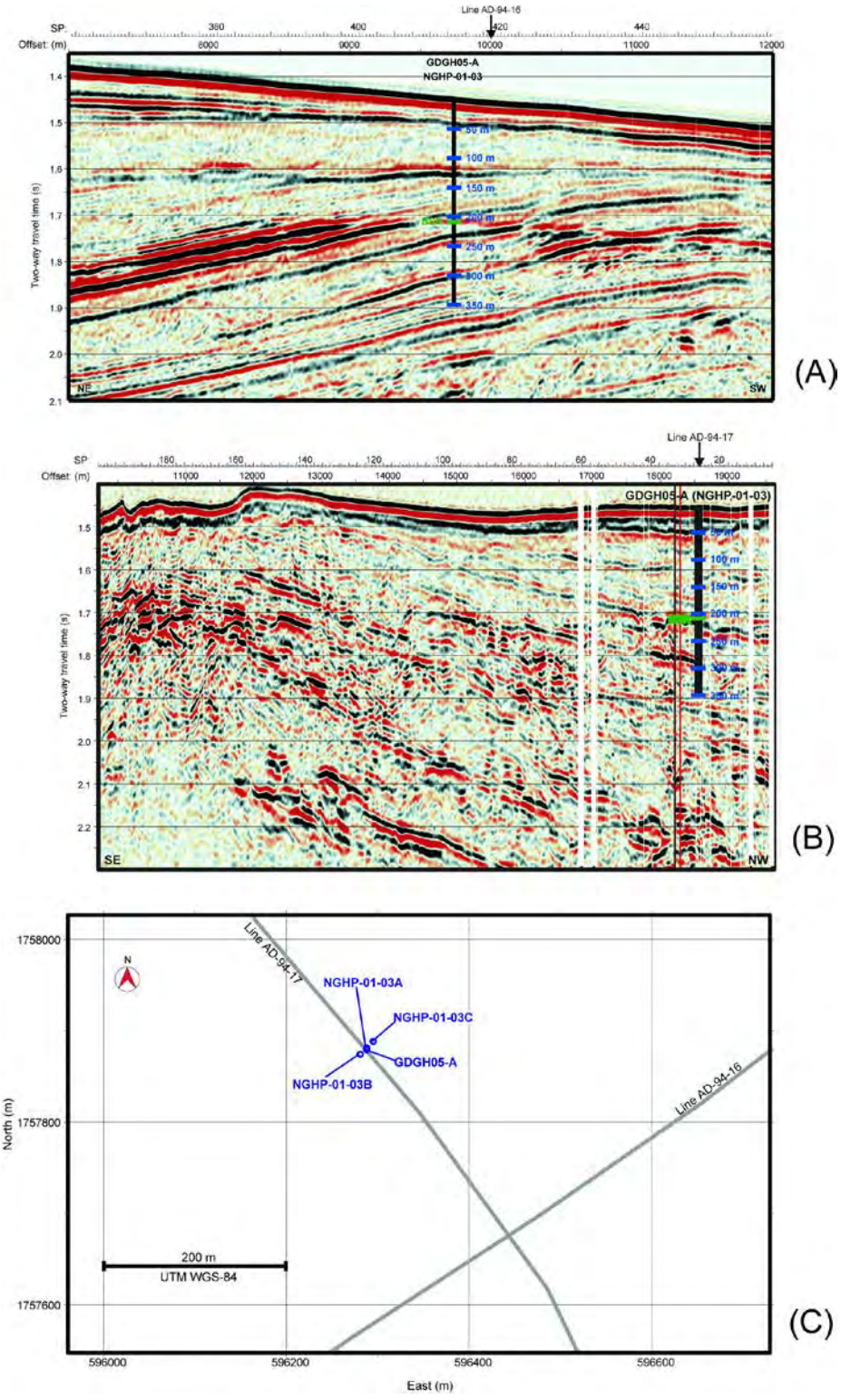
Line AD-94-16
SP
Offset: (m)
GDGH05-A
NGHP-01-03
50 m
100 m
150 m
200 m
250 m
300 m
350 m
Two-way travel time (s)
NE
SW
(A)
Line AD-94-17
GDGH05-A (NGHP-01-03)
SE
NW
(B)
North (m)
East (m)
Line AD-94-17
Line AD-94-16
NGHP-01-03A
NGHP-01-03C
GDGH05-A
NGHP-01-03B
200 m
UTM WGS-84
(C)

Figure 4

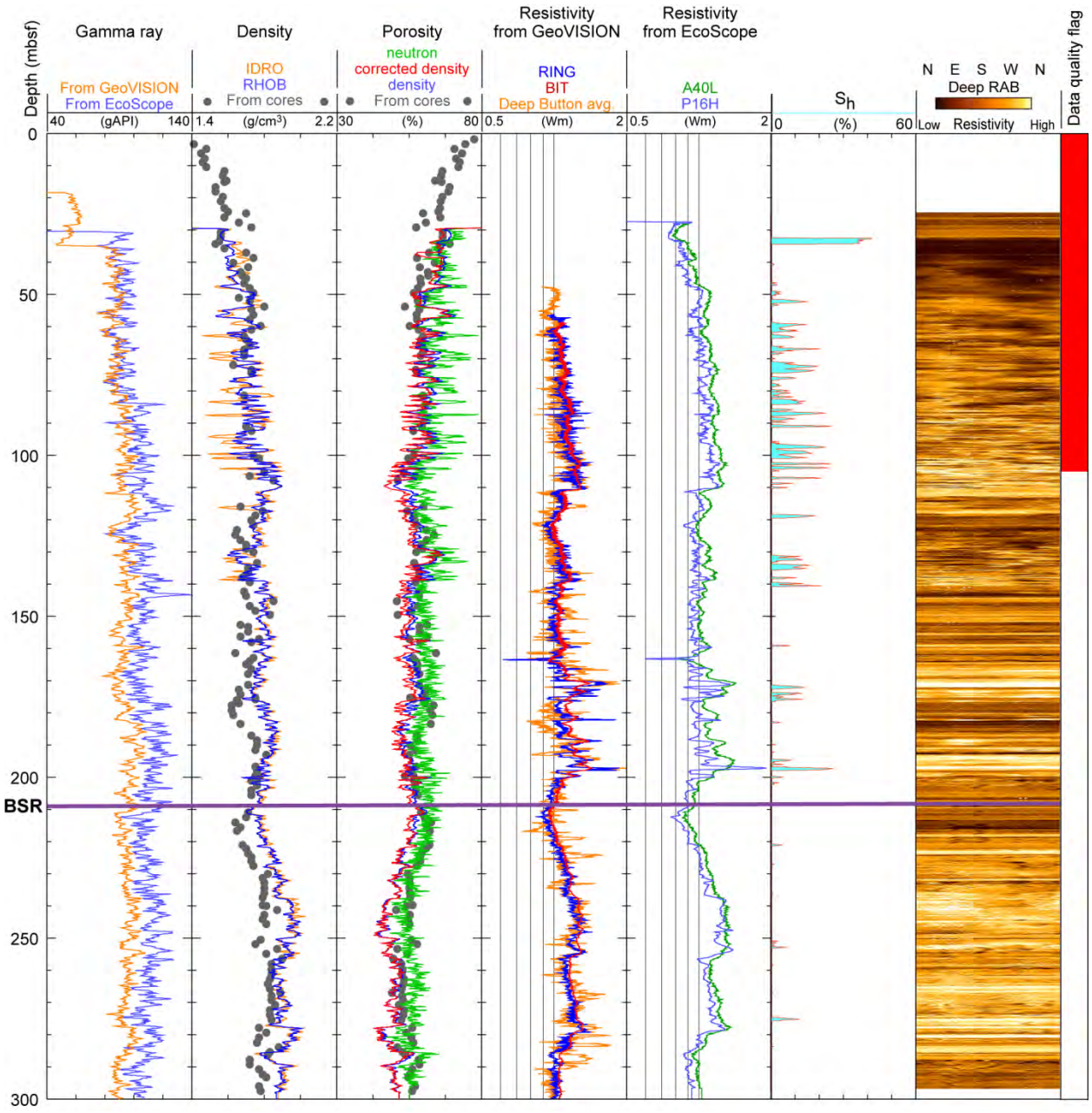
Depth (mbsf)
Gamma ray
From GeoVISION
From EcoScope
40 (gAPI) 140
Density
IDRO
RHOB
From cores
1.4 (g/cm3) 2.2
Porosity
neutron
corrected density
density
From cores
30 (%) 80
Resistivity from GeoVISION
RING
BIT
Deep Button avg.
0.5 (Wm) 2
Resistivity from EcoScope
A40L
P16H
0.5 (Wm) 2
Sh
0 (%) 60
N E S W N
Deep RAB
Low Resistivity High
Data quality flag
0
50
100
150
200
BSR
250
300

Figure 5

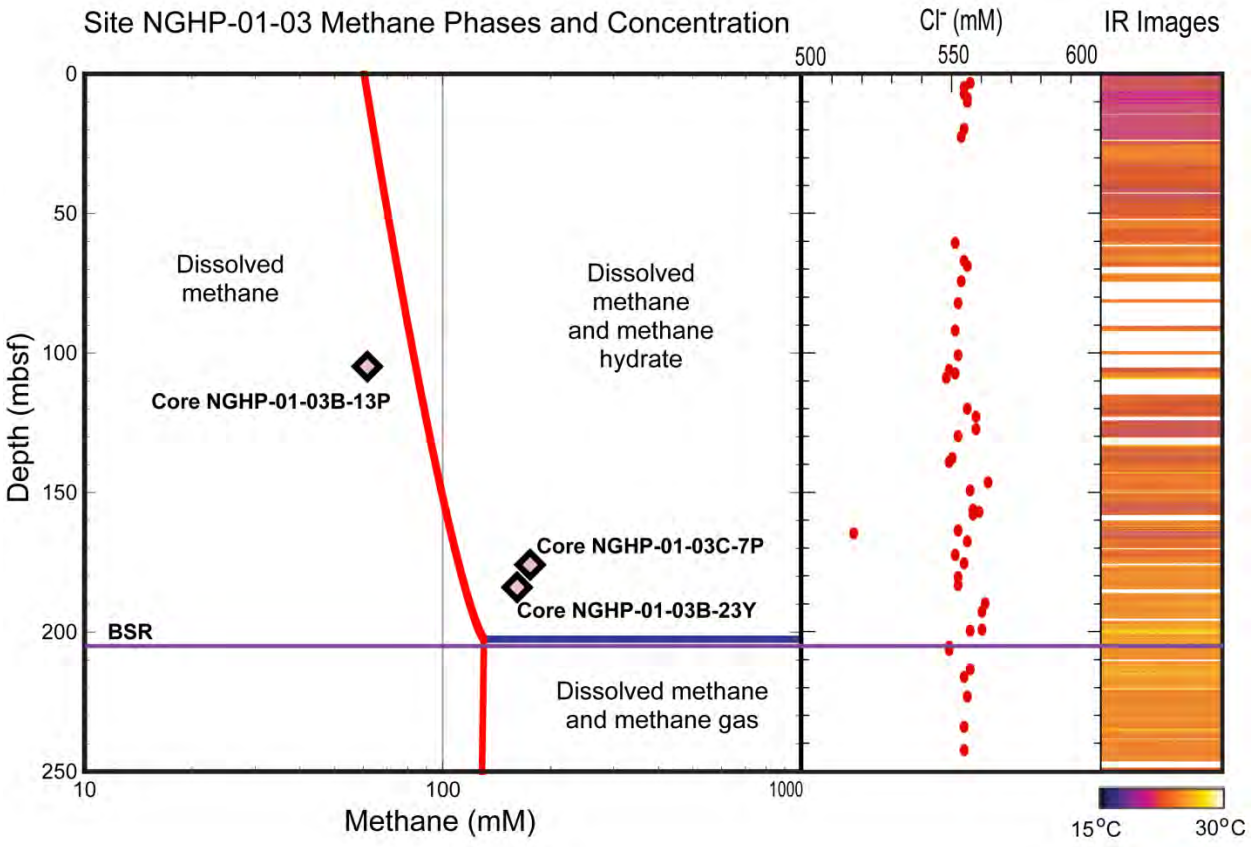
Site NGHP-01-03 Methane Phases and Concentration
Cl- (mM)
IR Images
500
550
600
0
50
100
150
200
250
Depth (mbsf)
Dissolved methane
Dissolved methane and methane hydrate
Core NGHP-01-03B-13P
Core NGHP-01-03C-7P
Core NGHP-01-03B-23Y
BSR
Dissolved methane and methane gas
10
100
1000
Methane (mM)
15°C
30°C

Figure 6

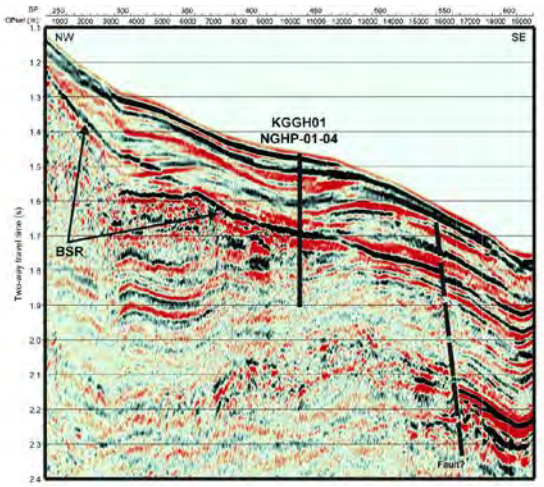
NW
SE
KGGH01
NGHP-01-04
BSR
Fault?
Two-way travel time (s)

(A)

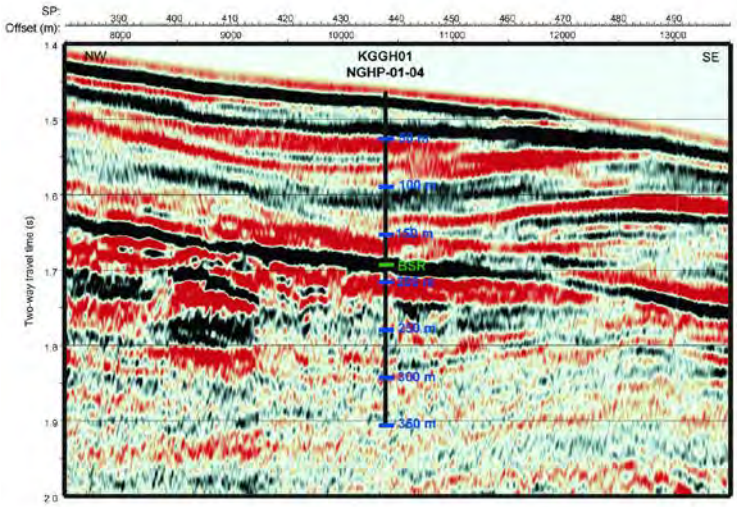
SP:
Offset (m):
NW
SE
KGGH01
NGHP-01-04
100 m
150 m
BSR
250 m
300 m
350 m
Two-way travel time (s)

(B)

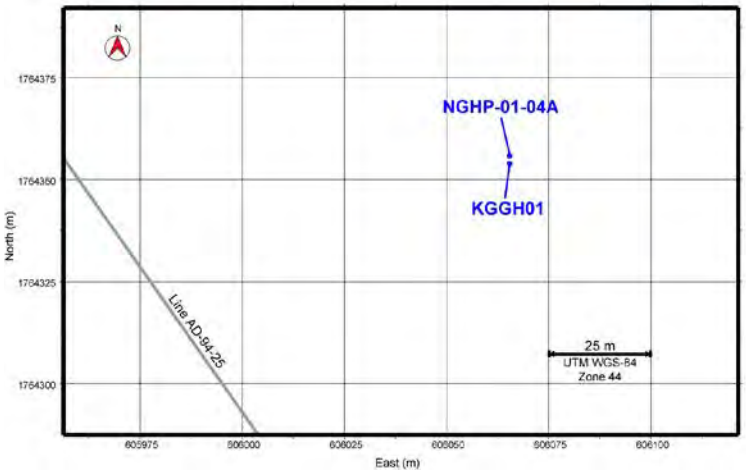
N
NGHP-01-04A
KGGH01
Line AD94-25
25 m
UTM WGS-84
Zone 44
North (m)
East (m)

(C)

Figure 7

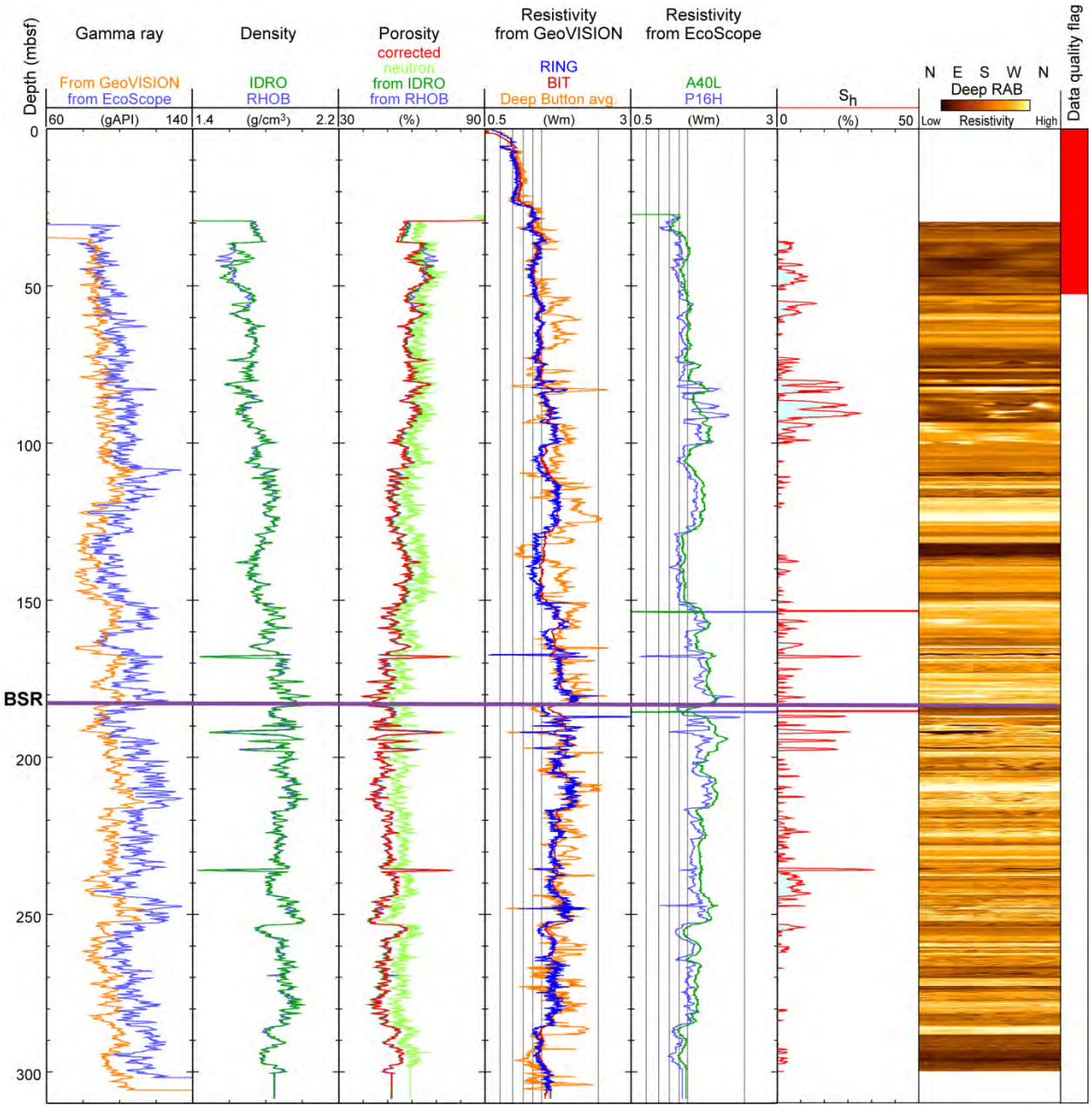
Depth (mbsf)
Gamma ray
From GeoVISION
from EcoScope
60 (gAPI) 140
Density
IDRO
RHOB
1.4 (g/cm3) 2.2
Porosity
corrected
neutron
from IDRO
from RHOB
30 (%) 90
Resistivity
from GeoVISION
RING
BIT
Deep Button avg
0.5 (Wm) 3
Resistivity
from EcoScope
A40L
P16H
0.5 (Wm) 3
Sh
0 (%) 50
N E S W N
Deep RAB
Low Resistivity High
Data quality flag
BSR
0
50
100
150
200
250
300

Figure 8

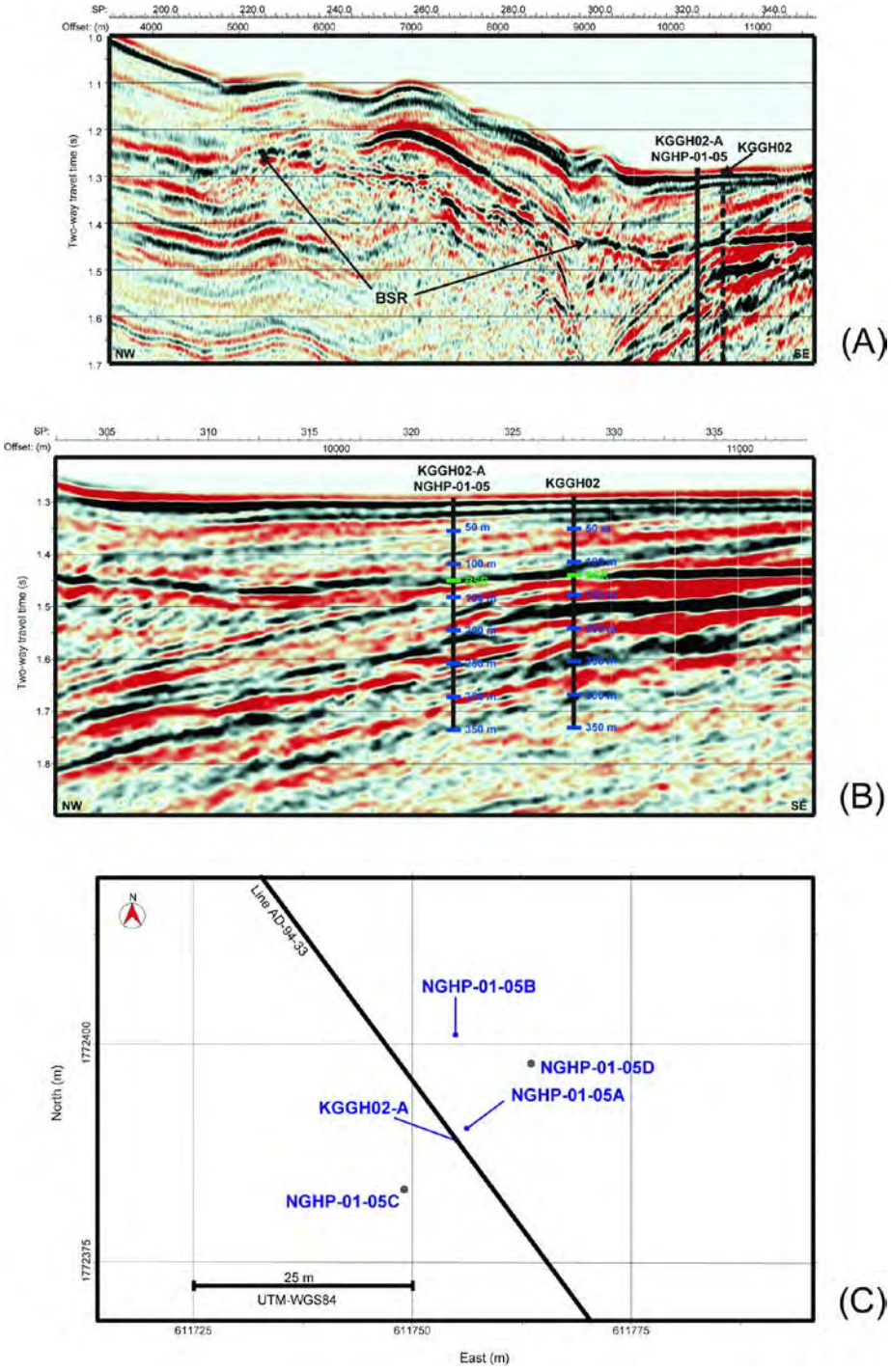
SP:
Offset: (m)
Two-way travel time (s)
KGGH02-A
NGHP-01-05
KGGH02
BSR
NW
SE
(A)
KGGH02-A
NGHP-01-05
KGGH02
50 m
100 m
350 m
(B)
Line AD-94-33
NGHP-01-05B
NGHP-01-05D
NGHP-01-05A
KGGH02-A
NGHP-01-05C
25 m
UTM-WGS84
North (m)
East (m)
(C)

Figure 9

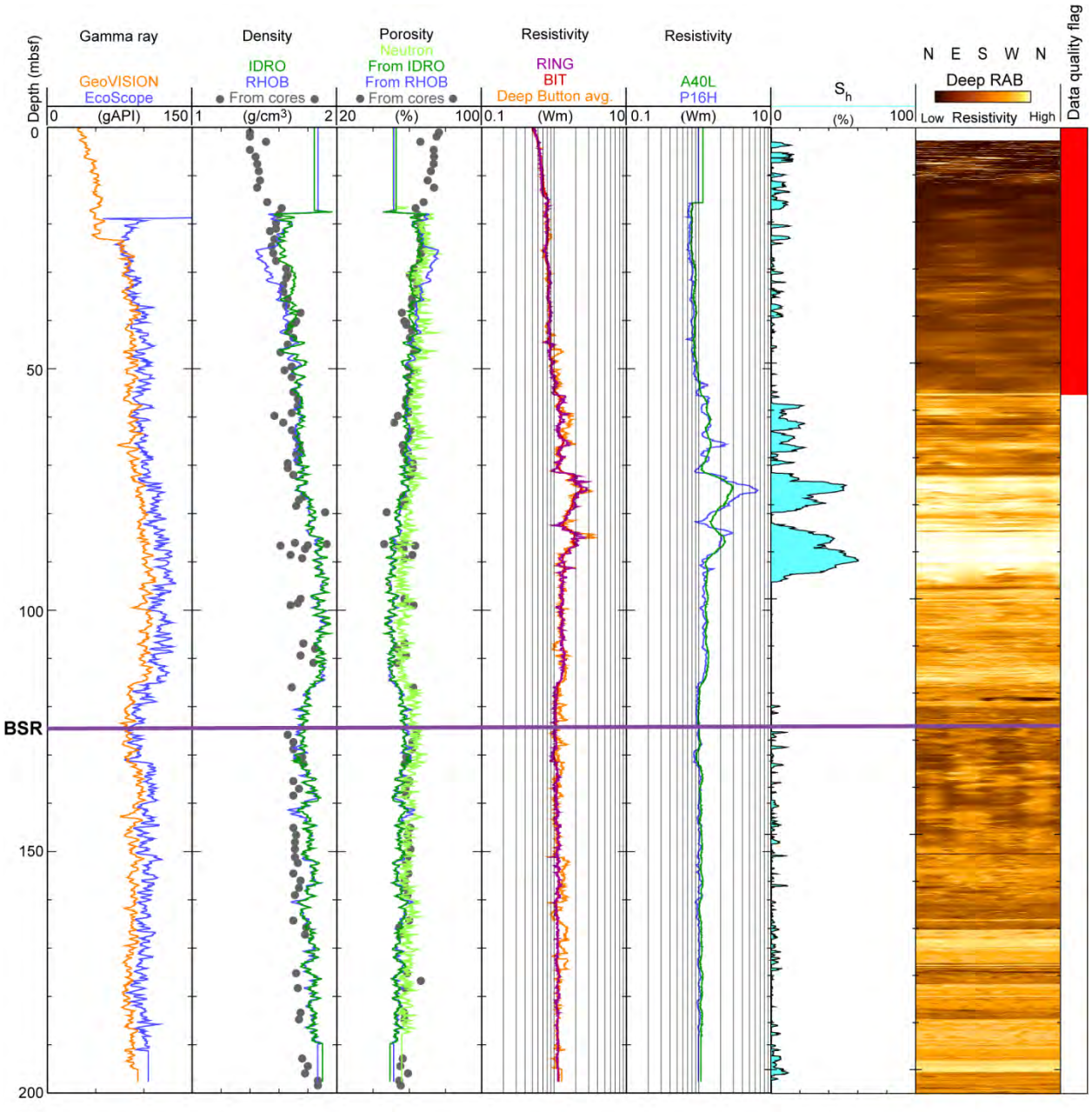
Depth (mbsf)
Gamma ray
GeoVISION
EcoScope
0
(gAPI)
150
Density
IDRO
RHOB
From cores
1
(g/cm3)
2
Porosity
Neutron
From IDRO
From RHOB
From cores
20
(%)
100
Resistivity
RING
BIT
Deep Button avg.
0.1
(Wm)
10
Resistivity
A40L
P16H
0.1
(Wm)
10
Sh
0
(%)
100
N E S W N
Deep RAB
Low Resistivity High
Data quality flag
0
50
100
BSR
150
200

Figure 10

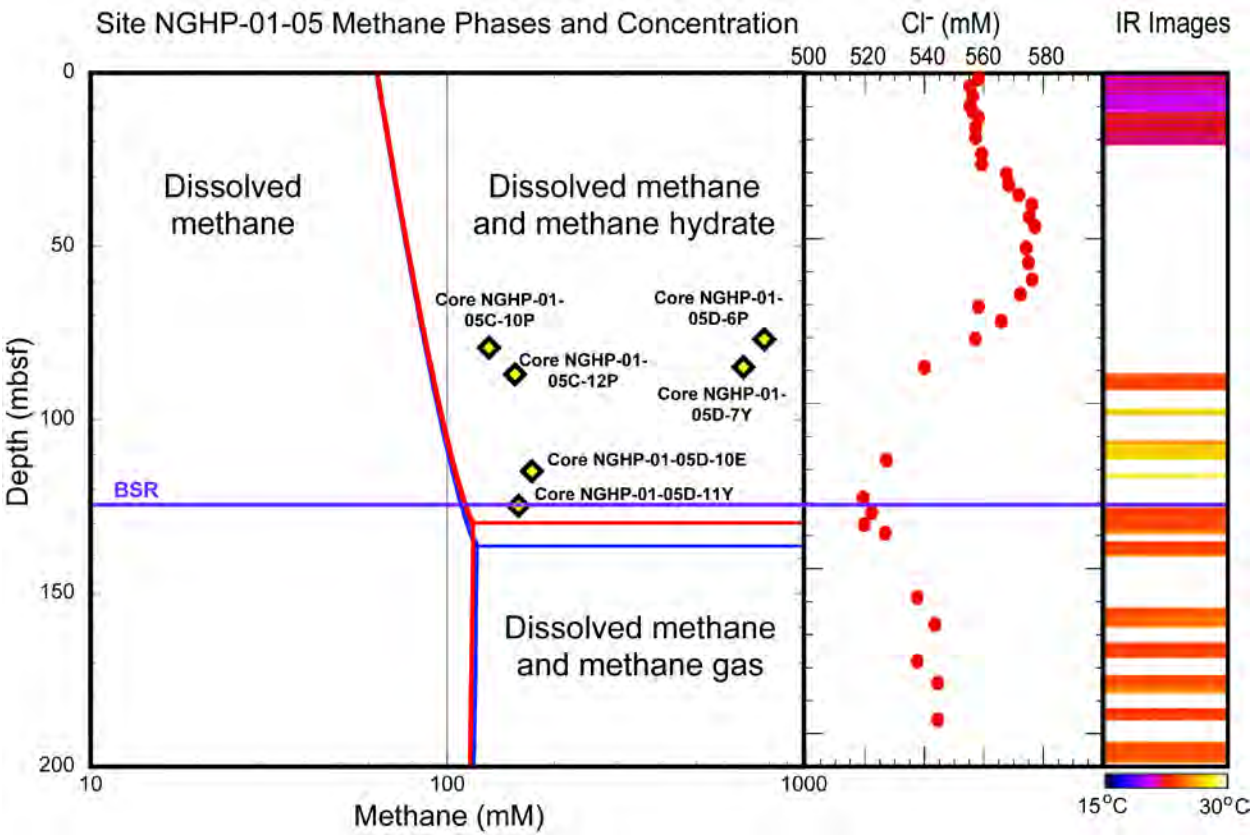
Site NGHP-01-05 Methane Phases and Concentration
Cl- (mM)
IR Images
500 520 540 560 580
0
50
100
150
200
Depth (mbsf)
Dissolved methane
Dissolved methane and methane hydrate
Core NGHP-01-05C-10P
Core NGHP-01-05C-12P
Core NGHP-01-05D-6P
Core NGHP-01-05D-7Y
Core NGHP-01-05D-10E
Core NGHP-01-05D-11Y
BSR
Dissolved methane and methane gas
10
100
1000
Methane (mM)
15°C
30°C

Figure 11

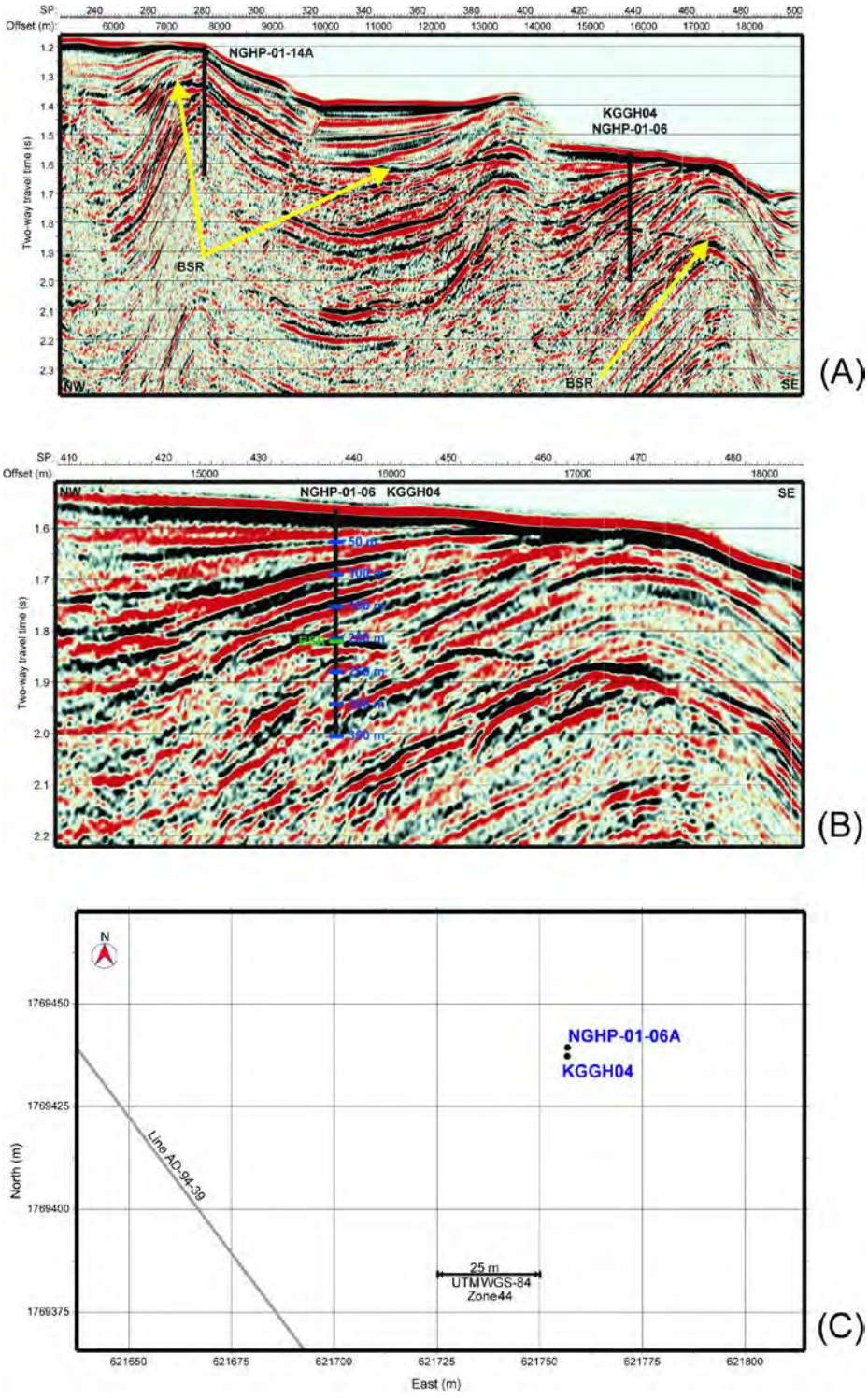
SP
Offset (m):
NGHP-01-14A
KGGH04
NGHP-01-06
BSR
BSR
NW
SE
Two-way travel time (s)
(A)
NW
NGHP-01-06
KGGH04
SE
50 m
100 m
150 m
200 m
250 m
300 m
350 m
(B)
N
NGHP-01-06A
KGGH04
Line AD-94-39
25 m
UTMWGS-84
Zone44
North (m)
East (m)
(C)

Figure 12

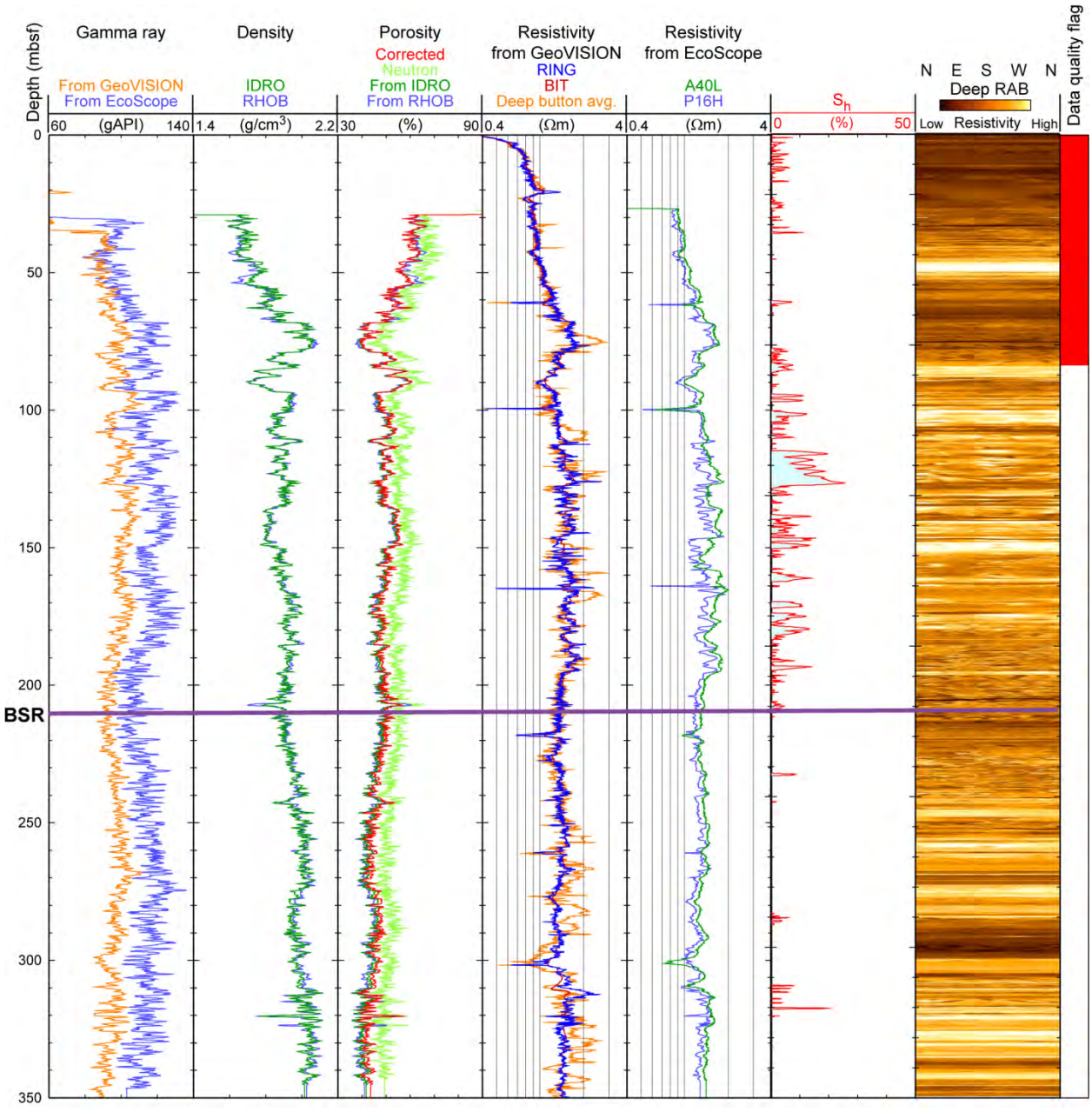
Depth (mbsf)
Gamma ray
From GeoVISION
From EcoScope
60 (gAPI) 140
Density
IDRO
RHOB
1.4 (g/cm3) 2.2
Porosity
Corrected
Neutron
From IDRO
From RHOB
30 (%) 90
Resistivity from GeoVISION
RING
BIT
Deep button avg.
0.4 (Ωm) 4
Resistivity from EcoScope
A40L
P16H
0.4 (Ωm) 4
Sh
0 (%) 50
N E S W N
Deep RAB
Low Resistivity High
Data quality flag
0
50
100
150
200
BSR
250
300
350

Figure 13

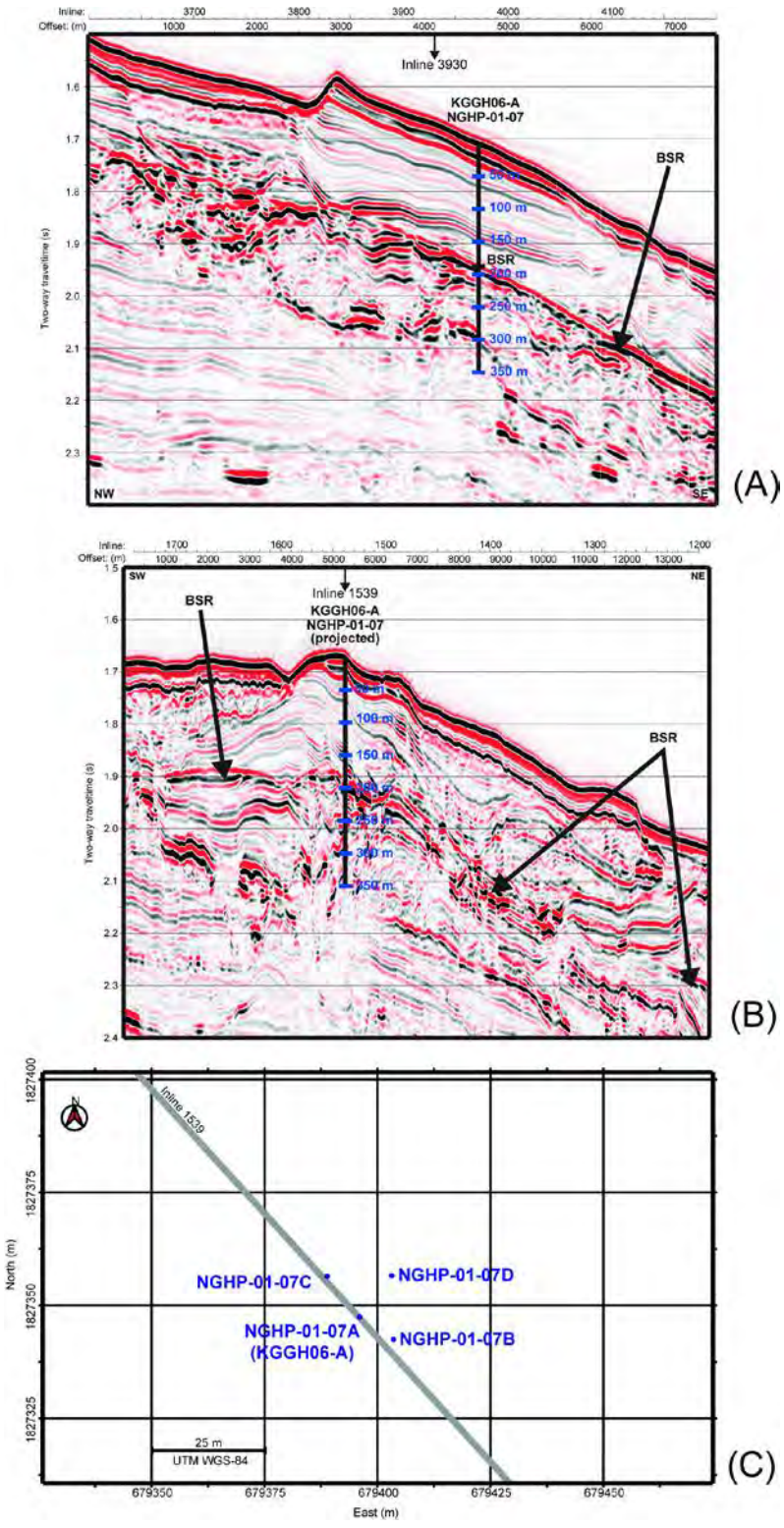
Inline:
Offset: (m)
Inline 3930
KGGH06-A
NGHP-01-07
BSR
100 m
150 m
BSR
200 m
250 m
300 m
350 m
Two-way traveltime (s)
NW
SE
(A)
Inline:
Offset: (m)
SW
NE
BSR
Inline 1539
KGGH06-A
NGHP-01-07
(projected)
100 m
150 m
BSR
300 m
350 m
Two-way traveltime (s)
(B)
Inline 1539
NGHP-01-07C
NGHP-01-07D
NGHP-01-07A
(KGGH06-A)
NGHP-01-07B
25 m
UTM WGS-84
North (m)
East (m)
(C)

Figure 14

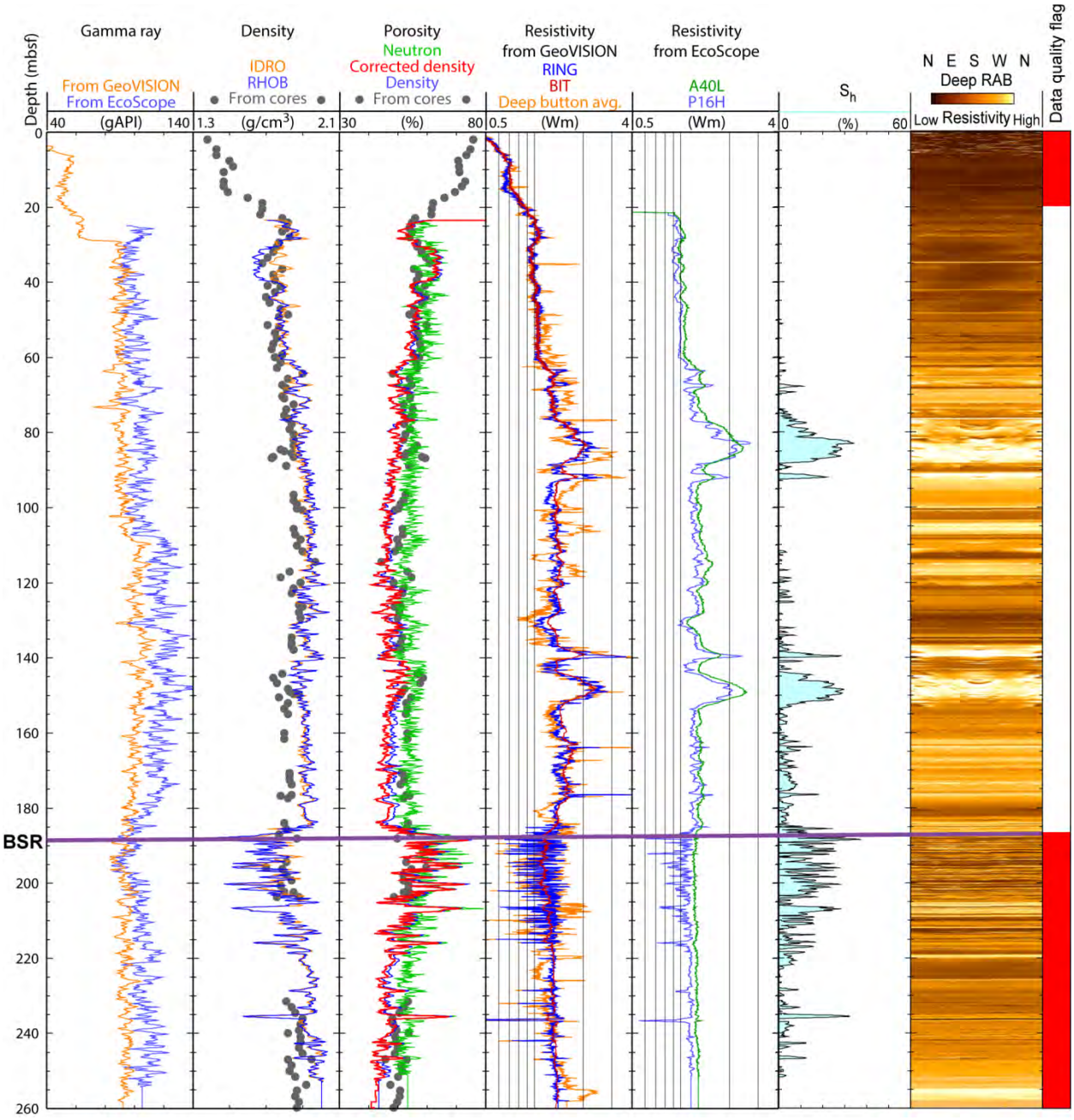
Depth (mbsf)
Gamma ray
From GeoVISION
From EcoScope
40 (gAPI) 140
Density
IDRO
RHOB
From cores
1.3 (g/cm3) 2.1
Porosity
Neutron
Corrected density
Density
From cores
30 (%) 80
Resistivity from GeoVISION
RING
BIT
Deep button avg.
0.5 (Wm) 4
Resistivity from EcoScope
A40L
P16H
0.5 (Wm) 4
Sh
0 (%) 60
N E S W N
Deep RAB
Low Resistivity High
Data quality flag
BSR
0
20
40
60
80
100
120
140
160
180
200
220
240
260

Figure 15

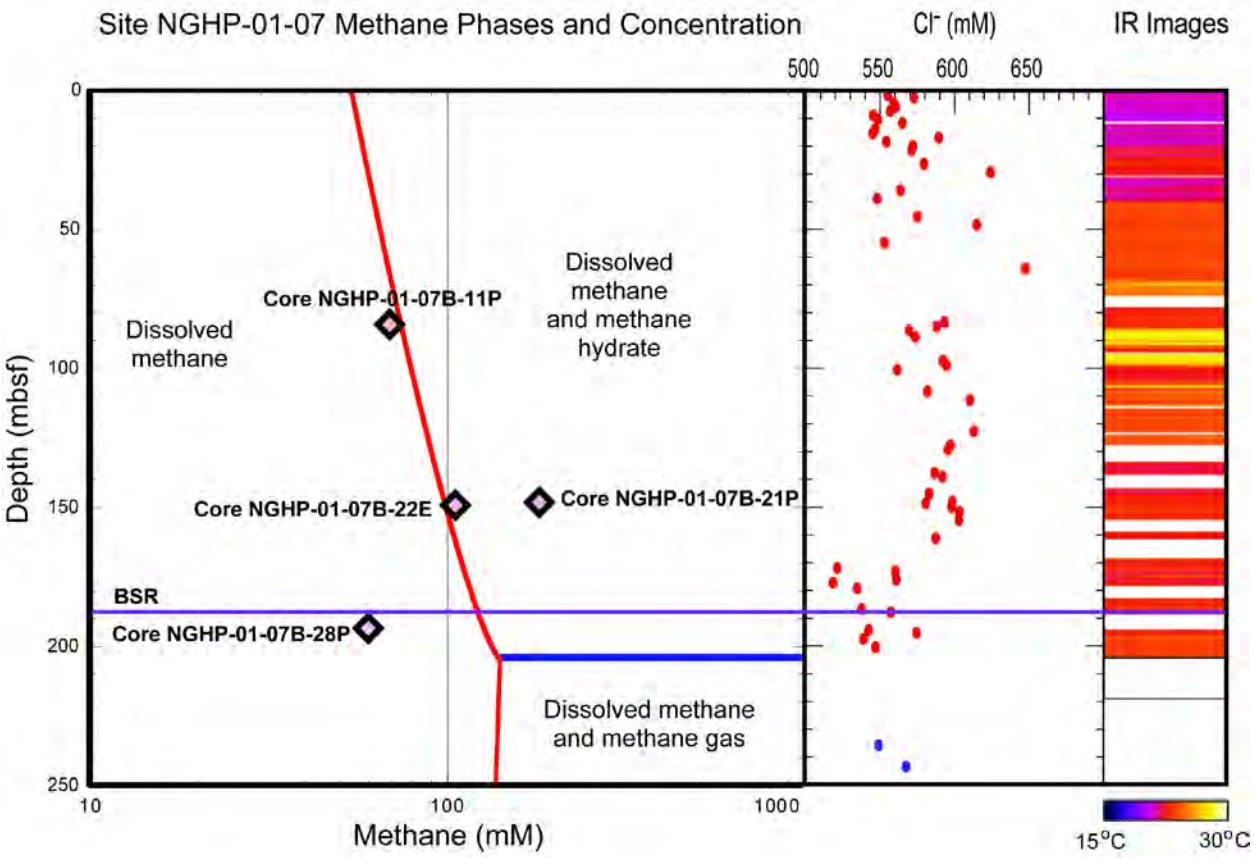
Site NGHP-01-07 Methane Phases and Concentration
Cl⁻ (mM)
IR Images
500
550
600
650
0
50
100
150
200
250
Depth (mbsf)
Dissolved methane
Core NGHP-01-07B-11P
Dissolved methane and methane hydrate
Core NGHP-01-07B-22E
Core NGHP-01-07B-21P
BSR
Core NGHP-01-07B-28P
Dissolved methane and methane gas
10
100
1000
Methane (mM)
15°C
30°C

Figure 16

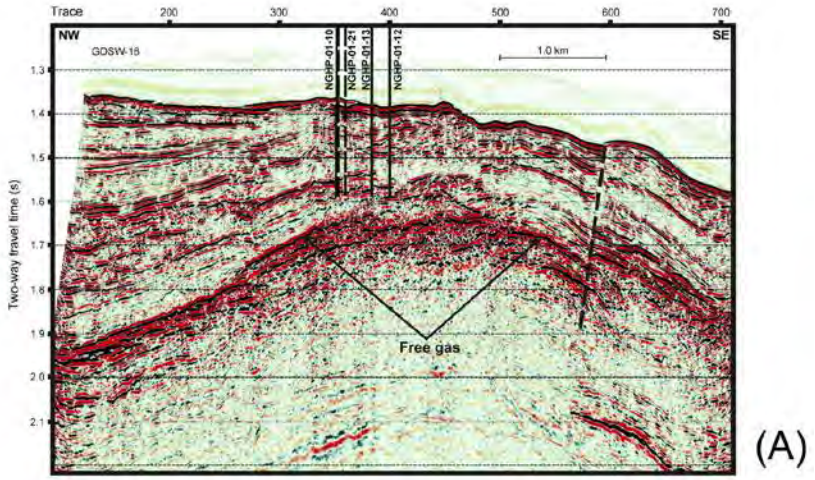

(A)

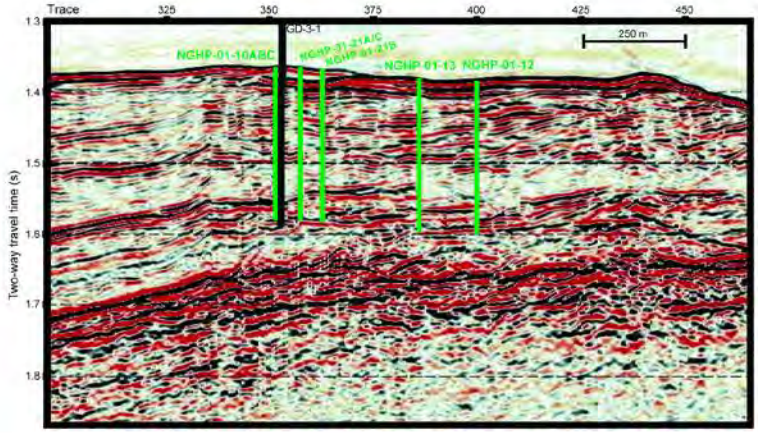

(B)

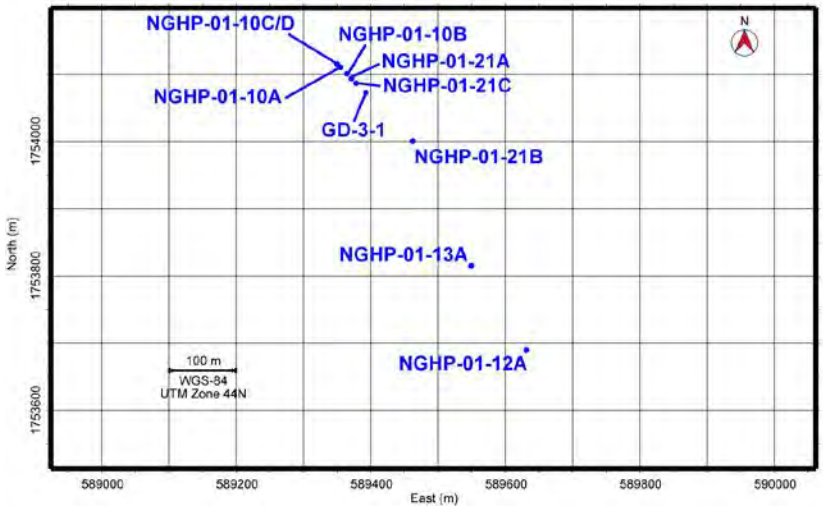

(C)

Figure 17

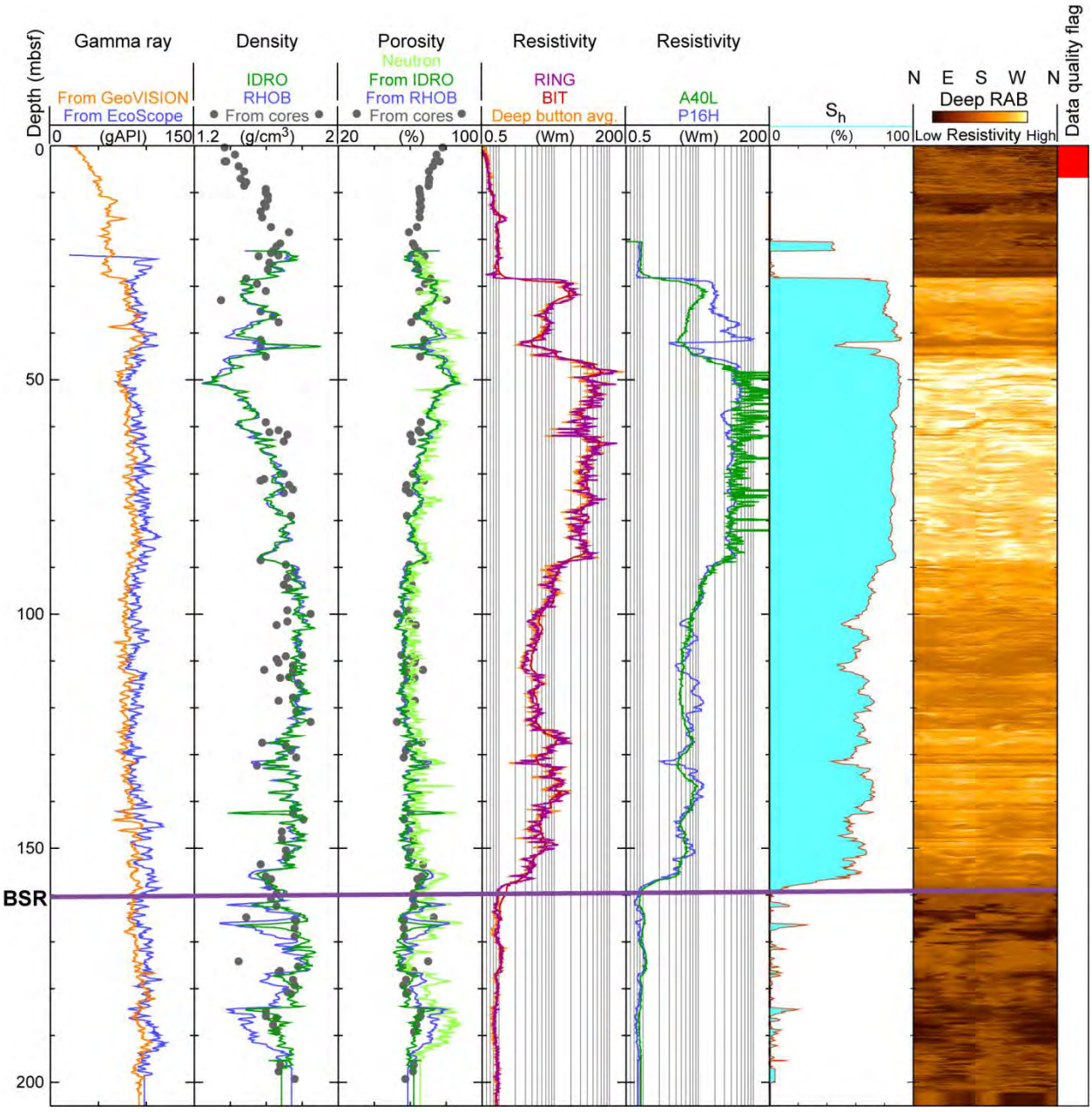
Depth (mbsf)
Gamma ray
From GeoVISION
From EcoScope
0 (gAPI) 150
Density
IDRO
RHOB
From cores
1.2 (g/cm3) 2
Porosity
Neutron
From IDRO
From RHOB
From cores
20 (%) 100
Resistivity
RING
BIT
Deep button avg.
0.5 (Wm) 200
Resistivity
A40L
P16H
0.5 (Wm) 200
Sh
0 (%) 100
N E S W N
Deep RAB
Low Resistivity High
Data quality flag
0
50
100
150
BSR
200

Figure 18

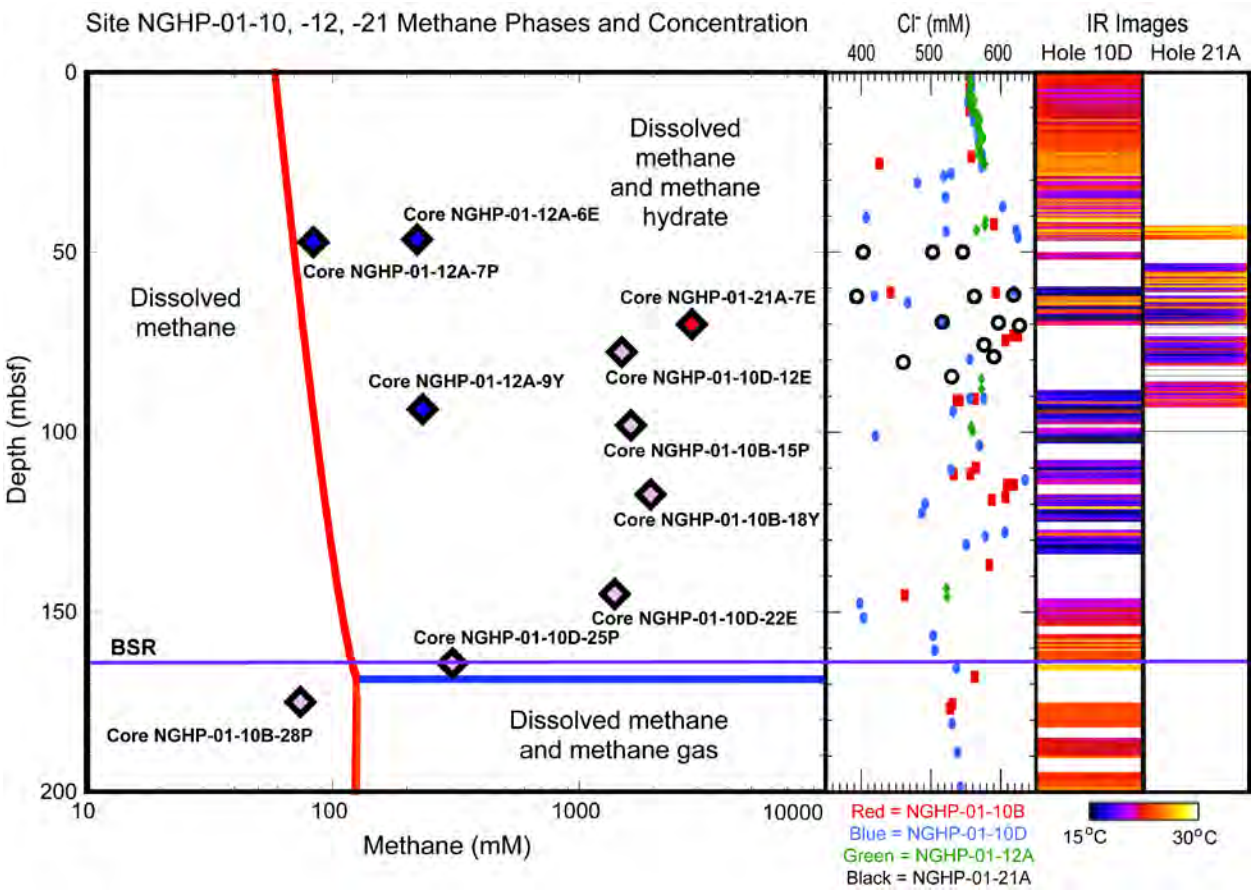
Site NGHP-01-10, -12, -21 Methane Phases and Concentration
Cl⁻ (mM)
400
500
600
IR Images
Hole 10D
Hole 21A
Depth (mbsf)
0
50
100
150
200
Dissolved methane
Dissolved methane and methane hydrate
Dissolved methane and methane gas
Core NGHP-01-12A-6E
Core NGHP-01-12A-7P
Core NGHP-01-21A-7E
Core NGHP-01-10D-12E
Core NGHP-01-12A-9Y
Core NGHP-01-10B-15P
Core NGHP-01-10B-18Y
Core NGHP-01-10D-22E
Core NGHP-01-10D-25P
BSR
Core NGHP-01-10B-28P
10
100
1000
10000
Methane (mM)
Red = NGHP-01-10B
Blue = NGHP-01-10D
Green = NGHP-01-12A
Black = NGHP-01-21A
15°C
30°C

Figure 19

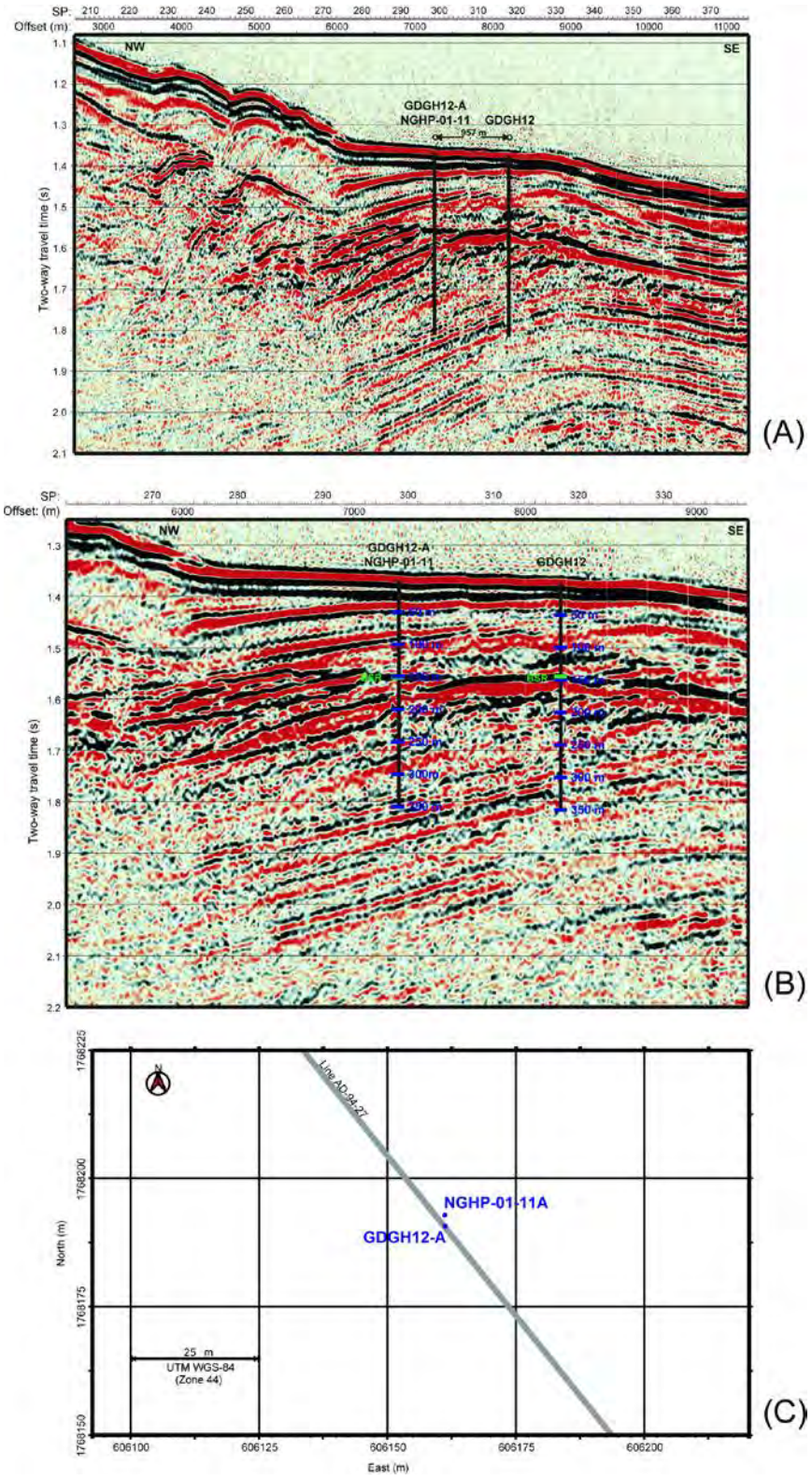
SP:
Offset (m):
NW
SE
GDGH12-A
NGHP-01-11
GDGH12
957 m
Two-way travel time (s)
(A)
(B)
(C)
Line AD-84-27
NGHP-01-11A
GDGH12-A
25 m
UTM WGS-84
(Zone 44)
North (m)
East (m)

Figure 20

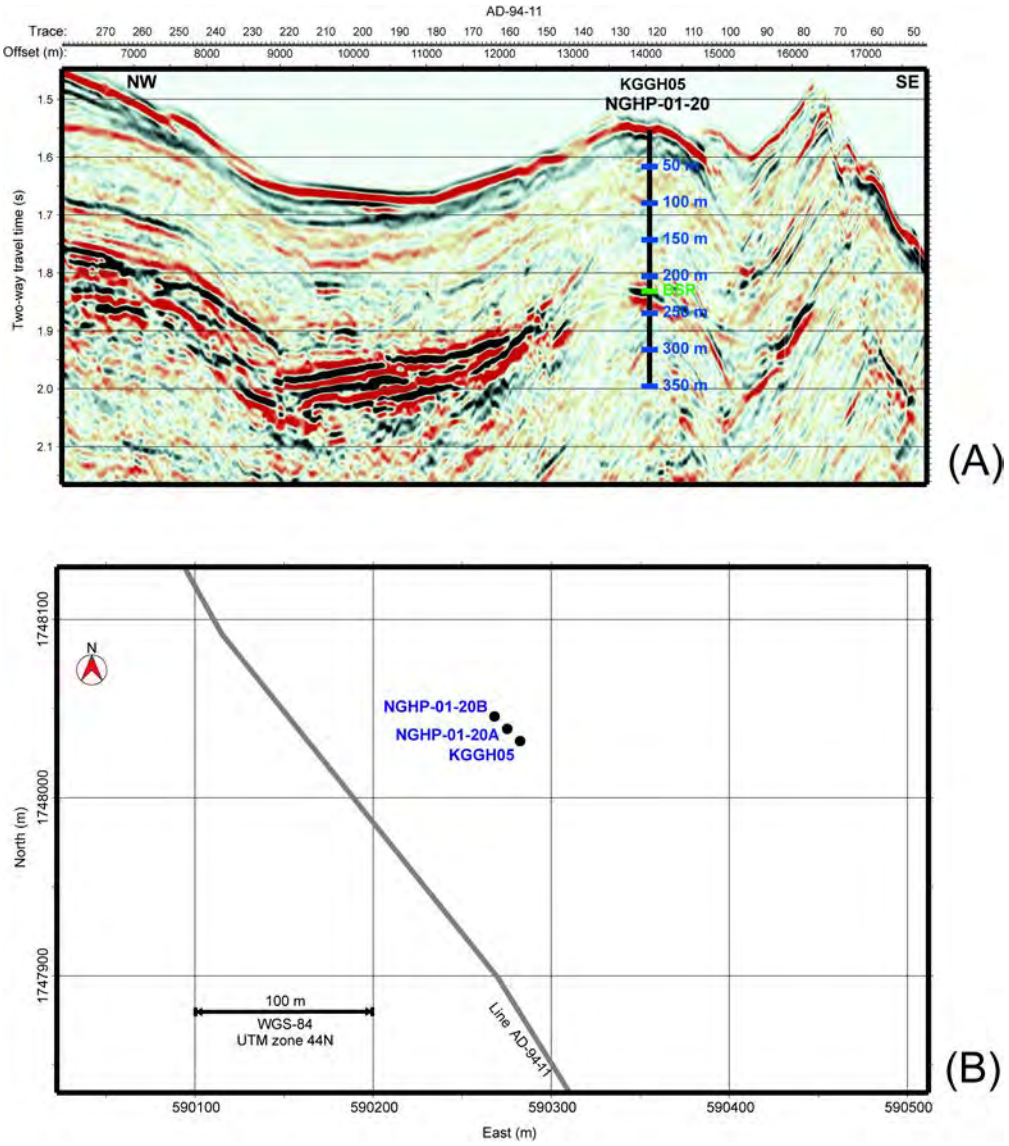
AD-94-11
Trace:
Offset (m):
NW
SE
KGGH05
NGHP-01-20
50 m
100 m
150 m
200 m
BSR
250 m
300 m
350 m
Two-way travel time (s)
(A)
NGHP-01-20B
NGHP-01-20A
KGGH05
N
100 m
WGS-84
UTM zone 44N
Line AD-94-11
North (m)
East (m)
(B)

Figure 31

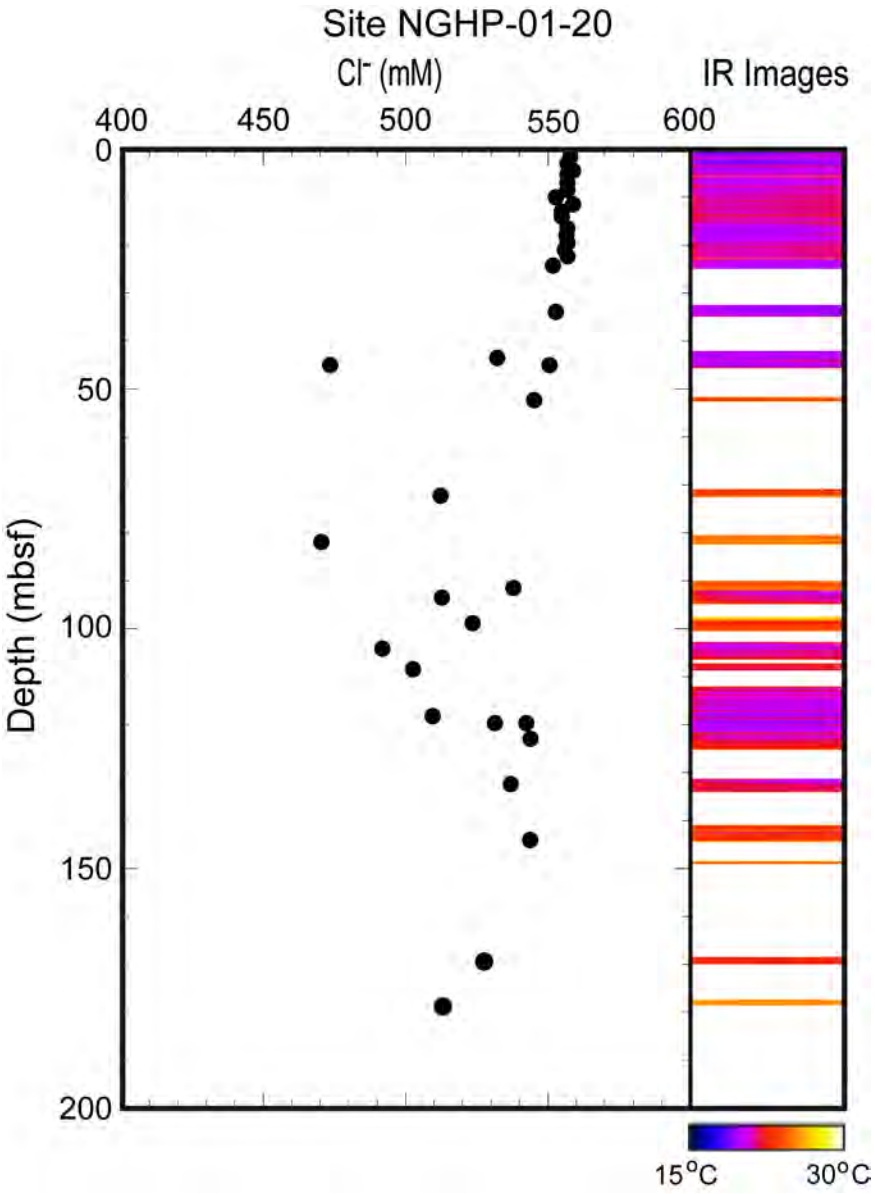
Site NGHP-01-20
Cl⁻ (mM)
IR Images
400
450
500
550
600
0
50
100
150
200
Depth (mbsf)
15°C
30°C

Figure 32

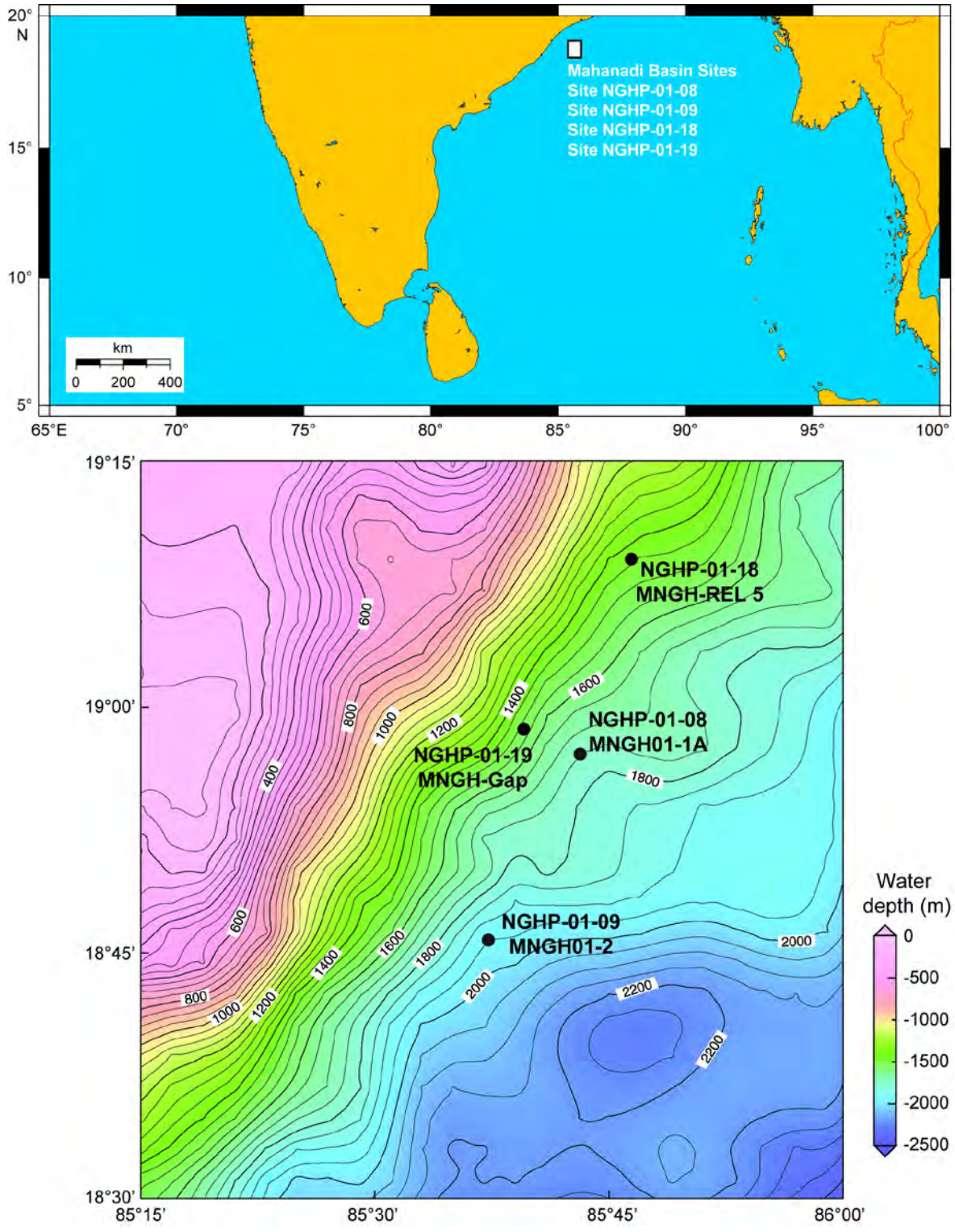
20° N
15°
10°
5°
65°E
70°
75°
80°
85°
90°
95°
100°
Mahanadi Basin Sites
Site NGHP-01-08
Site NGHP-01-09
Site NGHP-01-18
Site NGHP-01-19
km
0 200 400
19°15'
19°00'
18°45'
18°30'
85°15'
85°30'
85°45'
86°00'
NGHP-01-18
MNGH-REL 5
NGHP-01-08
MNGH01-1A
NGHP-01-19
MNGH-Gap
NGHP-01-09
MNGH01-2
600
800
1000
1200
1400
1600
1800
2000
2200
Water depth (m)
0
-500
-1000
-1500
-2000
-2500

Figure 33

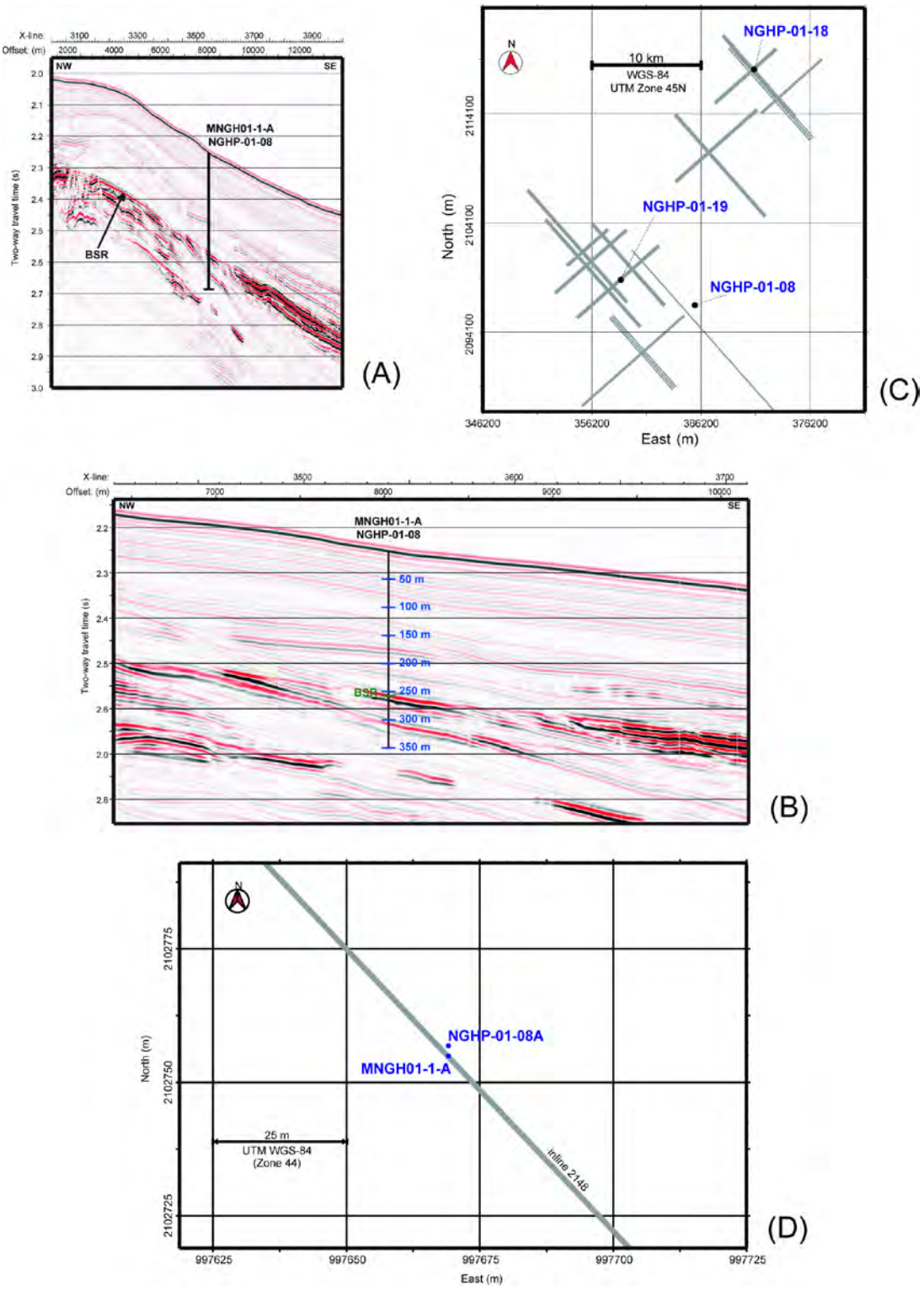
X-line:
Offset: (m)
NW
SE
MNGH01-1-A
NGHP-01-08
BSR
Two-way travel time (s)
(A)
N
10 km
WGS-84
UTM Zone 45N
NGHP-01-18
NGHP-01-19
NGHP-01-08
North (m)
East (m)
(C)
50 m
100 m
150 m
200 m
250 m
300 m
350 m
(B)
NGHP-01-08A
MNGH01-1-A
25 m
UTM WGS-84
(Zone 44)
Inline 2148
(D)

Figure 34

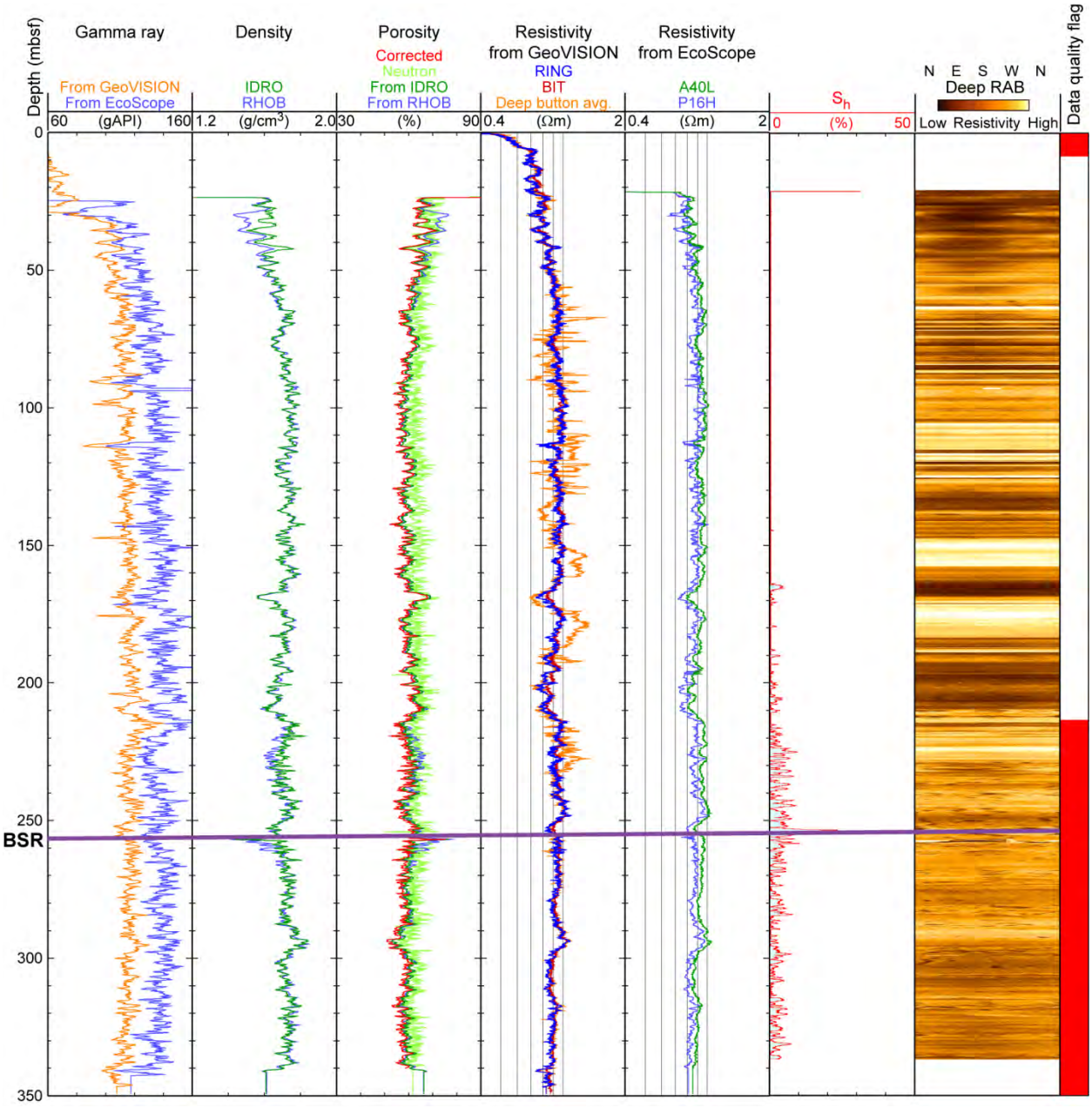
Depth (mbsf)
Gamma ray
From GeoVISION
From EcoScope
60 (gAPI) 160
Density
IDRO
RHOB
1.2 (g/cm3) 2.0
Porosity
Corrected
Neutron
From IDRO
From RHOB
30 (%) 90
Resistivity from GeoVISION
RING
BIT
Deep button avg.
0.4 (Ωm) 2
Resistivity from EcoScope
A40L
P16H
0.4 (Ωm) 2
Sh
0 (%) 50
N E S W N
Deep RAB
Low Resistivity High
Data quality flag
0
50
100
150
200
250
BSR
300
350

Figure 35

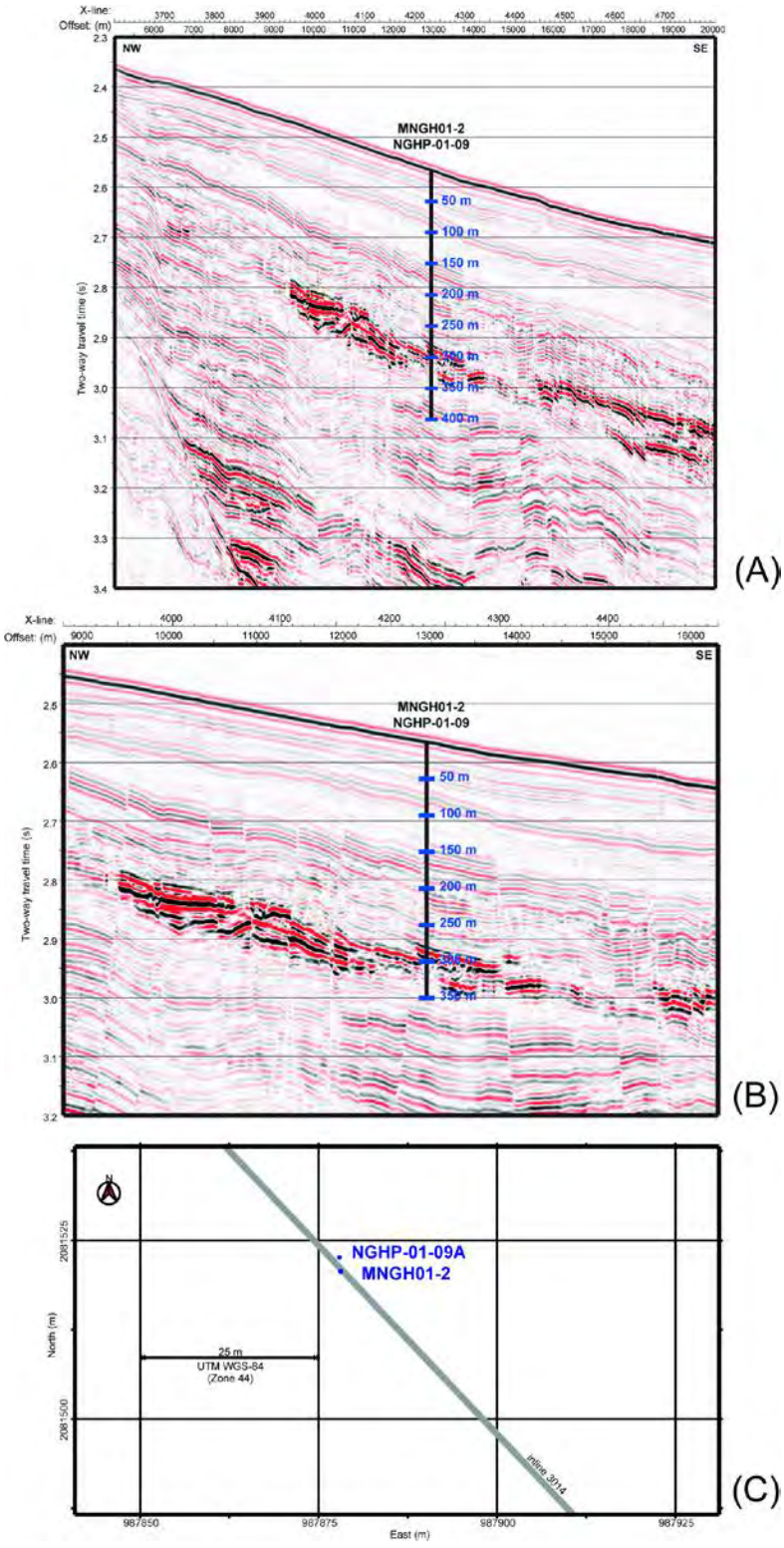
X-line:
Offset: (m)
NW
SE
MNGH01-2
NGHP-01-09
50 m
100 m
150 m
200 m
250 m
300 m
350 m
400 m
Two-way travel time (s)
(A)
X-line:
Offset: (m)
NW
SE
MNGH01-2
NGHP-01-09
50 m
100 m
150 m
200 m
250 m
300 m
350 m
Two-way travel time (s)
(B)
N
NGHP-01-09A
MNGH01-2
25 m
UTM WGS-84
(Zone 44)
inline 3114
North (m)
East (m)
2081525
2081500
987850
987875
987900
987925
(C)

Figure 36

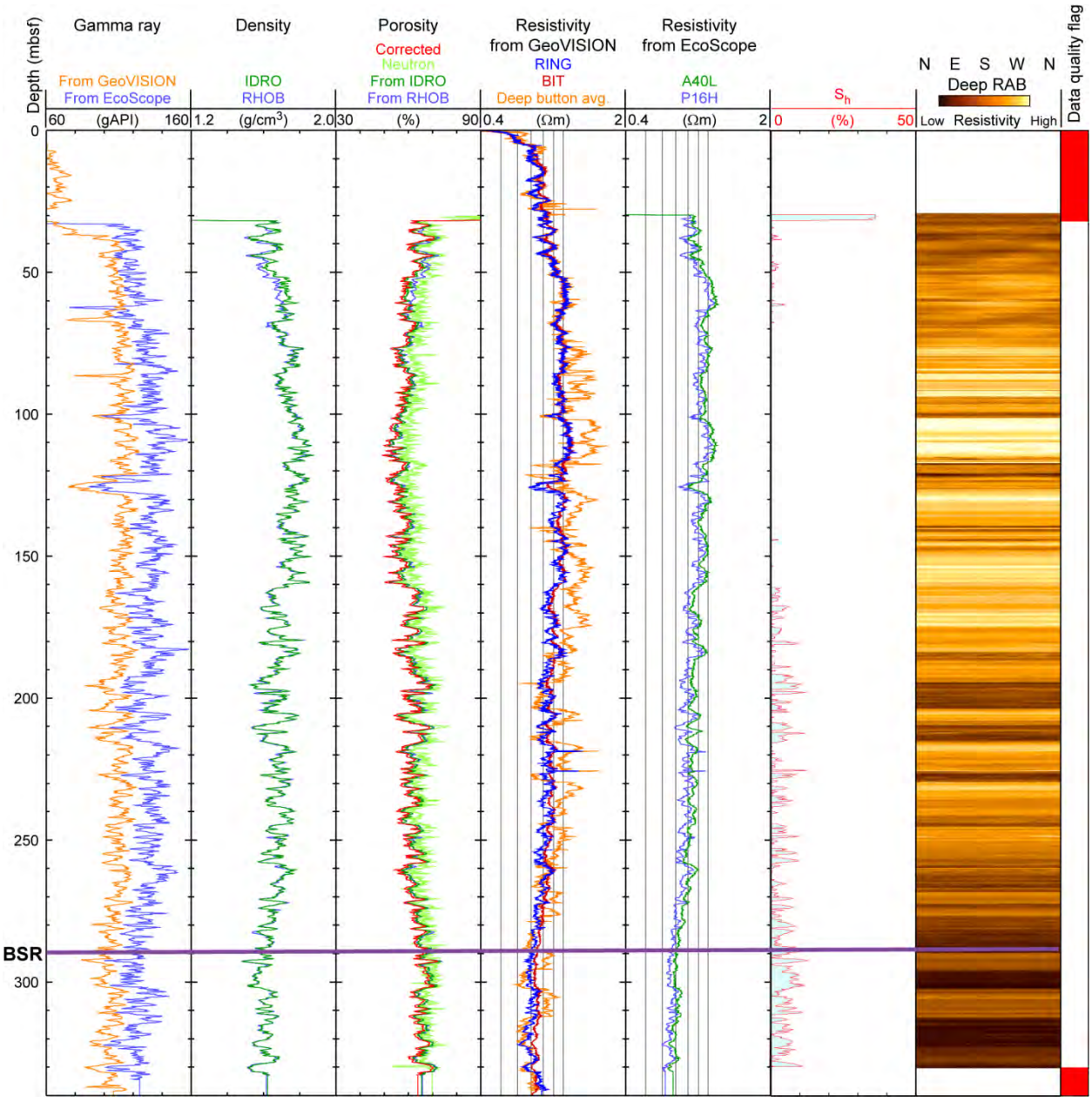
Depth (mbsf)
Gamma ray
From GeoVISION
From EcoScope
60 (gAPI) 160
Density
IDRO
RHOB
1.2 (g/cm3) 2.0
Porosity
Corrected
Neutron
From IDRO
From RHOB
30 (%) 90
Resistivity from GeoVISION
RING
BIT
Deep button avg.
0.4 (Ωm) 2
Resistivity from EcoScope
A40L
P16H
0.4 (Ωm) 2
Sh
0 (%) 50
N E S W N
Deep RAB
Low Resistivity High
Data quality flag
0
50
100
150
200
250
BSR
300

Figure 37

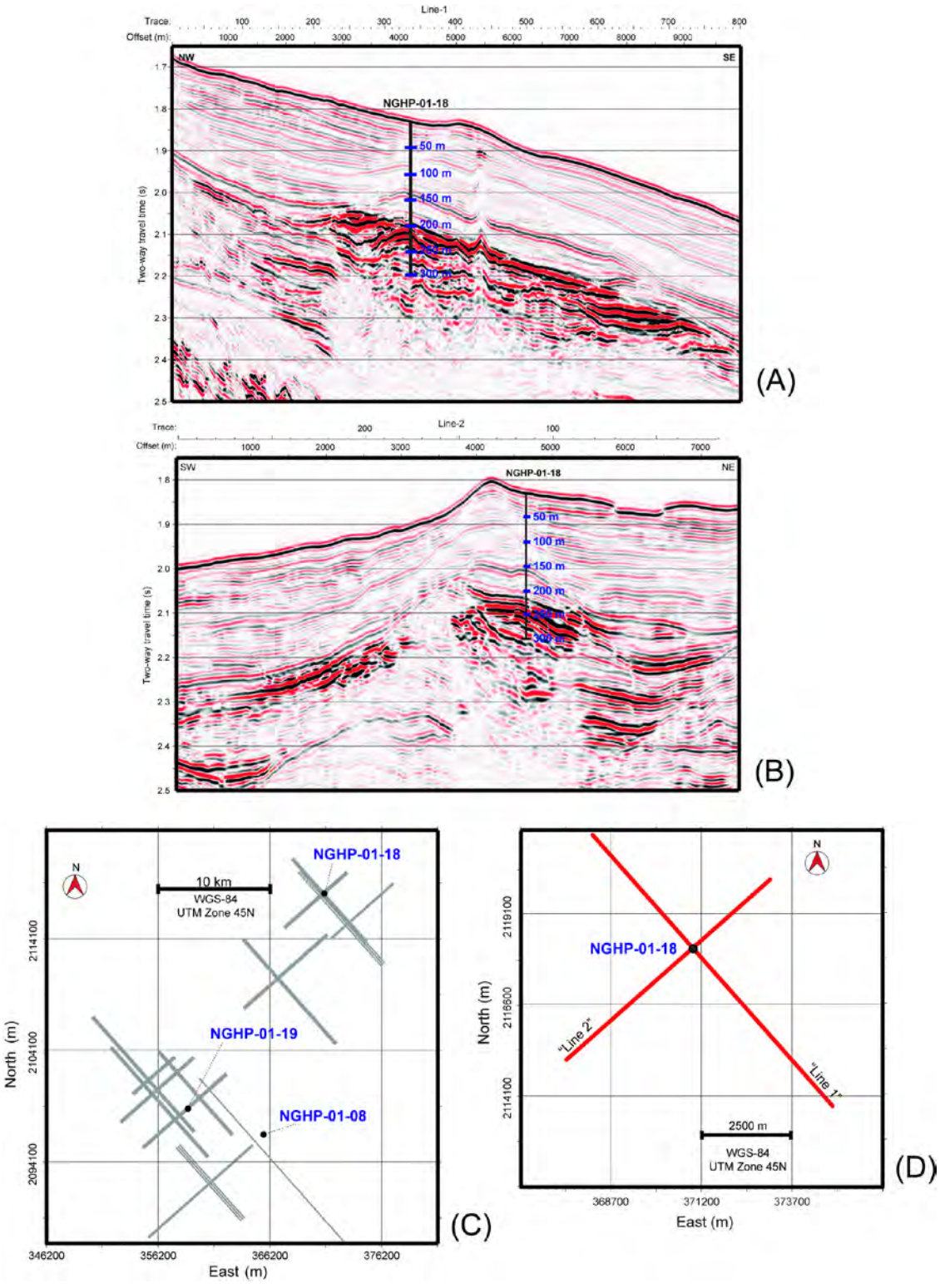
Line-1
Trace:
Offset (m):
NW
SE
NGHP-01-18
50 m
100 m
150 m
200 m
Two-way travel time (s)
(A)
Line-2
SW
NE
NGHP-01-18
(B)
N
10 km
WGS-84
UTM Zone 45N
NGHP-01-18
NGHP-01-19
NGHP-01-08
North (m)
East (m)
(C)
"Line 2"
"Line 1"
2500 m
(D)

Figure 38

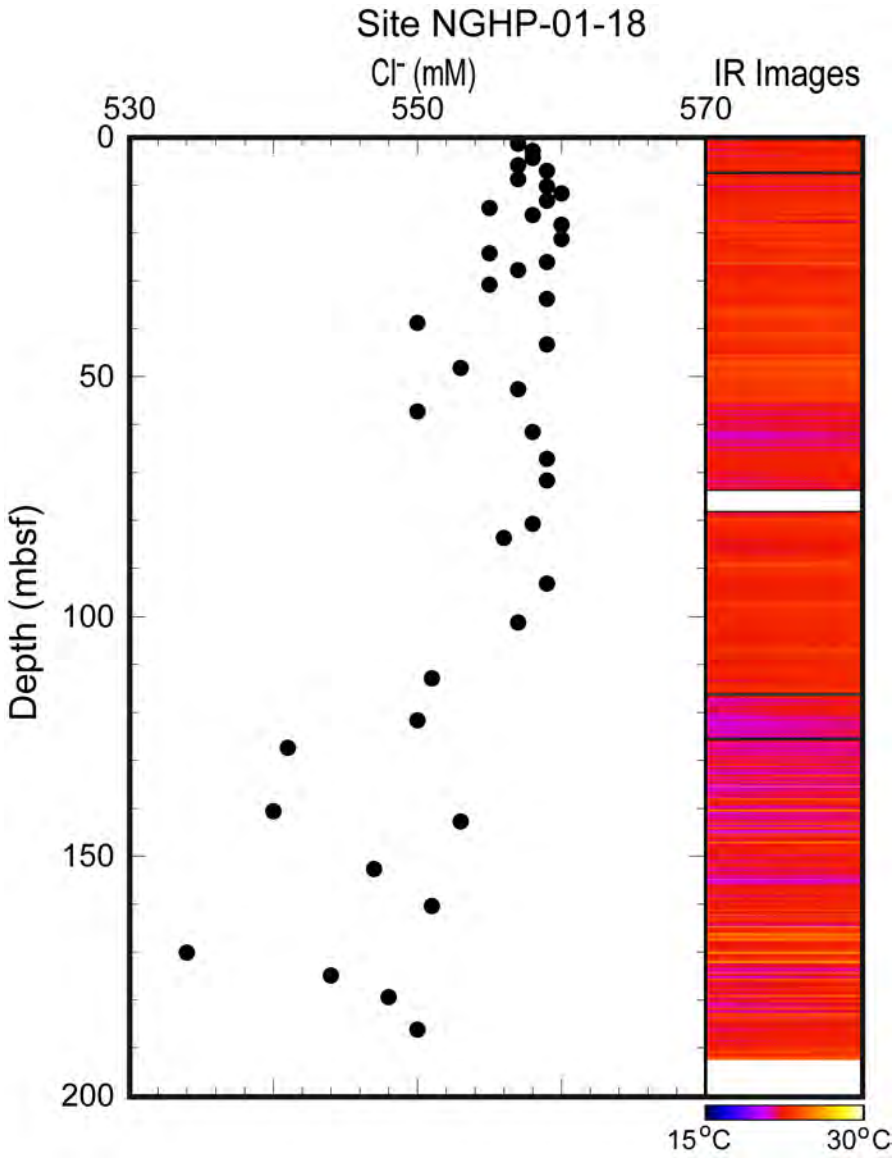
Site NGHP-01-18
Cl- (mM)
IR Images
530
550
570
0
50
100
150
200
Depth (mbsf)
15°C
30°C

Figure 39

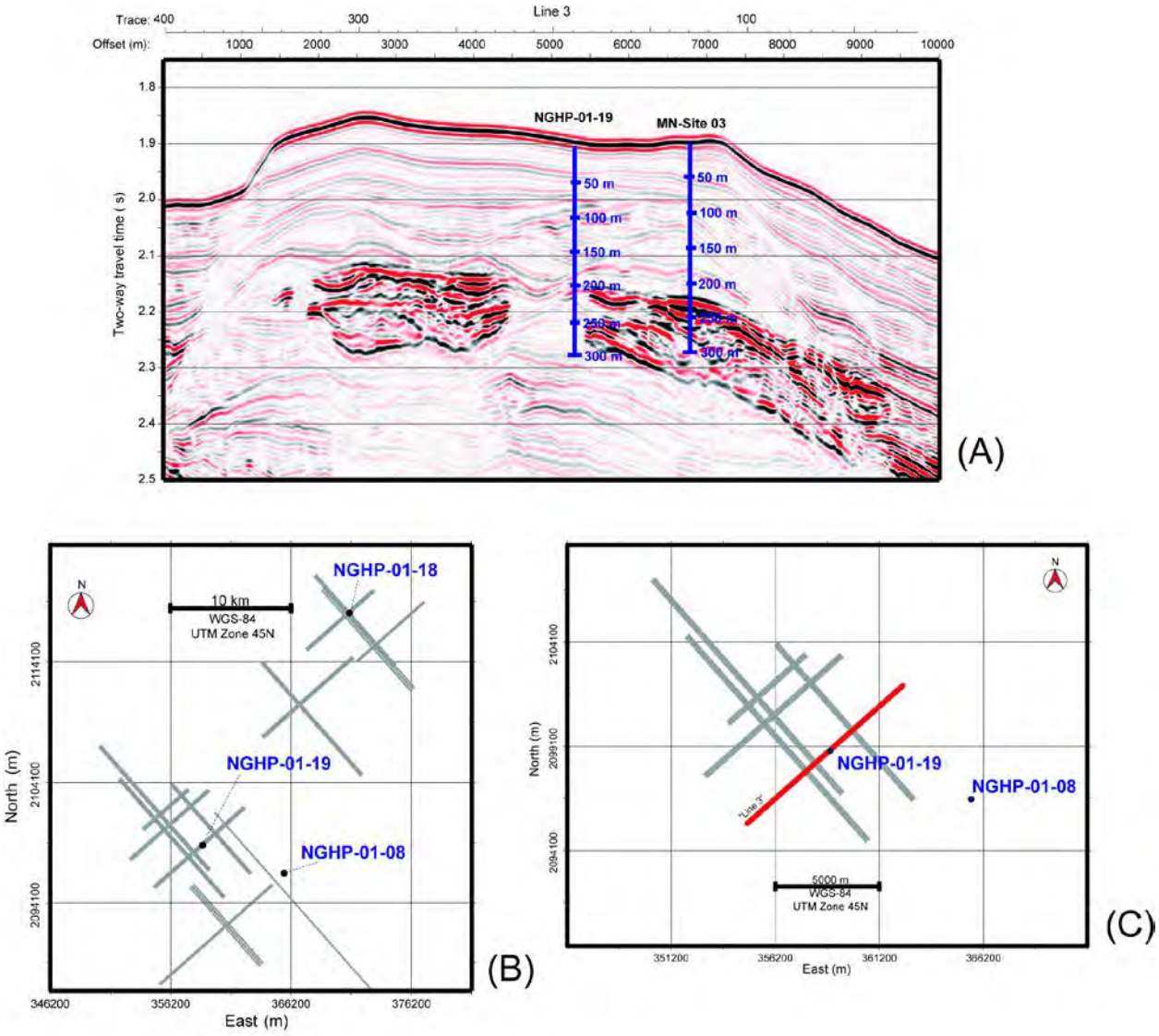
Trace: 400
300
Line 3
100
Offset (m):
1000
2000
3000
4000
5000
6000
7000
8000
9000
10000
Two-way travel time (s)
1.8
1.9
2.0
2.1
2.2
2.3
2.4
2.5
NGHP-01-19
MN-Site 03
50 m
100 m
150 m
200 m
250 m
300 m
(A)
N
10 km
WGS-84
UTM Zone 45N
NGHP-01-18
NGHP-01-19
NGHP-01-08
North (m)
2114100
2104100
2094100
346200
356200
366200
376200
East (m)
(B)
N
NGHP-01-19
NGHP-01-08
"Line 3"
5000 m
WGS-84
UTM Zone 45N
North (m)
2104100
2099100
2094100
351200
356200
361200
366200
East (m)
(C)

Figure 40

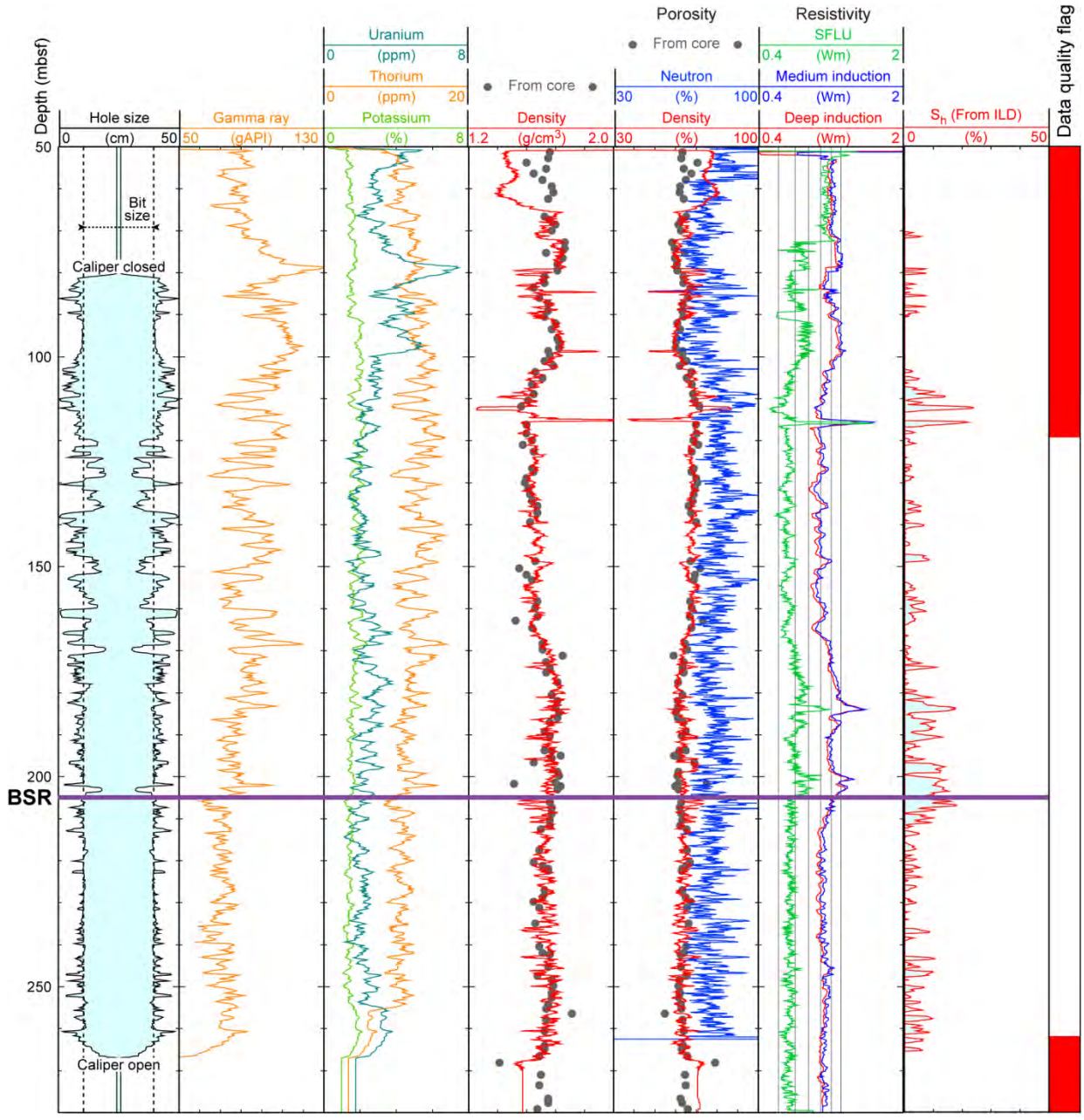
Depth (mbsf)
Hole size
0 (cm) 50
Gamma ray
50 (gAPI) 130
Uranium
0 (ppm) 8
Thorium
0 (ppm) 20
Potassium
0 (%) 8
From core
Density
1.2 (g/cm3) 2.0
Porosity
From core
Neutron
30 (%) 100
Density
30 (%) 100
Resistivity
SFLU
0.4 (Wm) 2
Medium induction
0.4 (Wm) 2
Deep induction
0.4 (Wm) 2
Sh (From ILD)
0 (%) 50
Data quality flag
Bit size
Caliper closed
Caliper open
BSR
50
100
150
200
250

Figure 41

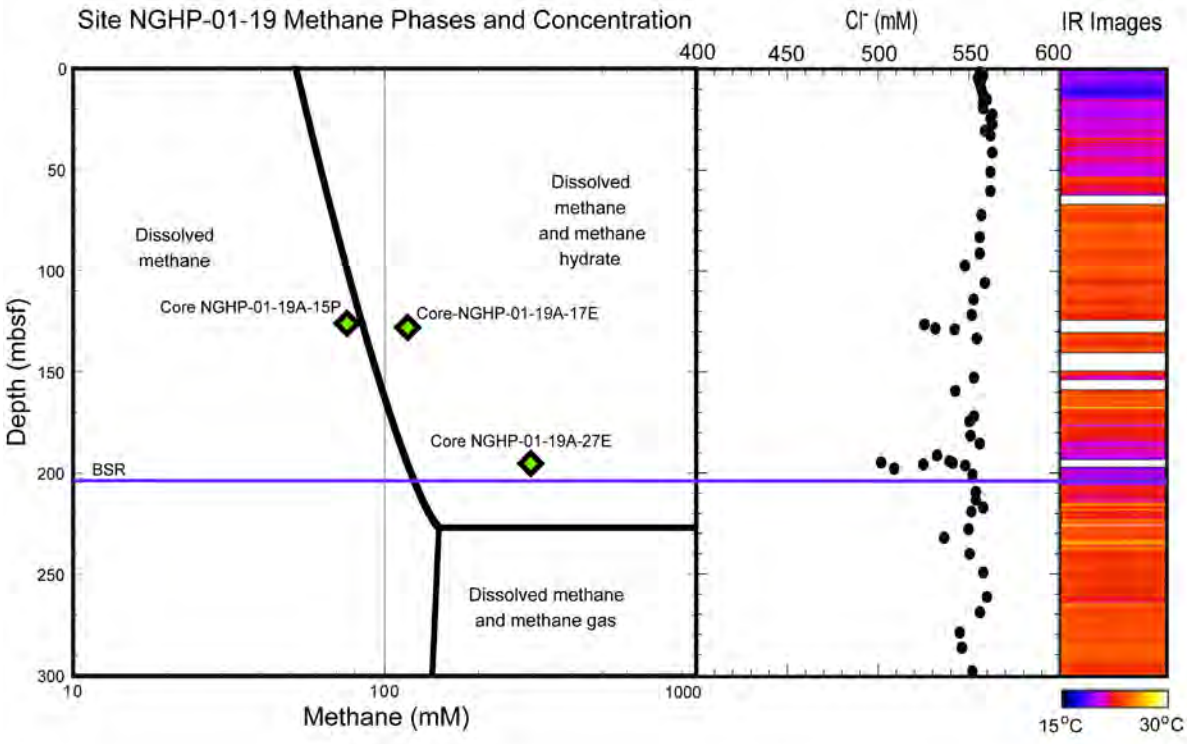
Site NGHP-01-19 Methane Phases and Concentration
Cl⁻ (mM)
IR Images
400
450
500
550
600
0
50
100
150
200
250
300
Depth (mbsf)
Dissolved methane
Dissolved methane and methane hydrate
Core NGHP-01-19A-15P
Core-NGHP-01-19A-17E
Core NGHP-01-19A-27E
BSR
Dissolved methane and methane gas
10
100
1000
Methane (mM)
15°C
30°C

Figure 42

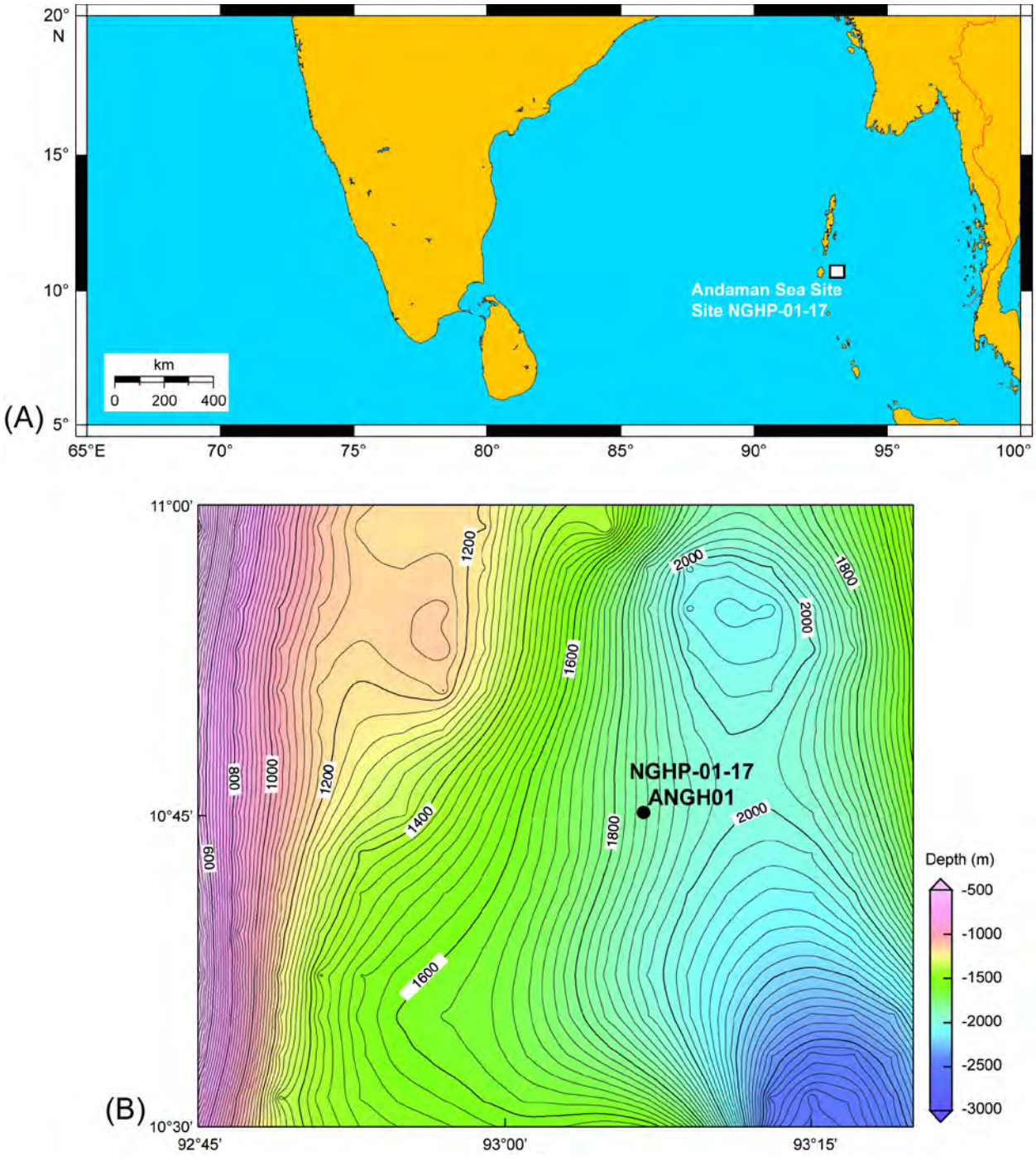
(A)
20° N
15°
10°
5°
65°E
70°
75°
80°
85°
90°
95°
100°
km
0 200 400
Andaman Sea Site
Site NGHP-01-17
(B)
11°00'
10°45'
10°30'
92°45'
93°00'
93°15'
NGHP-01-17
ANGH01
600
800
1000
1200
1400
1600
1800
2000
Depth (m)
-500
-1000
-1500
-2000
-2500
-3000

Figure 43

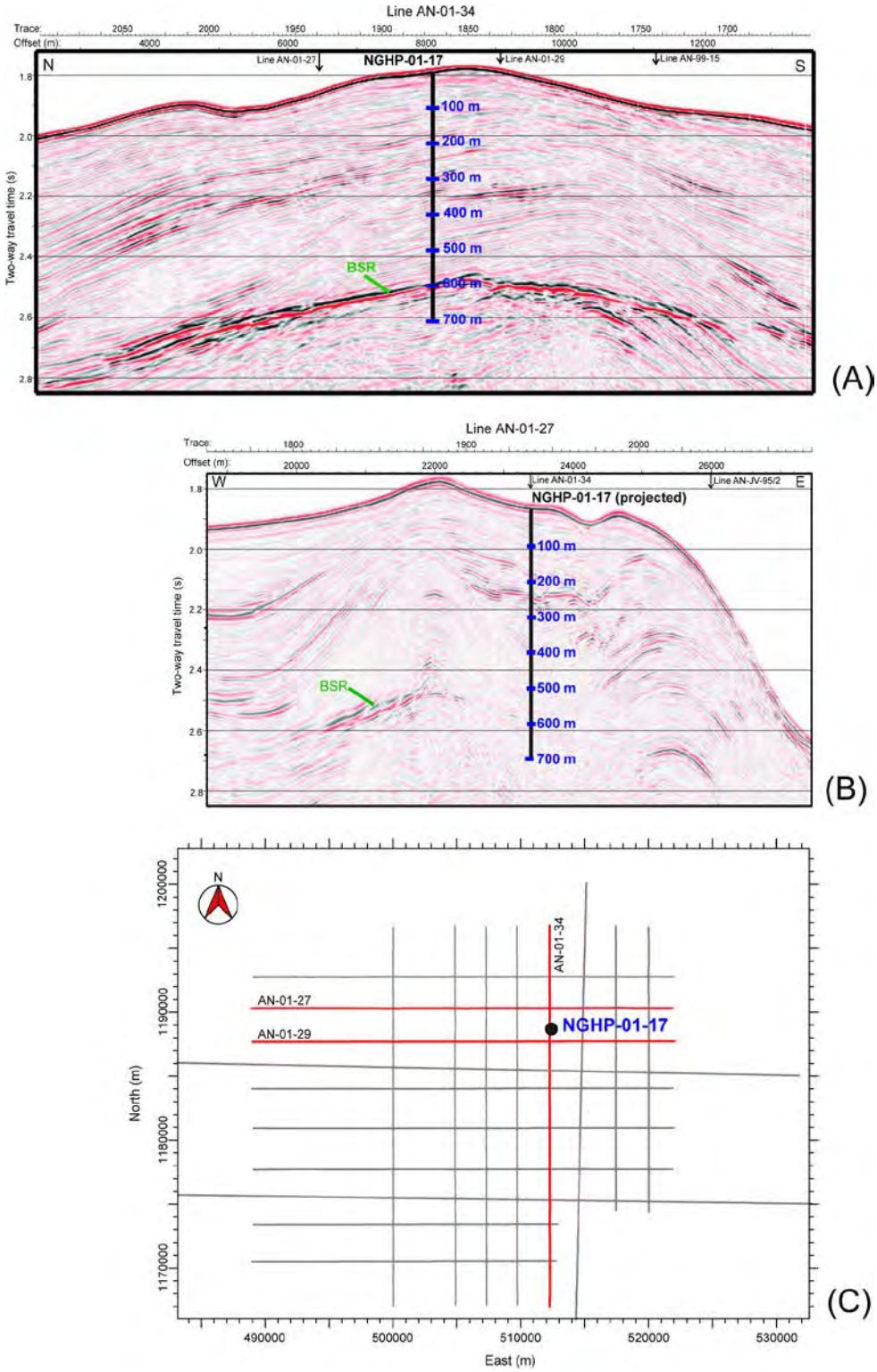
Line AN-01-34
Trace:
Offset (m):
N
S
Line AN-01-27
NGHP-01-17
Line AN-01-29
Line AN-99-15
100 m
200 m
300 m
400 m
500 m
600 m
700 m
BSR
Two-way travel time (s)
(A)
Line AN-01-27
W
E
Line AN-01-34
Line AN-JV-95/2
NGHP-01-17 (projected)
(B)
AN-01-34
AN-01-27
AN-01-29
NGHP-01-17
North (m)
East (m)
(C)

Figure 44

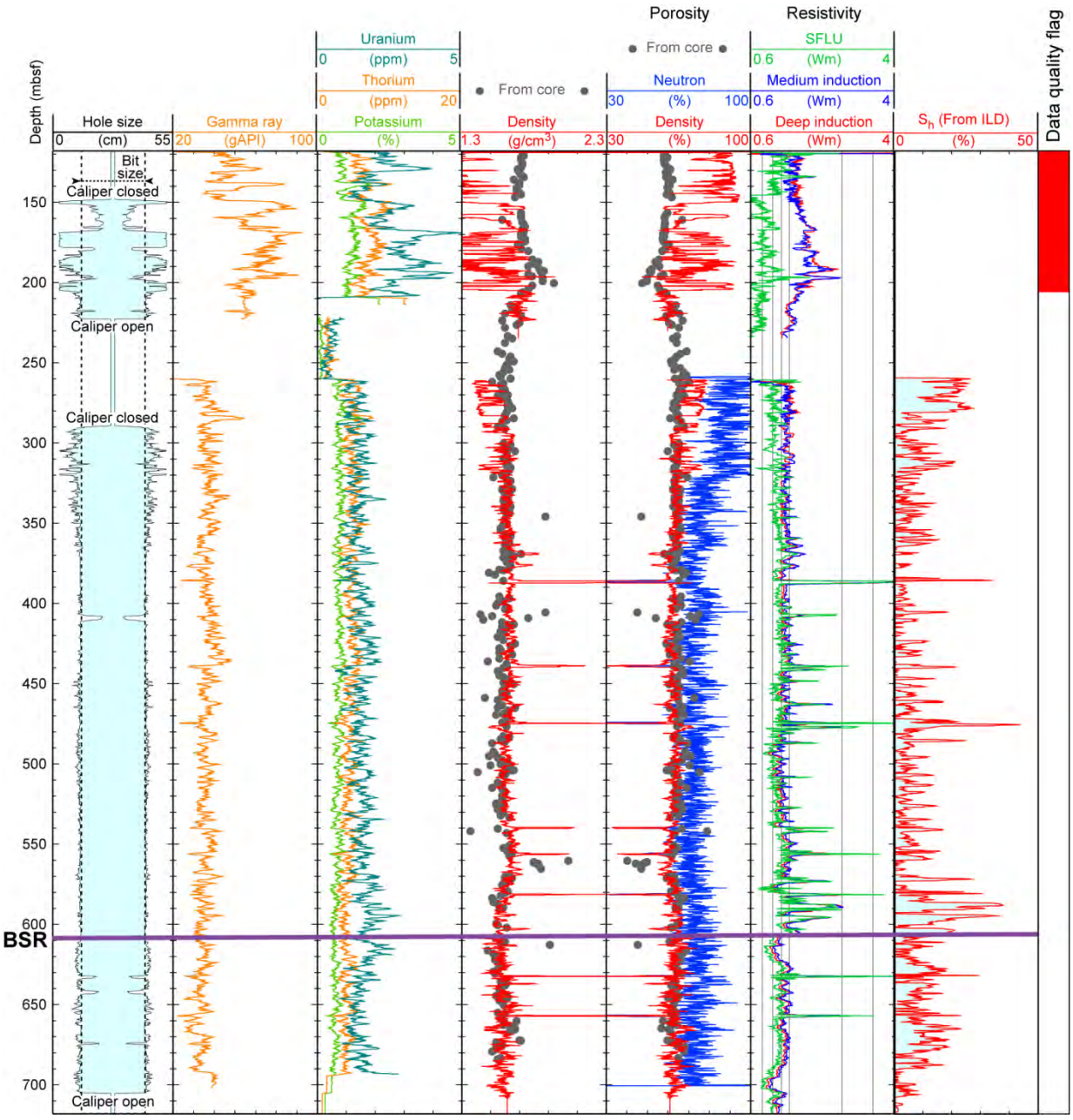
Porosity
Resistivity
Uranium
0 (ppm) 5
Thorium
0 (ppm) 20
From core
From core
SFLU
0.6 (Wm) 4
Neutron
30 (%) 100
Medium induction
0.6 (Wm) 4
Depth (mbsf)
Hole size
0 (cm) 55
Gamma ray
20 (gAPI) 100
Potassium
0 (%) 5
Density
1.3 (g/cm3) 2.3
Density
30 (%) 100
Deep induction
0.6 (Wm) 4
Sh (From ILD)
0 (%) 50
Data quality flag
Bit size
Caliper closed
Caliper open
Caliper closed
Caliper open
BSR
150
200
250
300
350
400
450
500
550
600
650
700

Figure 45

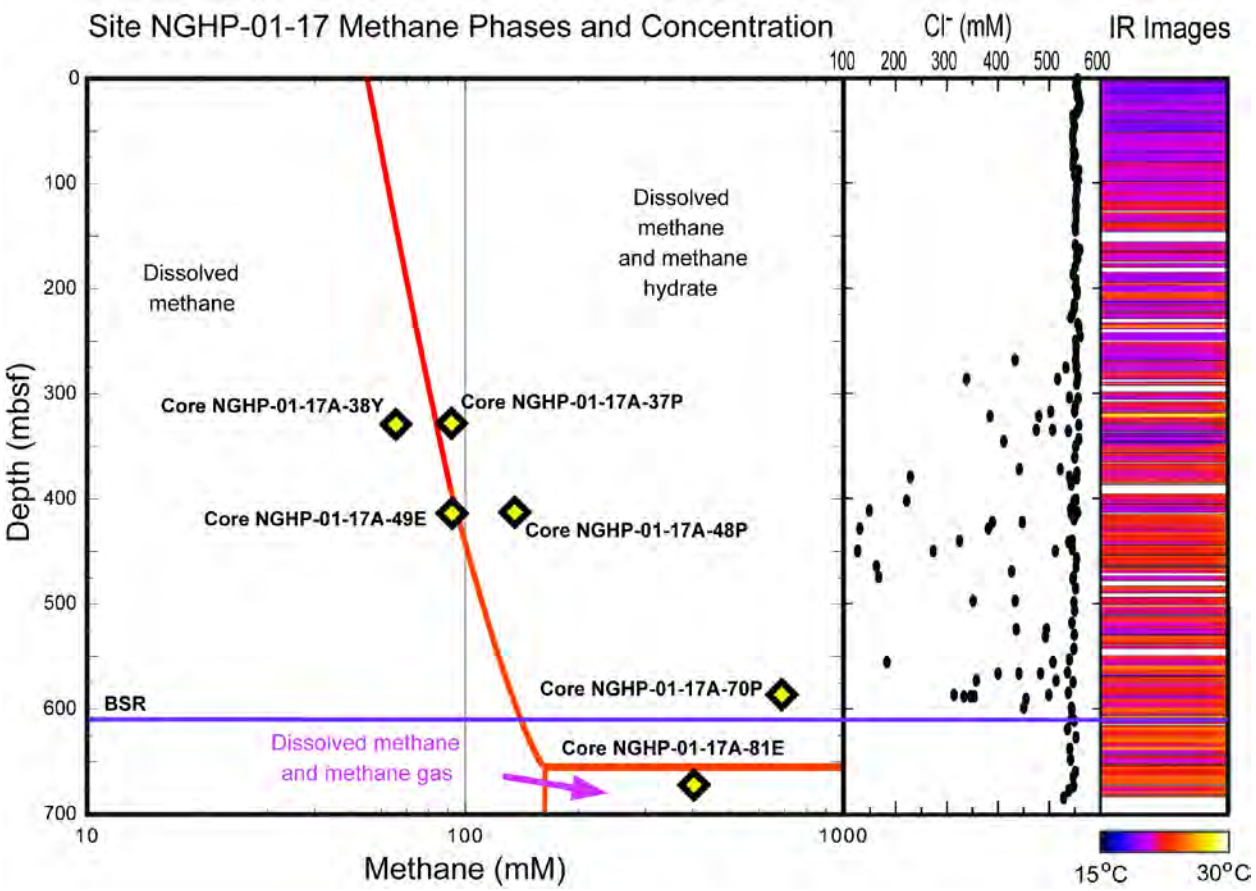
Site NGHP-01-17 Methane Phases and Concentration
Cl⁻ (mM)
IR Images
100
200
300
400
500
600
0
100
200
300
400
500
600
700
Depth (mbsf)
Dissolved methane
Dissolved methane and methane hydrate
Core NGHP-01-17A-38Y
Core NGHP-01-17A-37P
Core NGHP-01-17A-49E
Core NGHP-01-17A-48P
Core NGHP-01-17A-70P
BSR
Dissolved methane and methane gas
Core NGHP-01-17A-81E
10
100
1000
Methane (mM)
15°C
30°C

Figure 46

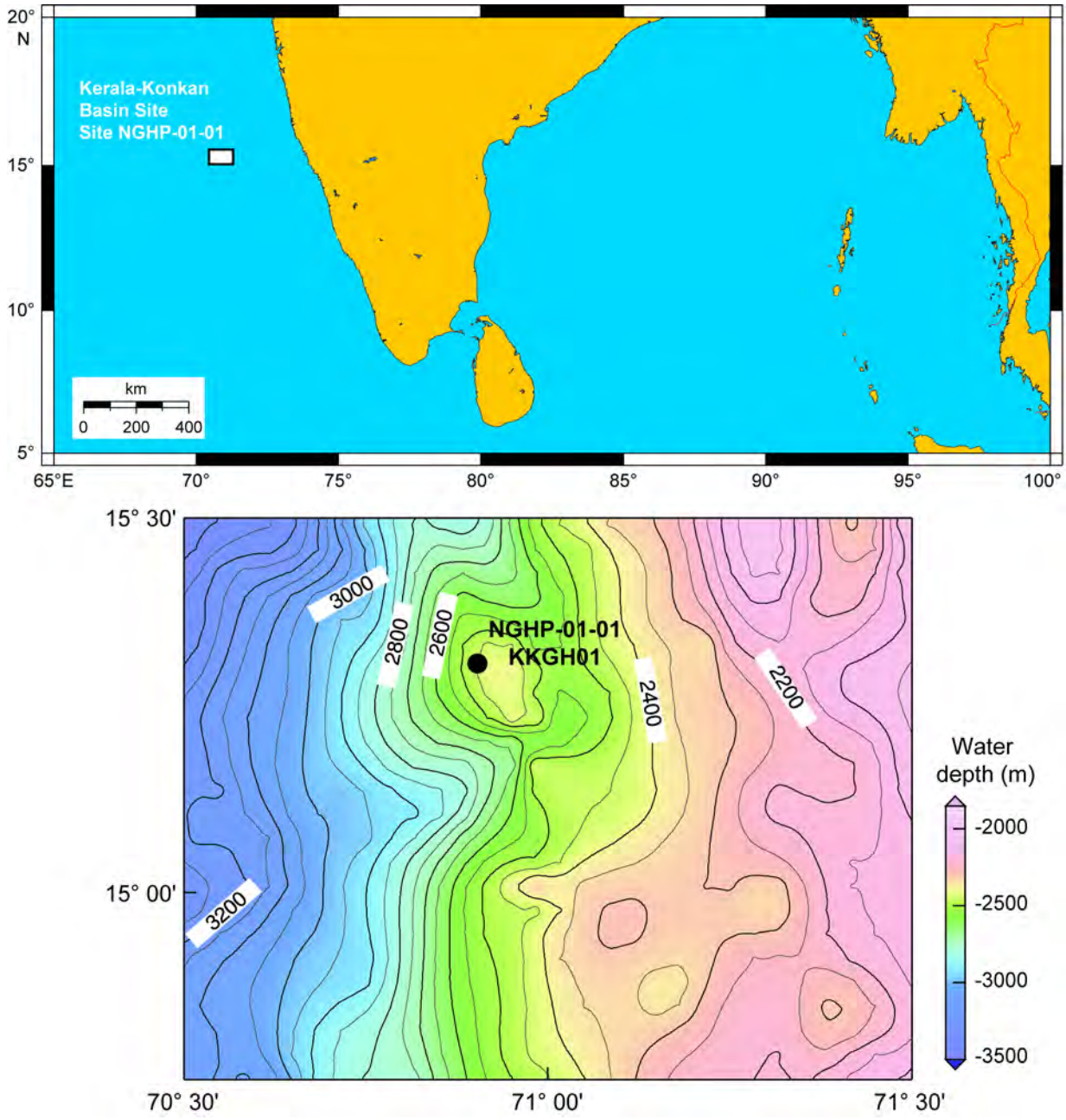
20° N
15°
10°
5°
65°E
70°
75°
80°
85°
90°
95°
100°
Kerala-Konkan
Basin Site
Site NGHP-01-01
km
0 200 400
15° 30'
15° 00'
70° 30'
71° 00'
71° 30'
3000
2800
2600
2400
2200
3200
NGHP-01-01
KKGH01
Water
depth (m)
-2000
-2500
-3000
-3500

Figure 47

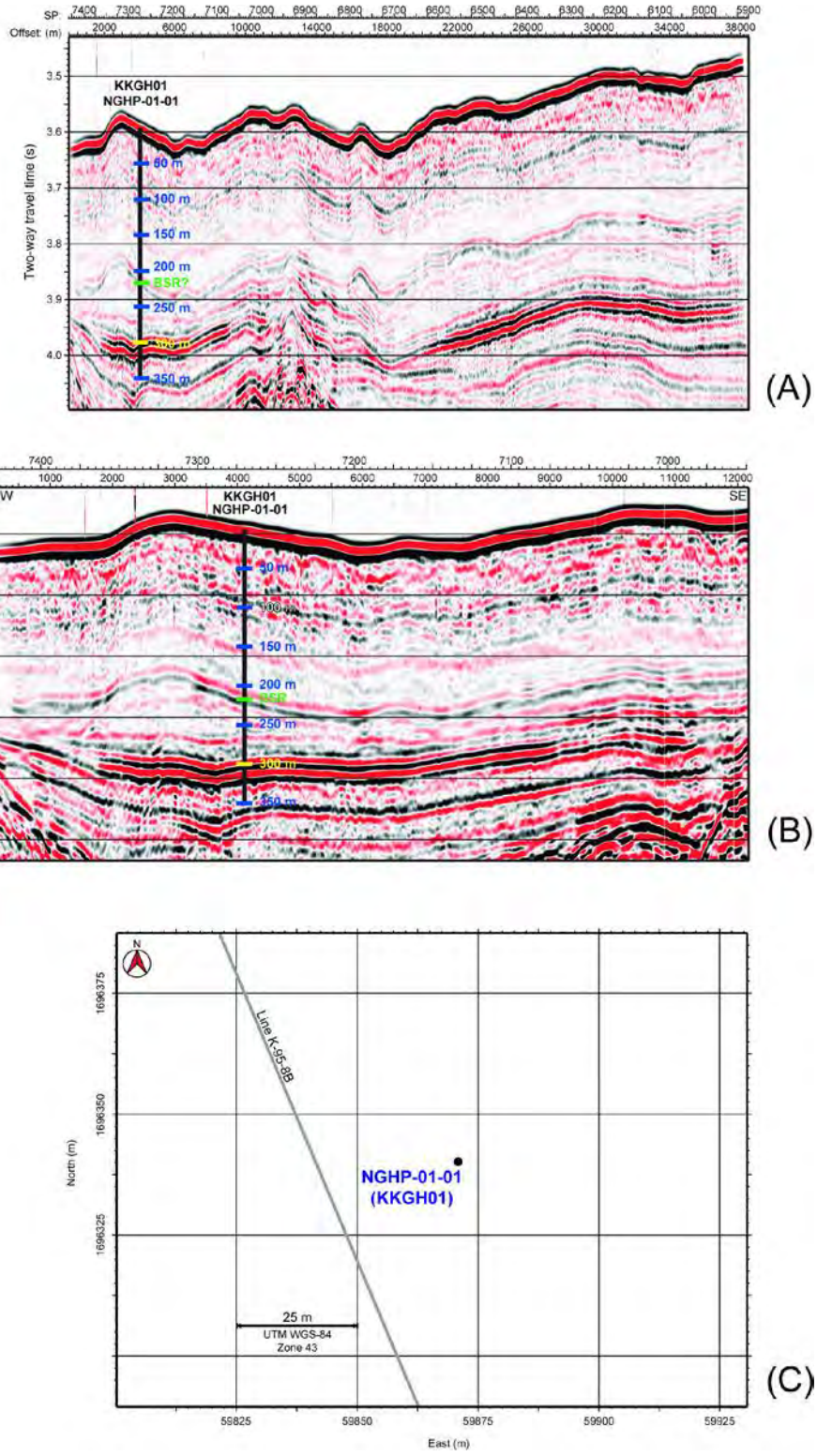
SP
Offset: (m)
KKGH01
NGHP-01-01
Two-way travel time (s)
60 m
100 m
150 m
200 m
BSR?
250 m
300 m
350 m
(A)
NW
SE
Two-way travel time(s)
BSR
(B)
Line K-95-8B
NGHP-01-01
(KKGH01)
25 m
UTM WGS-84
Zone 43
North (m)
East (m)
(C)

Figure 48

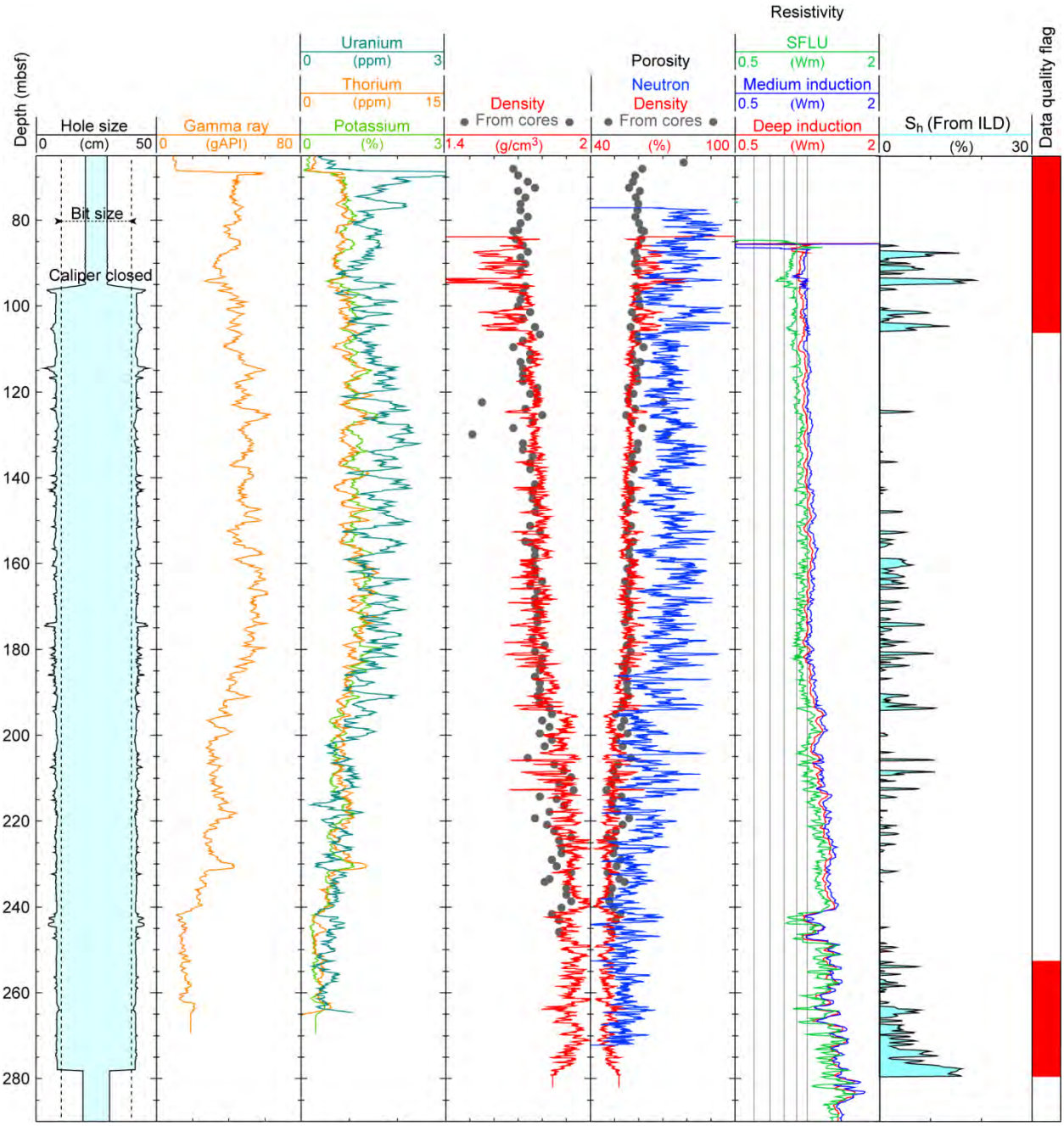
Depth (mbsf)
Hole size
0 (cm) 50
Bit size
Caliper closed
Gamma ray
0 (gAPI) 80
Uranium
0 (ppm) 3
Thorium
0 (ppm) 15
Potassium
0 (%) 3
Density
From cores
1.4 (g/cm3) 2
Porosity
Neutron
Density
From cores
40 (%) 100
Resistivity
SFLU
0.5 (Wm) 2
Medium induction
0.5 (Wm) 2
Deep induction
0.5 (Wm) 2
Sh (From ILD)
0 (%) 30
Data quality flag
80
100
120
140
160
180
200
220
240
260
280

Figure 49

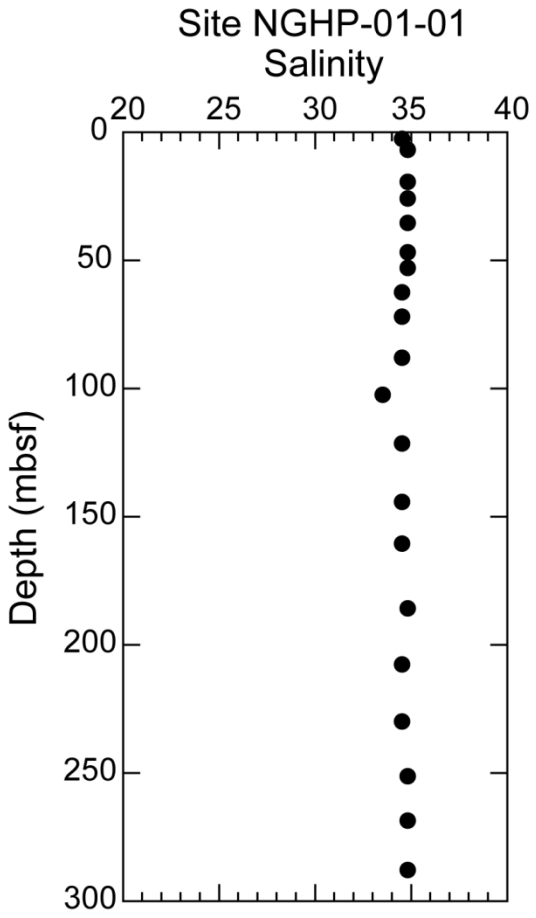
Site NGHP-01-01
Salinity
20
25
30
35
40
0
50
100
150
200
250
300
Depth (mbsf)

Figure 50

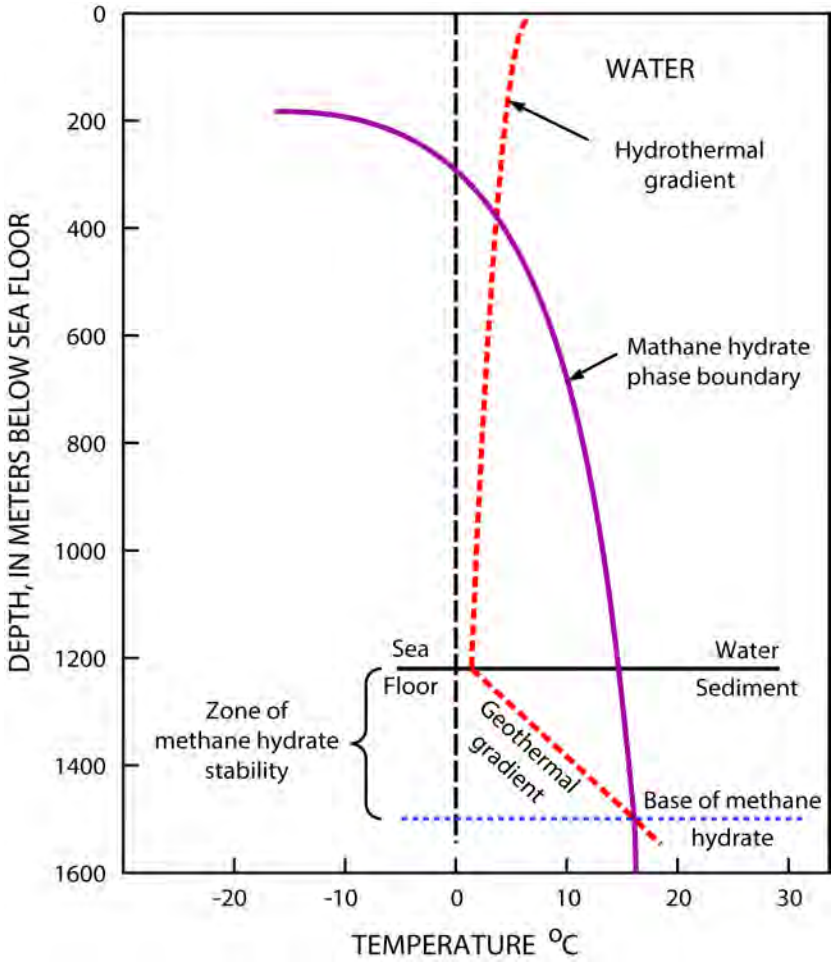
WATER
Hydrothermal gradient
Mathane hydrate phase boundary
Sea Floor
Water
Sediment
Zone of methane hydrate stability
Geothermal gradient
Base of methane hydrate
DEPTH, IN METERS BELOW SEA FLOOR
TEMPERATURE °C
0
200
400
600
800
1000
1200
1400
1600
-20
-10
0
10
20
30

Figure 51